



University Mohamed Khider of Biskra
Exact sciences and sciences of natural and life
Material sciences

MASTER MEMORY

Matter
Sciences
Physics

Material physics

Réf. :

Prsented by:
Boudjelida Meriem
Le : 27/6/2022

5G Filter-Antenna: ADS Design

Jury:

Sengouga Nouredine	Professor	Med Khider University-Biskra	President
Boudib Ouahiba	MCB	Med Khider University-Biskra	Examiner
Abdeslam N.Amele	MCB	Med Khider University-Biskra	Supervisor

Academic Year: 2021-2022

بِسْمِ اللَّهِ الرَّحْمَنِ الرَّحِيمِ

ملخص

اكتسب الجيل الخامس اهتمامًا كبيرًا بالبحث والتطوير حيث يمكنه توفير إنتاجية عالية للبيانات تلبي متطلبات مليارات البتات في الثانية من الاتصالات لعدة مستخدمين. تم إجراء محاكاة لمرشح تمرير نطاق صغير مدمج يعتمد على مرنان مستطيل بواسطة نظام تصميم متقدم باستخدام ركيزة بسماحية نسبية تبلغ 4.4 وسماكة 1.6 مم. تم استخدام الطريقة التحليلية لأول مرة لحساب خصائص المرشح مثل العازل الفعال الذي وجد أنه 4.086 وعرض 38.04 مم. هذان البعدان الرئيسيان مهمان لأنهما يؤثران بشكل مباشر على جودة وموثوقية الفلتر. ثم يُقترح أيضًا مرشح CMOS باستخدام دائرة مكافئة كهربائية مباشرة بتقنية 18 نانومتر CMOS. قيمة العناصر المجمعّة باستخدام الطريقة التحليلية متبوعة بغرس الدائرة الناتجة في التخطيطي داخل بيئة ADS ، ثم يتم محاكاتها. كانت النتائج مرضية بدرجة كافية مقارنة بأبحاث المرشح المنشورة.

الكلمات الرئيسية: مرشح 5 G ، Microstrip ، CMOS ، هوائي تصميم

Abstract

5G has gained condensed research and development land as it can provide high data throughput that meets the requirements of Gbps communications for multiple users. The simulation of the compact microstrip band-pass filter based on a rectangular-shaped resonator was carried out by Advanced Design System "ADS" using an FR4 substrate having a relative permittivity of 4.4 and a thickness of 1.6 mm. The analytical method was first used to calculate the filter characteristics such as the effective dielectric which was found of 4.086 and the width of 38.04. Those two main dimensions are important since they directly affect the quality and reliability of the filter. Then a CMOS filter is also proposed using the direct electric equivalent circuit with including 18nm CMOS technology then via the lumped elements after obtaining their value using analytical method followed by implanting the resulting circuit in the schematic ADS environment and then proceeding the simulation. The results were enough satisfying compared to the filter literature.

Key words: 5G filter, Microstrip, CMOS filter, design antenna

Résumé

La 5G a gagné un terrain de recherche et de développement condensé car elle peut fournir un débit de données élevé qui répond aux exigences des communications Gbps pour plusieurs utilisateurs. La simulation du filtre passe-bande microruban compact basé sur un résonateur de forme rectangulaire a été réalisée par Advanced Design System "ADS" en utilisant un substrat ayant une permittivité relative de 4,4 et une épaisseur de 1,6 mm. La méthode analytique a d'abord été utilisée pour calculer les caractéristiques du filtre telles que la constante diélectrique effectif qui a été trouvé de 4,086 et la largeur de 38,04mm. Ces deux dimensions principales sont importantes car elles affectent directement la qualité et la fiabilité du filtre. Puis un filtre CMOS est également proposé utilisant le circuit équivalent électrique ainsi qu'inclure la technologie 18nm CMOS puis par les éléments lumpés après l'obtention des valeurs des éléments par voie analytique et implantation du circuit résultant dans l'environnement schématique ADS, procédant à la simulation. Les résultats étaient assez satisfaisants comparer à la littérature sur les filtres.

Mots cle : les filtres 5 G, Microruban, filtre CMOS, conception des antennes.

DEDICATION

TO

*MY PARENTS FATIMA AND ABDEL
NASSER*

*MY BROTHERS WALID, YOUNES AND
OMAR*

MY SISTERS SAADIA AND IKRAM

MY AUNT SAMIRA

Acknowledgements

Thank first and foremost to Allah without grace this would never have been finished on time

I would like to thank the jury member for their helpful remarks, and evaluation, especially Professor Sengouga Nouredine as president of jury and teacher during my graduation and post- graduation. Doctor Boudib ouahiba as examiner of my work. Additionally, Dr.Nora Amele Abdeslam for her guidance, encouragement and help during my thesis work.

I would like to thank my family especially my parents and my sisters and my brothers.

Table of contents

Chapter I Filter Characterization and physics basis	
I-1 Introduction	1
I-2 Filters introduction	2
I-3 Role of the filter	2
I-4 Transfer function of a filter	3
I-5 Classification of filters	3
I-5-1 Analog filters	3
I-5-2 Digital Filters	4
I-6 The filter functions	4
I-6-1 First-order passive filters	5
I-6-2 first order Low pass filters	5
I-6-3 Second order low pass filter	8
I-6-4 First order high pass filter	9
I-7 Band Pass filter (BPF)	10
I-7-1 Pass band filter transfer function	11
I-8 Band stop filter (notch filter)	14
I-9 Active filter	16
I-9-1 Advantages and disadvantages of active filters	16
I-9-2 Active Low Pass Filter	17
References of Chapter I	23
Chapter II Transmission line characteristics	
II-1 Introduction	24
II-2 Electromagnetic field and Transmission Line theory	25
II-3 Transmission line characteristics	29
II-4 On the way to 5G and Internet of Things (IoT)	32
II-5 mm-Wave Spectrum, Challenges and Opportunities	34
II-6 Microstrip antenna	39
II-6-1 Microstrip structure and principle	39
II-6-2 Equivalent circuit of microstrip	41
II-6-3 Types of microstrip	42

II-7 CMOS-Technology	44
II-8 CMOS – Inversion	47
References of Chapter II	49
Chapter III Filter Design results	
III-1 Introduction	53
III-2 Design of Microstrip band pass filter	56
III-2-1 Specification of the proposed filter:	56
III-2-1 -1 Patch characterization	56
III-2-2 Theoretical Synthesis of the Filter	57
III-3 CMOS Filter	66
III-3-1 CMOS design	66
III-3-2 CMOS filter under lumped element form	67
References of Chapter III	71
Conclusion	73
Appendix A	76
A-1 Equivalent circuit	76
A-1-1 Role of different components:	76
1-Inductance L'	76
2-Capacitance C	77
3-Resistance R	77
4-Conductance G	77
A-2 The telegrapher equations	77
A-3 TEM Transmission Line -wave Equation	79
A-4 Characteristic Impedance	80
A-5 Wave propagation on a TEM TL.	82
A-6 Lossless and Low-Loss Transmission Lines	84
A-7 Coaxial line	84
A-8 Microstrip Line	86
A-9 Voltage reflection coefficient	88
A-10 Input Impedance for Open and Short-Circuit Terminations	91
A-11 Quarter-Wavelength Transmission Line	94

General Introduction

The mobile communication has seen a rapid evolution causing a strong impact on millions of people daily life's routine. Which continuously requires an upgrade of used technologies such mobile and antenna. For this purpose, the 5th generation (5G) has recently gained high research and development ground due to the possibility of providing high data rate that covers the huge communication needs (~ Gbps) of different operators. The Internet of Things (IoT) is following with intention to connect people regardless of time and/or place and 5G is the key catalyst of IoT.

To achieve the desired performance, 5G must be a leap forward from 4G which cannot be achieved by just step advance over previous technologies. The 5G consists on multi and different frequency range operational. The reason for the allocation of specific services in particular parts of the spectrum is due to the different propagation characteristics of the medium. In one side, the 5G is already compatible to 3G and 4G, and use from similar technology and solutions. On the side, in order to increase the speed of data transmission, mm-wave frequencies are a major progress versus previous technologies [Onoe, 2015].

The 57 to 66 GHz frequency band is kept to high-speed short range wireless communications. The two bands of 5 GHz each from 71 to 76 GHz and 81 to 86 GHz are allocated to backhauling systems. Benefited from the low atmospheric attenuation which could provide multi Gbps links for fiber extension or replacement over short medium [Vigilante and Reynaert,2018; Wells, 2010]. The frequency band from 77 to 81 GHz has been assigned for automotive radar applications. These radars can make Advanced Driver Assistance Systems (ADAS) reality, significantly enhancing the roads safety [Reger, 2016].

Indeed, a bandpass filter (BPF) is an important block in a transceiver system due to the existence of interferences (blocker), and the need for high image rejection. Thus, it is used to suppress noise and unwanted signals in various communication systems [Vigilante and Reynaert,2018], mainly in RF and microwave communications due to their efficient rejection of harmonic signals.

In this purpose, the manuscript has explored the filters for antenna applications by covering important concepts in order to comprehend and design a specific filter targeting 5 G applications. This manuscript is divided into three chapters. The first chapter is concentrated on the filter characteristics and their physics, their roles, transfer functions and classification are detailed, then

General Introduction

some advantages and disadvantages are mentioned. The second chapter focused on the transmission line and their electrical and physical properties. Followed by a third chapter where two band pass filters are designed, the microstrip and CMOS through two steps, the first one is analytically calculating the filter parameters and elements. Then using ADS Agilent software to simulate the resulting filters.

Appendix also has been added to this dissertation as it explains the transmission lines elements and parameters, their meanings and the dominant equations.

General Introduction

References of General Introduction

[Onoe, 2016] S. Onoe, 1.3 evolution of 5G mobile technology toward 1 2020 and beyond, in 2016 IEEE International Solid-State Circuits Conference (ISSCC), San Francisco, CA, pp. 23–28, 2016

[Reger, 2016] L. Reger, 1.4 the road ahead for securely-connected cars, in 2016 IEEE International Solid-State Circuits Conference (ISSCC), San Francisco, CA, pp. 29–33, 2016

[Vigilante and Reynaert,2018] M. Vigilante and P. Reynaert, '5G and E-Band Communication Circuits in Deep Scaled CMOS', Springer, ACSP Analog Circuits and Signal Processing, <https://doi.org/10.1007/978-3-319-72646-5>, 2018

[Wells, 2010] J. Wells, Multigigabit Microwave and Millimeter-Wave Wireless Communications (Artech House, Boston, 2010)

Chapter I Filter Characterization and physics basis

I-1 Introduction

Some unique properties of microwave region of the electromagnetic spectrum allow microwave signals to travel beyond prolonged distances across the atmosphere in all except the harshest weather conditions. Although military and civil applications abound, including radar, navigation and wireless communications, the microwave spectrum is a limited resource that must be divided, maintained and that's where microwave filters come in [Hunter, 2006].

Applications of RF and microwave filters Microwave systems have an enormous impact on modern society. Applications are diverse, from entertainment via satellite television, to civil and military radar systems. In the field of communications, cellular radio is becoming as widespread as conventional telephony. Microwave and RF filters are widely used in all these systems in order to discriminate between wanted and unwanted signal frequencies. Cellular radio provides particularly stringent filter requirements both in the base stations and in mobile handsets. A typical filtering application is shown in Figure I-1 which is a block diagram of the RF front end of a cellular radio base station. The Global System for Mobile (GSM) uses a time division multiple access technique TDMA [Redl et al, 1995]. Here the base station is transmitting and receiving simultaneously.

Thus, in order to comprehend the filter basis and functionality, this chapter cover the role, order and classification of multi categories of this device. Detailed analytical study is included showing the frequency response of different types of different filters according to their characteristics and applications. Additionally, their advantages and disadvantages for some applications are given.

I-2 Filters introduction

Microwave and Radio-Frequency (RF) filters constitute fundamental elements in the wireless communication systems. They are a dual port block (the input port and output port). The filters are passive or active devices, both are used to select, remove or differentiate signals located in different frequency bands, while the other parts of the signals are rejected. In our domain, this discrimination is done according to specifications in frequency translates the fact that some bands

of frequency experience severe attenuation when passing through the filter, meanwhile others do not undergo practically any loss.

Filters are categorized by type as being high pass, low pass, band pass and band stop or by technologies being passive, active, analog or digital. The low pass and high pass filters are intended for the ends of the frequency range, while the band pass acts "inside". From 3dB, the attenuation becomes tolerable. The analog filters can be passive or active. In passive filter, the power supply is not provided, thus there is no gain. Nowadays, digital filters are very powerful and accurate, but they consume energy. Consequently, realizing a balance between performance and energy efficiency is needed. The filter attaches to an antenna is responsible of filtering the signals transmitted and received from the transceiver-device. Particularly stringent filter requirements are provided by cellular radio both in the base stations and mobile handset. Figure I-1 is a block diagram of the RF front end of a cellular radio base station.

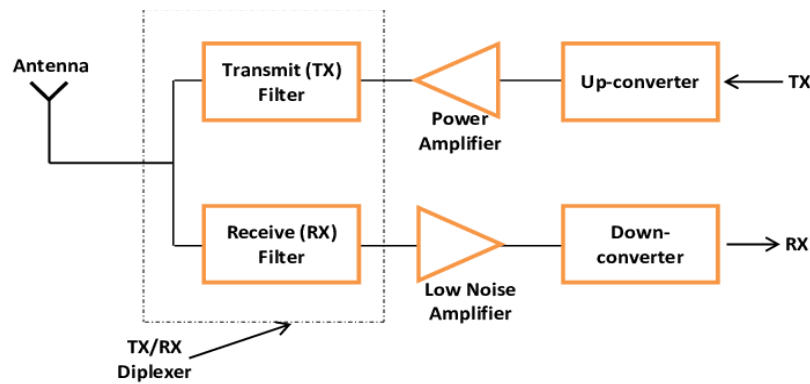


Figure I-1: The filter designed will be placed between the antenna and the transceiver (transmitter-receiver) [Hunter, 2006]

In this chapter, one can find almost all the definition of filters types, their expressions and their classifications regarding to the band frequency selected.

I-3 Role of the filter

Widely used in electronic signal processing circuits, filters are particularly used in telecommunication systems, they play a fundamental role since it is a question of eliminating all the parasitic components of the useful signal, which can be assimilated to a noise. There are various sources of the noise, it can be external, carried by the channel, or internal, transported by the passive and active elements constituting the system itself.

The signal to noise ratio (SNR) which designates the quality of an information transmission and which also defines the ratio of the power of the useful signal to that of the noise. The SNR is therefore an essential parameter in the systems. Also, the separation of interference from useful signals is necessary because the transmitted and received signals are interfered with relative to each other. Finally, according to the architecture chosen for the system, the appearance of parasitic frequencies, called images, is also a problem. In all these cases, filtering techniques are used [Khireddine, 2019].

I-4 Transfer function of a filter

Both analog and digital filters can be edited like a "black box". The signals enter one side of the black box and exit the other side. The voltage amplitude of the output signal (or its equivalent numerical representation) depends on frequency of the applied input signal and on the design of the filter itself.

The output voltage can be found mathematically by multiplying the input voltage by the transfer function, which is a frequency dependent equation [Winder, 2002]

Since the filter depends on the value of the frequency, it will amplify, attenuate, or phase shift-differently the spectral components of a signal. In other words, a transfer function can be established as pulse function w , the frequency f , or of the Laplace variable $p=j.w$, or yet again of the reduced variable x (with $x=w/w_c$, $x=f/f_c$) where w_c and f_c represent the cutoff pulse or frequency. The degree of the denominator, always greater than or equal to the degree of the numerator, defines the order of the filter [Fourniols and Escriba, 2012].

I-5 Classification of filters

Filters can be classified as analog or digital filters depending on the format of input, output and internal working signals. For analog filters, the operating signals vary in voltage and current, whereas in digital filters they are coded in a binary format and they have the advantage of flexibility because it is possible to modify their programs progressively. as mathematical models develop [Les Thede, 2004].

I-5-1 Analog filters

Analog filters were originally invented for use in radio receivers and long-distance telephone systems and continue to be the most essential components in all types of communication systems [Les Thede, 2004]. Analog filters can be classified according to their components:

- Passive RLC filters consist of passive elements (resistors, inductors, capacitors).
- Crystal filters consist of piezoelectric resonator which can be modeled by resonant circuits.
- Mechanical filters which consist of mechanical resonators and acts on mechanical vibrations.
- Microwave filters which are composed of microwave resonators and cavities that can be represented by resonant circuits.
- Active RC filters which include resistors, capacitors and amplifiers.
- Capacitor filters include resistors, capacitors, amplifiers and switches [Chen, 2009].

I-5-2 Digital Filters

In its most general sense, a digital filter is a linear shift-invariant discrete-time system, realized using finite-precision arithmetic [Andreas, 2006]. It receives an entrance under the form of a discrete-time signal and produce an output as a discrete-time signal as shows Figure I.2 [Les Thede, 2004].

The most used digital filters are the FIR (Finite Impulse Response) and IIR (Infinite Impulse Response) also called recursive filters.

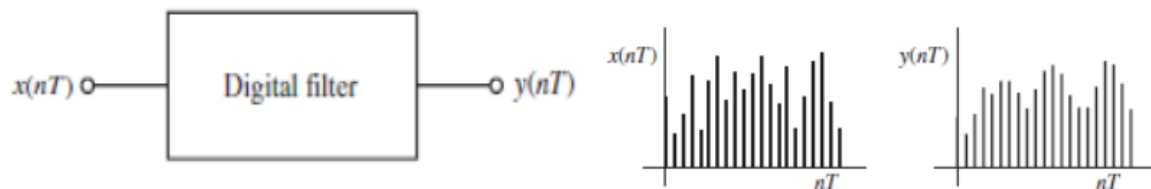


Figure I-2: A digital filter as a discrete-time system [Les Thede, 2004]

Passive filters contain only passive components such as capacitors, inductors and resistors, and do not have amplifying elements (example: transistors, op-amps). Thus, there is no signal gain, which means that their output level is always less than the input.

Filters are classified according to:

I-6 The filter functions

According to the frequency range of signals allowed or to that blocked (attenuated), filters are also termed [Hunter, 2006]. The most generally used filter designs are:

- ✓ The Low Pass Filter: Only allows low frequency signals from 0 Hz to its cutoff frequency, f_c point to pass while blocking those higher.

- ✓ The High Pass Filter: Only allows high frequency signals from its cutoff frequency, f_c point and higher to infinity to pass through.
- ✓ The Band Pass Filter: Allows signals falling within a certain frequency band setup between two points to pass through while blocking both the lower and higher frequencies in either side of this frequency band.

I-6-1 First-order passive filters

Simple First-order passive filters (1st order) is a connection of a single resistor and a single capacitor in series and an input signal across them V_{in} . Depending on which way around we connect the resistor and the capacitor with regards to the output signal determines the type of filter construction resulting in either a low pass filter or a high pass filter as it is shown on Figure I-3.

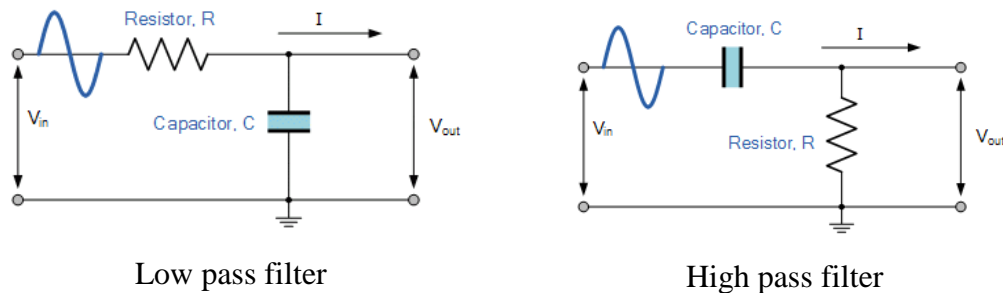


Figure I-3: First order low pass filter and high pass filter [Hunter, 2006].

As the function of any filter is to allow signals of a given band of frequencies to pass unaltered while attenuating or removing all others, one can define the amplitude response characteristics of an ideal filter by using an ideal frequency response curve of the four basic ideal filter types as shown on Figure I-4.

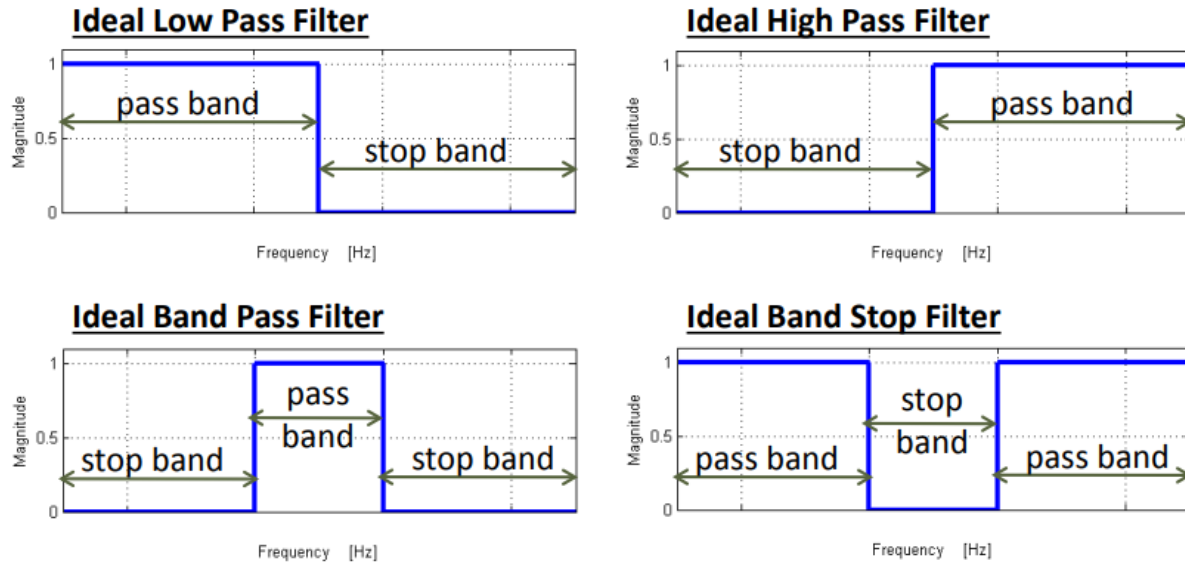


Figure I-4: Ideal Filter Response Curves [Hunter, 2006].

I-6-2 Low pass filters

A Low pass filter can be a combination of capacitance, inductance or resistance intended to produce higher order filter and high attenuation above a specified frequency and slight or no attenuation below that frequency. The frequency at which the transition occurs is called the “cutoff” or “corner” frequency. By plotting the networks (Figure I-3 left) output voltage against different values of input frequency, the frequency response curve or Bode plot function of the low pass filter circuit can be found, as shown on Figure I-5 and explained as follow.

By consider figure I-3 left, by using the potential divider equation, the output voltage is given as:

$$V_{\text{out}} = V_{\text{in}} \cdot \left(\frac{Z_c}{Z_c + Z_R} = \frac{1/jc\omega}{1/jc\omega + R} = \frac{1}{1 + j\omega RC} \right) \quad \text{I-1}$$

$$\Gamma(\omega) = \frac{V_{\text{out}}}{V_{\text{in}}} = \frac{1}{1 + j\omega RC} \quad \text{I-2}$$

Then, the voltage gain (modulus of the transmittance) is

$$|\Gamma(\omega)| = \left| \frac{1}{1 + j\omega RC} \right| \quad \text{I-3}$$

Where $\omega_0 = \frac{1}{RC}$, Bode diagram for the gain is

$$G(\omega)|_{dB} = 20 \log_{10} |\Gamma(\omega)| = 20 \log_{10} \left| \frac{1}{1+j\omega RC} \right| \quad \text{I-4}$$

Hence,

$$G(\omega)|_{dB} = 20 \log_{10} \left(\frac{1}{\sqrt{1 + \left(\frac{\omega}{\omega_0}\right)^2}} \right) = -10 \log_{10} \left(1 + \left(\frac{\omega}{\omega_0}\right)^2 \right) \quad \text{I-5}$$

$$\text{And } \varphi = -\arctan \left(\frac{\omega}{\omega_0} \right) \quad \text{I-6}$$

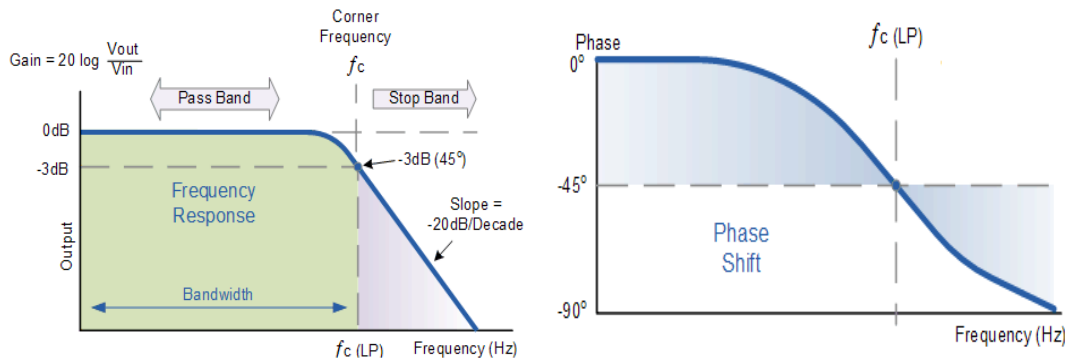


Figure I-5: Frequency response of 1st order low pass filter [Khiredine, 2019]

From Bode plot, for low frequencies, the frequency response is nearly flat which means almost all of the input signal passed to the output, ensuing a gain of nearly 1, until it reaches its f_0 . This is because the reactance of the capacitor is high at low frequencies and blocks any current flow through the capacitor. After this cutoff frequency the response of the circuit decreases to zero at a slope of -20dB/ Decade (-6dB/Octave) “roll-off”. Note that the angle of the slope, is -20dB/ Decade roll-off will always be the same for any RC combination.

Any higher frequency signals applied to the low pass filter circuit above this cutoff frequency will become greatly attenuated. This happens because at very high frequencies the reactance of the capacitor becomes so small that it gives the effect of a short circuit condition on the output terminals resulting in zero output.

For this type of low pass filter circuit, all the frequencies below f_0 point are unaltered with little or no attenuation and are known as Pass band zone. This pass band region also represents the

Bandwidth of the filter. Any signal frequencies above this point cutoff point are generally recognized as Stop band region and are greatly attenuated.

This Cutoff frequency ($1/2.\pi RC$) is defined as the frequency point where the capacitive reactance and resistance are equal, $R = X_c (1/C.w_0)$. When this occurs the output signal is attenuated to 70.7% of the input signal value or -3dB ($20 \log (V_{out}/V_{in})$) of the input. Although $R = X_c$, the output is not half of the input signal. This is because it is equal to the vector sum of the two and is therefore 0.707 of the input.

As the filter contains a capacitor, the phase angle (ϕ , where the phase shift $\phi = -\arctan(2.\pi.f.RC)$) of the output signal lags behind that of the input and at the -3dB cut-off frequency is -45° out of phase. This is due to the time taken to charge the plates of the capacitor as the input voltage changes, resulting in the output voltage (the voltage across the capacitor) “lagging” behind that of the input signal. The higher the input frequency applied to the filter the more the capacitor lags and the circuit becomes more and more “out of phase”.

I-6-3 Second order low pass filter

In the RLC circuit, second order low pass filter as represented on Figure I-6, the current is the input voltage divided by the sum of the impedance of the inductor Z_L , the impedance of the resistor $Z_R=R$ and that of the capacitor Z_C . The output is the voltage over the capacitor and equals the current through the system multiplied with the capacitor impedance.

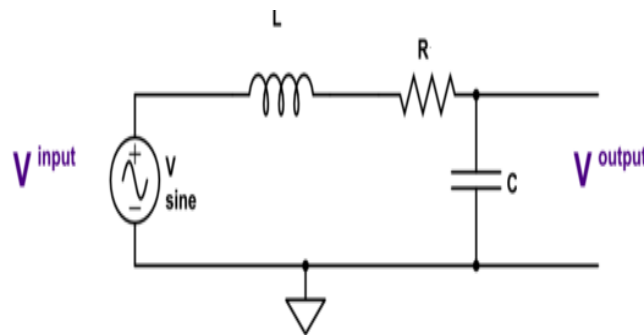


Figure I-6: RLC circuit, 2nd order low pass filter [Khiredine, 2019].

The transfer function is then given by the following equation

$$\Gamma(w) = \frac{Z_c}{Z_c + Z_L + Z_R} = \frac{1/jc\omega}{1/jc\omega + jL\omega + R} = \frac{1}{1 + jwRC - LCw^2} \quad \text{I-7}$$

By substituting x in the last equation $x = w/w_0$ equation I-7 is rewritten as:

$$\Gamma(w) = \frac{1}{1-x^2+jx/Q} \quad \text{I-8}$$

And just by comparison, one can find $w_0 = 1/\sqrt{LC}$ and $Q = \frac{1}{R}\sqrt{\frac{L}{C}}$.

Furthermore, in the equation I-7, the denominator is a second-order polynomial. The roots to this polynomial are called the system's poles, and we can reform the equation as

$$\Gamma(w) = K \cdot \frac{1}{(jw-p_1)(jw-p_2)} \quad \text{I-9}$$

Where $K=1/LC$ and

$$p_{1,2} = -\frac{R}{2L} \pm \sqrt{\left(\frac{R}{2L}\right)^2 - \frac{1}{LC}} \quad \text{I-10}$$

K is also expressed as the product of $p_1.p_2$. Since the poles in equation I-9 can be real or complex conjugates, and in order to put this in evidence, one can parameterize the poles in terms of w_0 and the damping ratio ζ , so

$$p_{1,2} = -\frac{R}{2L} \pm \sqrt{\left(\frac{R}{2L}\right)^2 - \frac{1}{LC}} = \frac{1}{\sqrt{LC}} \left(-\sqrt{LC} \cdot \frac{R}{2L} \pm \sqrt{LC} \cdot \sqrt{\left(\frac{R}{2L}\right)^2 - \frac{1}{LC}} \right) \quad \text{I-11}$$

$$p_{1,2} = \frac{1}{\sqrt{LC}} \left(-\frac{R}{2} \sqrt{\frac{C}{L}} \pm \sqrt{\left(\frac{R}{2} \sqrt{\frac{C}{L}}\right)^2 - 1} \right) \quad \text{I-12}$$

Where $\zeta = \frac{R}{2} \sqrt{\frac{C}{L}}$ and $p_{1,2} = w_0 (-\zeta \pm \sqrt{\zeta^2 - 1})$

This dampening coefficient ζ determines the behavior of the system.

I-6-4 First order high pass filter

Effectively, the high pass filter is the same circuit as the low pass circuit with reversed location of the resistor and capacitance as represented in Figure I-3 right. Then the transfer function in this case is given by the following equation:

$$\Gamma(w) = \frac{Z_R}{Z_C+Z_R} = \frac{R}{1/jcW+R} = \frac{jwRC}{1+jwRC} \quad \text{I-13}$$

By substituting w_0 one can get:

$$\Gamma(w) = \frac{j(w/w_0)}{1+j(w/w_0)} \quad \text{I-14}$$

Hence the gain in potential is given by:

$$|\Gamma(w)| = \left| \frac{jw/\omega_0}{1+jw/\omega_0} \right| = \frac{1}{\sqrt{1+\left(\frac{\omega_0}{w}\right)^2}} \quad \text{I-15}$$

With $\omega_0 = \frac{1}{RC}$. Bode diagram for the gain is

$$G(w)|_{dB} = 20 \log_{10} \left(\frac{1}{\sqrt{1+\left(\frac{\omega_0}{w}\right)^2}} \right) \quad \text{I-16}$$

Hence,

$$G(w)|_{dB} = -10 \log_{10} \left(1 + \left(\frac{\omega_0}{w} \right)^2 \right) \quad \text{I-17}$$

$$\text{And } \varphi = \frac{\pi}{2} - \arctan \left(\frac{\omega_0}{w} \right) \quad \text{I-18}$$

And just by qualitative study the bode gain and phase are represented on figure I-7.

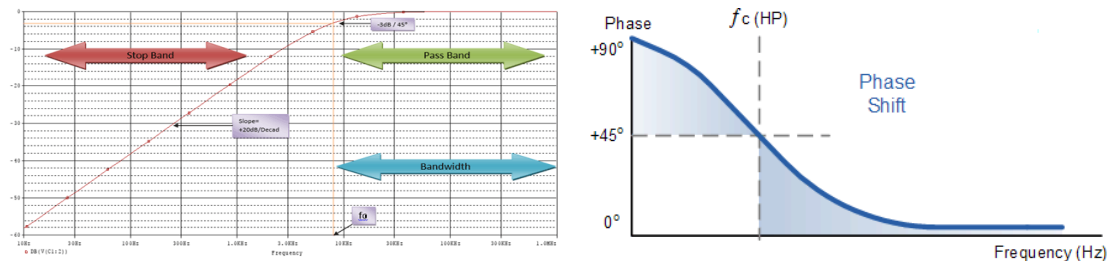


Figure I-7.: High pass filter responses on Bode plane (Gain and phase shift)

Widely used within RF circuits-also for RF applications, high and low pass filters are normally based around both inductors and capacitors. The LC based filters provide much better performance than just RC ones and consequently they tend to be used for RF applications.

I-7 Band Pass filter (BPF)

Band-pass filters can be made by stacking (cascading) a low-pass filter on the end of a high-pass filter, or vice versa (no difference in its overall operation) and it acts as a screen to frequencies lying in a certain range while giving easy transit only to frequencies within a particular range. Examples of these band pass filter-circuits are presented on Figure I-8.

Although, making a bandpass filter by combining low-pass and high-pass filters together is sturdy, it is not without certain limitations. Furthermore, and since this type depends on either section to block unwanted frequencies, it can be tough to design such a filter to enable unhindered passage within the desired frequency range.

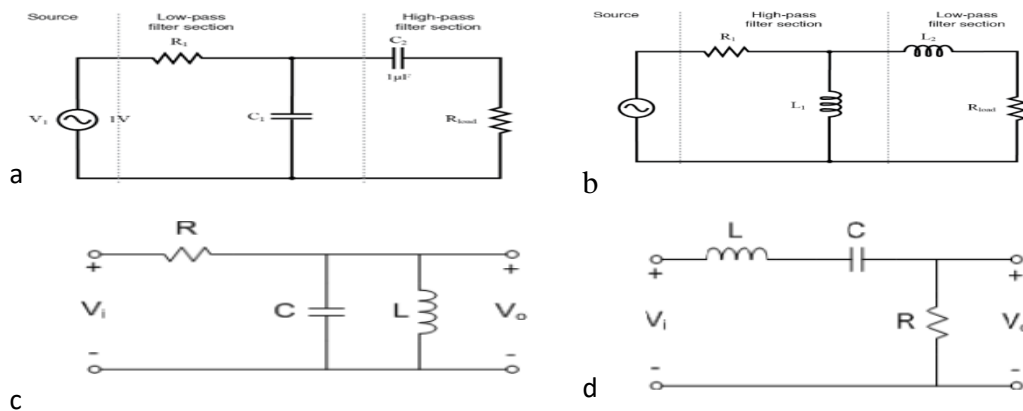


Figure I-8: Band pass filter examples [Hunter, 2006]

The two sections (LPF and HPF) permanently block signals to some degree, and their combined effort results in an attenuated signal at best (reduced amplitude), even at the peak of the pass-band frequency band.

Audio amplifier applications or circuits such as in loudspeaker crossover filters or pre-amplifier tone controls is one of simple use for these types of passive filters. In these cases where, it is needed to just pass a specific range of frequencies that do not begin at 0 Hz, (DC) or end at certain upper high frequency point but essentially to be within a certain range or band of frequencies, either narrow or wide

I-7-1 Pass band filter transfer function

The frequency response function of pass filter option given by Figure I-8-c is:

$$\Gamma(\omega) = \frac{Z_1}{Z_1 + Z_2} \quad \text{I-19}$$

$$\left\{ \begin{array}{l} \Gamma(W) = \frac{\frac{jLw}{1-LCw^2}}{\frac{jLw}{1-LCw^2} + R} = \frac{jwL}{R + jwL - RLCw^2} \\ Z_1 = R \\ Z_2 = \left[jCw + \frac{1}{jLw} \right]^{-1} = \frac{jLw}{1-LCw^2} \end{array} \right. \quad \text{I-20}$$

$$\Gamma(W) = \frac{jw/RC}{(1/LC) + (jw/RC) - w^2} \quad \text{I-21}$$

By considering the filter's behavior at the limit's cases of frequency, three cases can be distinguished as shown on figure I-9

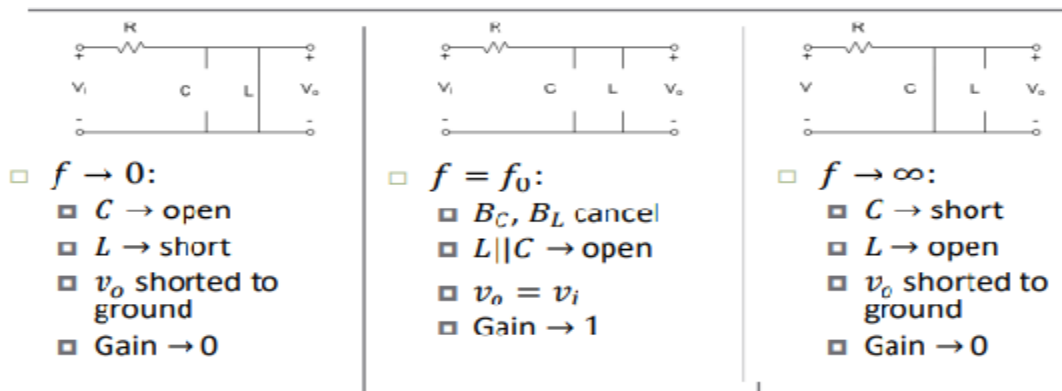


Figure I-9: the behavior of pass band filter (Figure I-8-c).

For the case of Figure I-8-d, the second order band pass filter has a transfer function as:

$$\left\{ \begin{array}{l} \Gamma(W) = \frac{R}{R + \frac{1-LCw^2}{jCw}} = \frac{jwRC}{1 + jwRC - LCw^2} \\ Z_2 = R \\ Z_1 = \left[jLw + \frac{1}{jCw} \right] = \frac{1-LCw^2}{jCw} \end{array} \right. \quad \text{I-22}$$

Then, the frequency response function is given as follow:

$$\Gamma(W) = \frac{jwR/L}{\frac{1}{LC} + jw\frac{R}{L} - w^2} \quad \text{I-23}$$

And the quantitative filter's behavior study at the frequency limits is shown on figure I-10

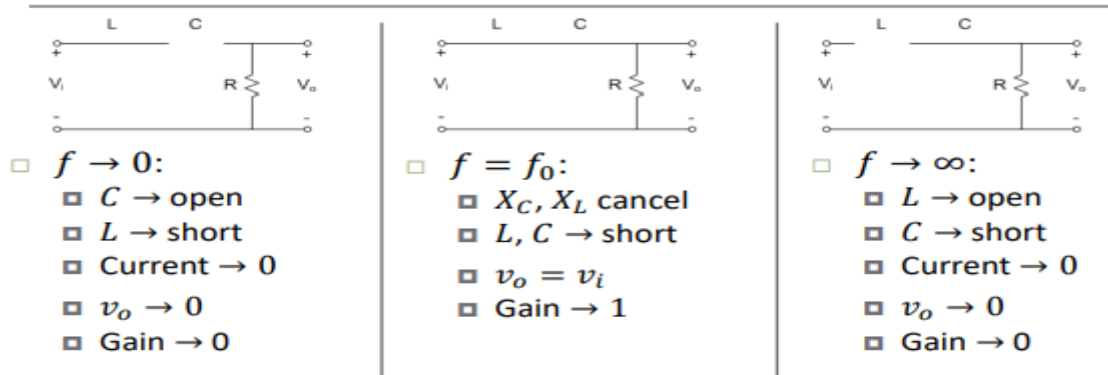


Figure I-10: the behavior of pass band filter (Figure I-8-d).

Even the last band pass filters (c and d) have different response functions and a different quality factor Q , they have the same resonant frequency f_0 as summarized in table I-2.

Band pass circuit	quality factor Q	response function $\Gamma(\omega)$	$\Gamma(\omega)$ in terms of ω_0 and Q	Resonant frequency f_0
	$RC \cdot \omega_0 = \frac{R}{L\omega_0}$	$\frac{j\omega/RC}{\frac{1}{LC} + (j\frac{\omega}{RC}) - \omega^2}$	$\frac{j\omega \frac{\omega_0}{Q}}{(j\omega \frac{\omega_0}{Q}) + \omega_0^2 - \omega^2}$	$\frac{1}{2\pi \cdot \sqrt{LC}}$
	$\frac{1}{RC\omega_0} = \frac{\omega_0 L}{R}$	$\frac{j\omega R/L}{\frac{1}{LC} + j\omega \frac{R}{L} - \omega^2}$		

Table I-2: Band pass filters characterizations [Hunter, 2006].

Since the last two band pass filter have the same frequency response, we present Figure I-11 which shown their response in frequency domain.

Q determines the sharpness of the response; higher value for Q provides higher selectivity which means a narrower pass band and steeper transition to the stop bands. The band width of the pass band is the difference between the upper and lower frequency of the band in response.

$$Bw = f_u - f_l = \frac{f_0}{Q}$$

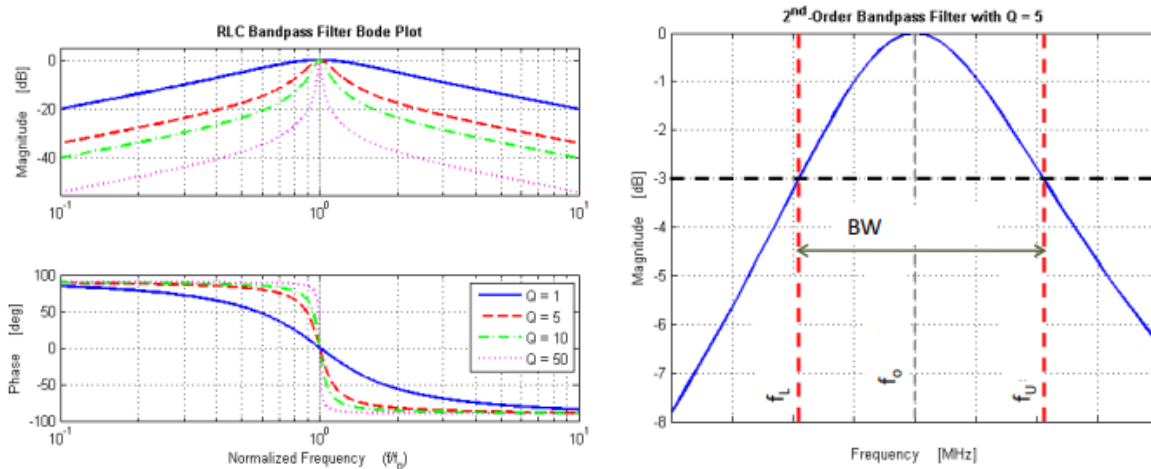


Figure I-11: a representative frequency response of band pass filter (not to scale).

I-8 Band stop filter (notch filter)

As example, the band stop filter (a 2nd order filter) can be just the same filter as the one on Figure I-8-d (series RLC) but in this time the output is taken across the inductor and the capacitance as represented by Figure I-12.

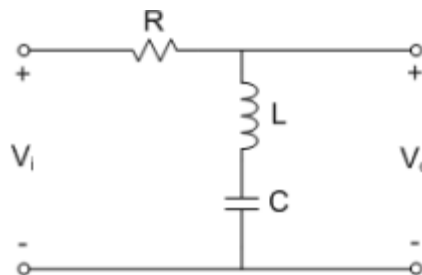


Figure I-12 Band stop Filter.

Here the capacitor behaves as an open circuit at low frequencies, therefore the output voltage is the same as the input voltage but at high frequencies, it is the inductor that behaves as an open circuit leading the output voltage to take the same amount voltage as the input. At the resonant frequency, the impedance of inductor cancels the impedance of capacitance mutually and so there is only the effect of resistance. The transfer function of this circuit is obtained by the analyzing the electrical diagram as follows:

$$\Gamma(\omega) = \frac{Z_2}{Z_1 + Z_2}$$

I-25

$$\left\{ \begin{array}{l} \Gamma(\omega) = \frac{\frac{1-LC\omega^2}{jC\omega}}{\frac{1-LC\omega^2}{jC\omega} + R} = \frac{1-LC\omega^2}{1+j\omega RC-LC\omega^2} \\ Z_1 = R \\ Z_2 = jL\omega + \frac{1}{jC\omega} = \frac{1-LC\omega^2}{jC\omega} \end{array} \right. \quad \text{I-26}$$

Then,

$$\Gamma(\omega) = \frac{\frac{1}{LC} - \omega^2}{\frac{1}{LC} + j\omega \frac{R}{L} - \omega^2} \quad \text{I-27}$$

By a qualitative study, Figure I-13 gathers the filter behavior at its three limiting cases for frequency:

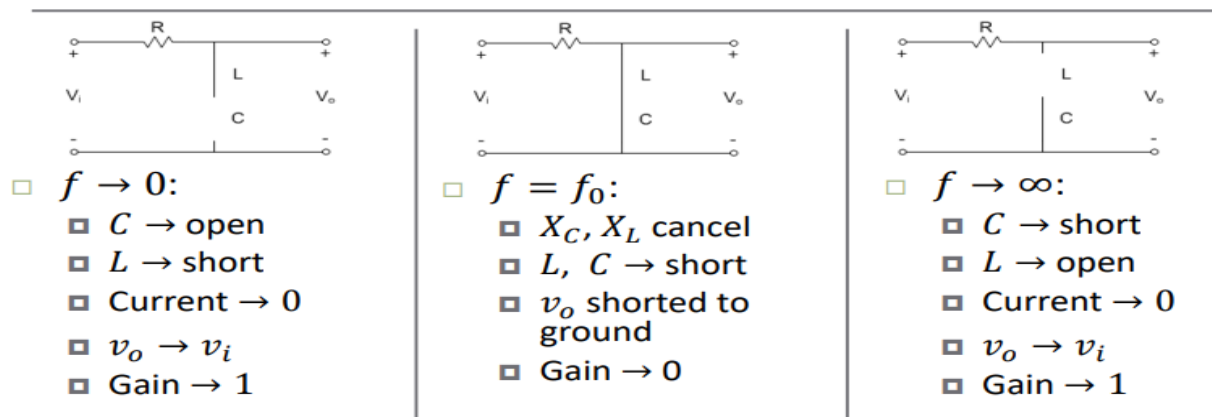


Figure I-13: The filter behavior at its three limiting cases for frequency.

The general form of the frequency response function in terms of ω_0 and Q is then:

$$\Gamma(\omega) = \frac{\omega_0^2 - \omega^2}{\omega_0^2 + j\omega \frac{\omega_0}{Q} - \omega^2} \quad \text{I-27}$$

With the resonant frequency $f_0 = \frac{1}{2\pi\sqrt{LC}}$ is and the Quality factor is $Q = \frac{1}{RC\omega_0} = \frac{\omega_0 L}{R}$.

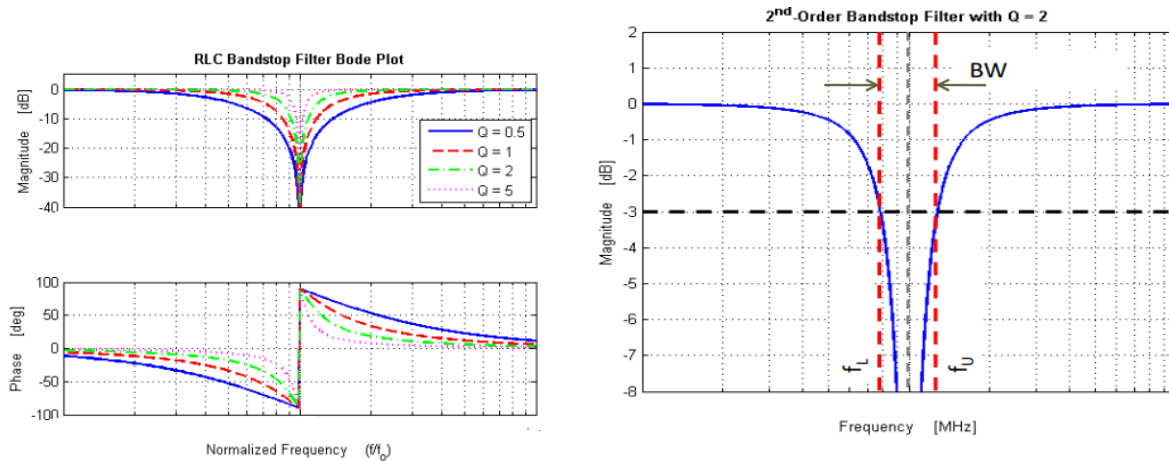


Figure I-14: the frequency response of band stop filter (note that all 2nd order band stop filters provide same response as function of Q and ω_0)

I.9 Active filter

Active filters include at least one active gain component such as transistor, or operational amplifier. It is essentially about an amplifier circuit whose frequency response is regulated by the phase-shifting elements both in the direct circuit and in the negative feedback. As a result, they can have a total gain greater than 1 and they can amplify certain frequencies as well as cut (attenuate) them. Operational amplifiers can also be used to form or change the circuit frequency response by making the filter's output bandwidth narrower or even wider by generating a more selective output reaction.

The active filter is well suited for low amplitude and low power signals. It is therefore widely used in audio amplifiers and electronic instruments of all kinds [Bouaouina, 2018].

I.9.1 Advantages and disadvantages of active filters

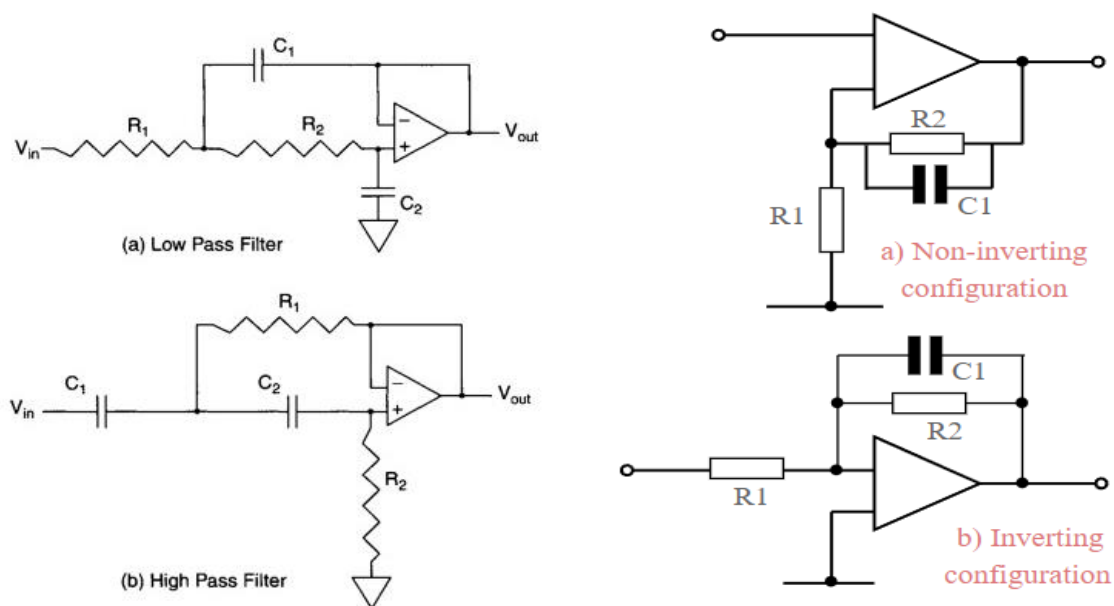
Each filter technology offers a unique set of advantages and disadvantages that make it an almost ideal solution to some filtering problems and completely unacceptable in other applications. Thus, in this section a brief overview of the most important differences between passive and active filters:

Amplifier operational (AOP) can be used to replace inductor of passive filters. Indeed, inductors, for lower frequencies, are lossy and coils of quality are difficult to manufacture, bulky, are comparatively heavy, and are not compatible with standard integrated circuit manufacturing technologies advantage of active filters in terms of cost, size and weight.

Due, among other things, to the reduction in open-loop gain of Amp-OPs at high frequencies, the use of active filters is limited to frequencies of the order of MHz at most, as instance of application audio, ultrasonic, instrumentation. Beyond that, the passive RLC circuits are used again, and the coils are then easier to integrate in smaller size at high frequency.

I-9-2 Active Low Pass Filter

The active filter which permits only low-frequency components and denies all other high-frequency components, it is called Active Low Pass Filter. It is essentially equipped with an operational amplifier and powered by a symmetrical voltage and passive components to ensure the feedback. An example given by Figure I.15 illustrates this type of filter. The input to the operational amplifier is high impedance signals, which produces a low impedance signal as output.



High and low pass filter using a 2-pole Salen-Key topology

Single pole low pass inverting & non-inverting configurations

Figure I-15: Simple active filters, using a 2-pole Salen-Key topology.

It is suitable to use the switched capacitor filter type to avoid the use of external components (as they are with op amp active filters). besides, when a computer-controlled filter is required, this filter can be a good option since they can be tuned by varying the frequency of the applied clock signal, usually a digital waveform.

A switched capacitor filter is a sampled-data device, shown in Figure I-16, where an internal capacitor is switched between the input signal and an integrating amplifier (the integrator simulates a resistor). Initially, when switch s_1 is at position (a), the capacitor C_1 charges to the input voltage at that moment. Then s_1 switches to position (b) where C_1 discharges into C_2 , the integrating capacitor, via the operational amplifier. Over several switching cycles, this process is repeated, and C_2 averages the input signal voltage. The time constant of the filter depends upon the switching frequency, which determines the cutoff frequency [Austerlitz, 2003].

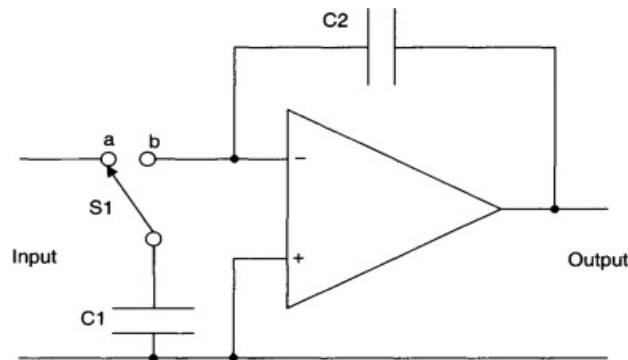


Figure I-16: Switched capacitor filter [Austerlitz, 2003].

The performance of the amplifier plays a very important factor when designing an active low pass filter. There are two primary kinds of active low-pass filters namely switched capacitor type and continuous capacitor type. The filters are available from first-order until the eighth order of design.

The frequency response of the circuit will be the same as that of the passive RC filter, except that the passband voltage gain rises the amplitude of the output signal. The bandwidth starts at 0 Hz or DC for a low pass filter and remains at -3 dB to the designated cutoff frequency. Then, the signals are attenuated above that point.

As previously mentioned, the inverse of a low pass filter is a high pass filter. Moreover, the bandpass filters combine the functionality of lowpass filters and high pass filters to only allow frequencies within a specific frequency range.

The transfer function of the filter (example: the single pole low pass inverting configuration) is expressed as:

$$\begin{cases} \Gamma(\omega) = \frac{v_o(j\omega)}{v_i(j\omega)} \\ v_o(j\omega) = \frac{R_2}{R_2 + jCR_2\omega} \times I \\ v_o(j\omega) = R_1 \times I \end{cases} \quad \text{I-28}$$

Therefore, the transfer function of this type of filter will become

$$\Gamma(\omega) = -\frac{R_2}{R_1} \cdot \frac{1}{1 + j\tau\omega} \quad \text{I-29}$$

Where $\tau = CR_2$ and $f_0 = 1/2 \cdot \pi\tau$. The frequency response of this filter is given by Figure I.17 below:

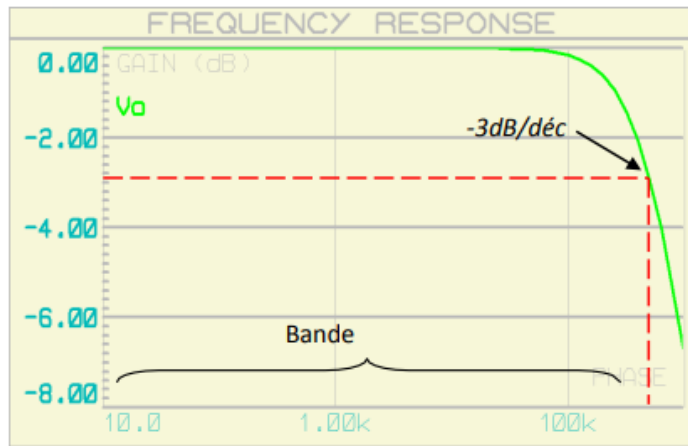


Figure I.17 Frequency response of an active low-pass filter [Austerlitz, 2003].

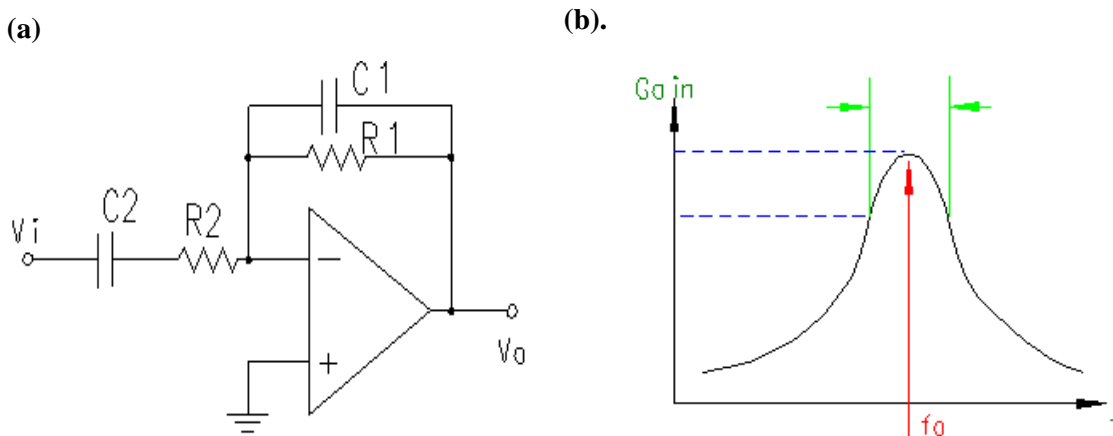


Figure I-18: A simple band pass filter with operational amplifier (a) and the transfer function response (b) [Austerlitz, 2003].

For the band-pass filter, the simplest one can be made by combining the first order low pass and high pass filters as mentioned above and an example is given by Figure I-18 (a). The attenuation happens for low frequencies ($\omega \ll \frac{1}{R_2 C_2}$) and high frequencies ($\omega \gg \frac{1}{R_1 C_1}$), and the signals pass within intermediate frequencies with a gain of $\frac{R_1}{R_2}$. However, to make a filter with a very narrow band, it is required a more complex filter.

For a second-order band-pass filter the transfer function is given by

$$\Gamma(\omega) = \frac{v_o(j\omega)}{v_i(j\omega)} = \frac{j\omega\Gamma_0.BW}{-\omega^2 + j\omega.BW + \omega_0^2} \tag{I-30}$$

Γ_0 is the maximum amplitude of the filter when $\omega = \omega_0$. Often the transfer function equation is written in terms of the quality factor, Q. Thus, quality factor of a filter goes up as it becomes narrower and its bandwidth decreases as represented on Figure I-18 (b). Another type of active pass filter is Rauch filter Figure I-19, its characteristics are given as follows:

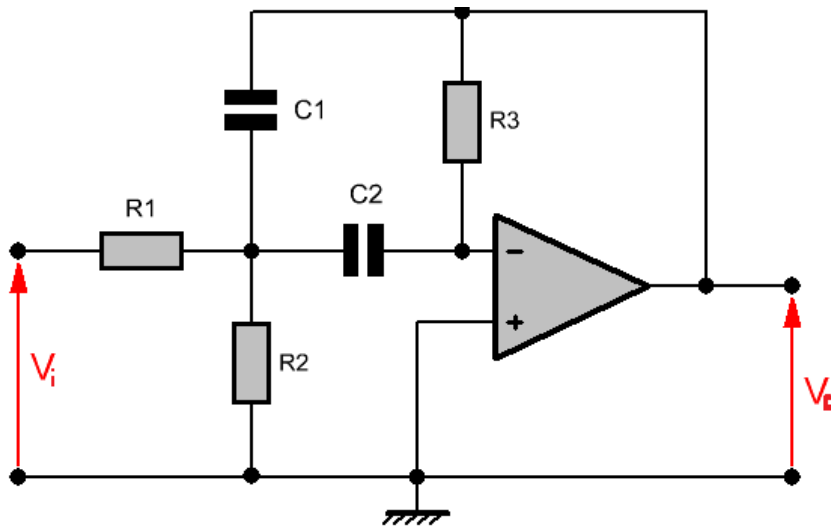


Figure I-19: Band pass filter type Rauch [Austerlitz, 2003].

$$\Gamma(\omega) = \frac{v_o(j\omega)}{v_i(j\omega)} = \frac{Y_1 Y_3}{Y_3 Y_4 + Y_5 (Y_1 + Y_2 + Y_3 + Y_4)} \tag{I-31}$$

With $Y_1 = \frac{1}{R_1}$, $Y_2 = \frac{1}{R_2}$, $Y_3 = jC_2\omega$, $Y_4 = jC_1\omega$ and $Y_5 = \frac{1}{R_3}$

Then

$$\Gamma(\omega) = \frac{\frac{jC_2\omega}{R_1}}{-C_1C_2\omega^2 + \frac{1}{R_3}\left(\frac{1}{R_1} + \frac{1}{R_2} + jC_2\omega + jC_1\omega\right)} = \frac{\frac{jC_2\omega}{R_1}}{-C_1C_2\omega^2 + \frac{R_1+R_2}{R_1R_2R_3} + j\omega\left(\frac{C_2+C_1}{R_3}\right)} \quad \text{I-32}$$

So, if $C_1 = C_2 = C$, then:

$$\Gamma(\omega) = \frac{j\omega\frac{C}{R_1}}{-C^2\omega^2 + \frac{R_1+R_2}{R_1R_2R_3} + 2j\omega\left(\frac{C}{R_3}\right)}$$

$$\Gamma(\omega) = -\frac{R_3}{2R_1} \cdot \frac{2 \cdot j\omega\frac{R_1R_2}{R_1+R_2}C}{1 - C^2\omega^2 \cdot R_3\frac{R_1R_2}{R_1+R_2} + 2j\omega\left(\frac{R_1R_2}{R_1+R_2}C\right)}$$

$$\text{Hence } \Gamma_0 = -\frac{R_3}{2R_1}, \omega_0 = \frac{1}{C} \sqrt{\frac{R_1+R_2}{R_1R_2R_3}} \text{ and the band width } BW = \frac{2}{CR_3},$$

The previous types of filters were named as per their functionalities of operation. Based on technical design specifications there are four classical analogue filter types such as Butterworth, Chebyshev, Bessel and Elliptic filters. Each filter is convenient in some areas but poor in others. They have their own unique characteristics and hence they have been chosen for different applications.

-Butterworth filter is a flatten pass band, moderate phase distortion but has a poor roll of rate.

-Chebyshev filter has ripple in its pass band and better roll off (steeper) rate. In addition to the ripples and with comparison to the Butterworth, Chebyshev filter is characterized by sharper transition band and poorer group delay.

-For Bessel filter, has the worse roll off rate among the other filters but the best phase response, knowing that the filter with poor phase response will react poorly to a change in signal level

As represented on the last figure I-20, when square wave (non-sinusoidal waveform) is applied to the input to Butterworth low pass filter it results into distortion. Which result in an output waveform having ringing and overshoot.

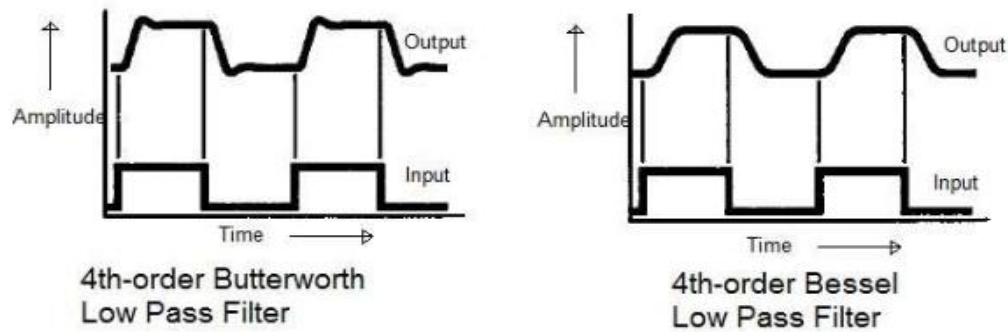


Figure I- 20: The frequency response (gain as function to time) of Butterworth.vs. Bessel filter [Austerlitz, 2003].

This is due to the fact that component frequencies of square wave will shift in time versus to each other (delay in the output signal by certain constant time period) due to the linearly increase of the phase with frequency.

In addition, that Bessel filter avoids the situation mentioned above, it introduces a linear phase shift with respect to frequency. Hence it acts as a delay line having low pass characteristics. And as it can be depicted from the last figure, the output waveform will not have any ringing and overshoot as it is the case for Butterworth and where high frequency harmonic components are present in the input waveform, Bessel filter round off the input square wave.

Elliptic filter has same pass and stop band ripples at amplitude response with the steepest roll off rate (cutoff slope is sharper) and it has a nonlinear phase response.

So, the best-known filter approximation is the Butterworth (maximum flat response) exhibits a nearly flat passband with no ripple. The roll-off is smooth and monotonic with a low pass or high pass roll-off of 20 dB/decade for every pole.

Chebyshev at its turn, the response is a mathematical strategy for achieving a faster roll-off by allowing ripples in frequency response. Even if increasing the unwanted ripples leads to a sharper roll off, this makes the Chebyshev response an optimal trade-off between these two parameters. Chebyshev filter is called Chebyshev type-1 one when the ripples are only in the passband and type-2 when they are present only in the stopband but are rarely used.

References of Chapter I

- [Andreas, 2006] Andreas Antoniou, “Digital Signal Processing”. PhD thesis, London University UK, 2006
- [Austerlitz, 2003] Howard Austerlitz, Analog Signal conditioning, in Data Acquisition Techniques Using PCs 2nd Edition, 2003
- [Bouaouin, 2018] Bouaouin Belouadah ‘ ‘ étude et conception d’un filtre RF pour des applications en télécommunications’, Master thesis, Tlemcen university, 2018
- [Chen, 2009] Wai-Kai Chen, “Passive, active, and digital filter”. Handbook, 2009
- [Fourniols and Escriba] Jean-Yves Fourniols and Christophe Escriba, ‘ système électronique analogiques Amplification, filtrage et optronique’
- [Hunter, 2006] Ian Hunter, ‘Theory and Design of Microwave Filters,’ IET electromagnetic Waves Series 48, 2006
- [Khireddine, 2019] Khireddine Hana, Etude et conception d’un filtre RF ULB pour des applications en télécommunications, Master thesis, 2019
- [REDL et al, 1995] REDL S.M., WEBER M.K. and OLIPHANT M.W.: ‘An introduction to GSM’, Artech House, Norwood, MA, pp.71-75, 1995
- [Les Thede, 2004] Les Thede,” Practical Analog and Digital Filter Design”. Book, 2004
- [WINDER, 2002] Steve Winder, “analog and digitalfilter design Second Edition”. 2002

II-1 Introduction

As crucial components in a wide variety of electronic systems, microwave filters are used in cellular radio, satellite communications, radar. Their specifications are generally stringent, frequently approaching the limit of what is theoretically realisable in terms of frequency selectivity and phase linearity. And their design is specific in which it uses network synthesis, where it is possible to apply systematic procedures to go from a specification to a final theoretical design. This is the contrary of the majority of engineering disciplines which tend to utilize analysis-based design rules.

As a necessary requirement for network synthesis skills, an exhaustive knowledge of the circuit theory of passive networks. But, knowledge of network synthesis is not enough to design filters. The designed structure provides a modular network that can then be transformed into a variety of microwave networks, plus TEM transmission lines, waveguides, and dielectric resonator realizations. Consequently, it is also necessary to have reasonable leeway knowledge of the electromagnetism properties of these filters.

Fifth-generation (5G) is the novel future wireless devices communication where numerous licensed frequency bands are allocated for the 5G communication systems in different parts of the global as shown in figure II-1.

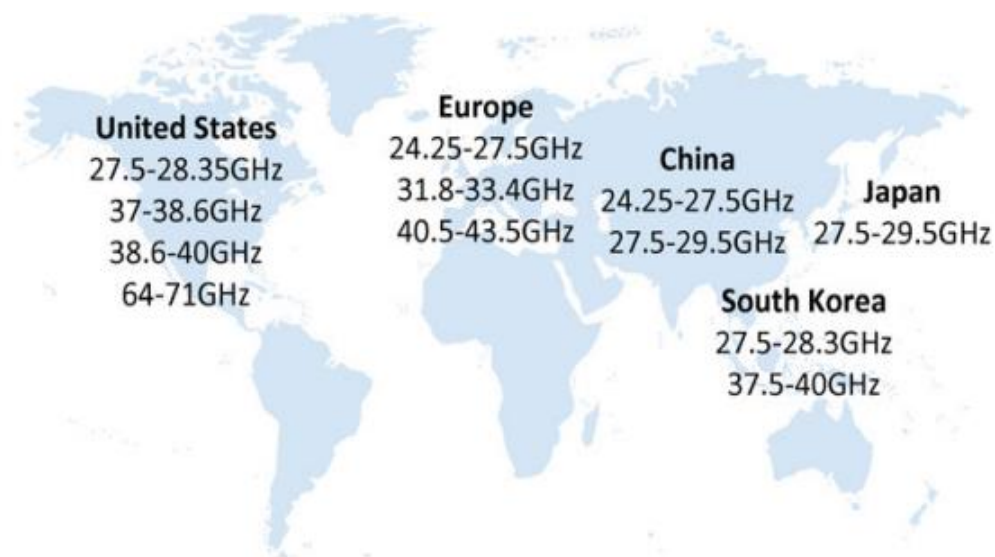


Figure II-1: The mm-wave frequency bands allocated in different part of the world for future 5G wireless communication systems [Hu et al, 2017].

The most popular bands for the 5G spectrums are the frequency spectrums 26-29, 36-39, and the sub-six spectrums [Wang, 2014]. The easy fabrication, the multiple bands covering and the compactness are the most interesting features of 5G millimeter wave devices, such as filters, antennas, and power dividers [Choudhury et al, 2018] Radio frequency filters are one of the most applicable components in communication systems.

filters have structures such as stepped impedance resonators, parallel coupled lines and multimode resonators [Choudhury et al, 2018]. Some proposed filters are investigated in order to improve their characteristics such as a dual-band filter with high rejection at the stopband and low bandwidth (BW) [Leu et al, 2018]. A low-pass filter with high BW rejection of 1.1 GHz on the stopband [Kumar and Karthikeyan, 2018]. A band-pass microwave filter with a single band and adequate BW [Chen et al, 2009]. Those filters work in the microwave bands. However, in the 5G mm-wave bands, rare researches for mm-wave filters compared to the lower microwave band are available [Syrtsin et al, 2018; Bowrothu and Zhang, 2018; Shaman et al, 2014; Yang et al, 2018]

This chapter has evolved from a series of readings on filters and its physical, structural and electrical properties in order to design the 5G filter. The purpose of this section is to provide a convenient source for filters design, types and their advantages. Also, comparisons of filters are given based on their Transmission lines model and their structures.

II-2 Electromagnetic field and Transmission Line theory

In fact, the electric charges create electric fields (E) and by moving, they establish electric currents (I), which induce magnetic fields (B) that loops around. However, James Clerk Maxwell observed that there is another way to create electric field besides having charges and another way to create magnetic field besides having a current. Which is by changing the electric field in space, it creates a magnetic field, and verse versa. Consequently, a time-space varying electric field produces a varying magnetic field at right angles to it, and the time-space varying magnetic field in its turn produces an electric field at right angles to it. This remains establishing oscillations of magnetic and electric field components, so, they are coupled in a way that they behave like waves known as electromagnetic waves as shown on figure II-1-a.

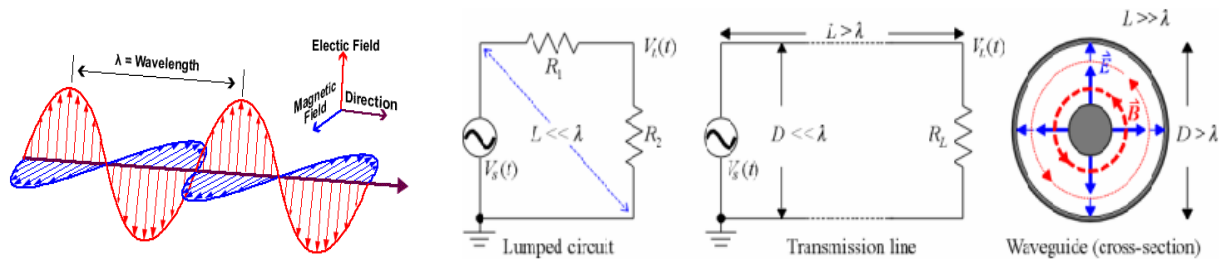


Figure II-1: a-Electromagnetic wave in space b- Schematic diagram of different types of EM problems [Yang, 2018]

Any structure or media, figure II-1-b, that enables transfer of energy or information between two points (in term of circuits, it is the wires) is transmission line (TL). This means that transmission lines are wave-guides where they guide electromagnetic signals from a sending point to a receiving point. Thus, this TL theory bridge the gap between the EM field analysis and circuit theory.

The fundamental difference between the circuit and transmission line theory is the electrical size where it is assumed that in circuit the electrical length is considerably greater than the physical length while in TL is not true. Table II-1 gives a quick comparison among EM problems.

Conditions	theory	Unknowns	Math tool	Description
$L \ll \lambda$	Lumped circuits Kirchhoff's laws	$V(t)$ $I(t)$	Ordinary differential equation (ODEs)	All points react to the source instantly
$L > \lambda, D \ll \lambda$	Transmission lines Kirchhoff's laws	$V(z, t)$ $I(z, t)$	Partial differential equations (PDEs)	Delay along the longitudinal (z) direction exists
$L \gg \lambda, D > \lambda$	Waveguides Maxwell's equations	$\vec{E}(x, y, z, t)$ $\vec{H}(x, y, z, t)$	Full vectorial PDEs	Delay along the longitudinal (z) and transversal (x, y) directions exist

Table II-1: A comparison among EM [Yang, 2018]

The TLs are fraction of wavelength or several wavelengths long, so it results in a distributed parameter network and the voltage and currents vary in magnitude and phase over its length (Figure II-3-a).

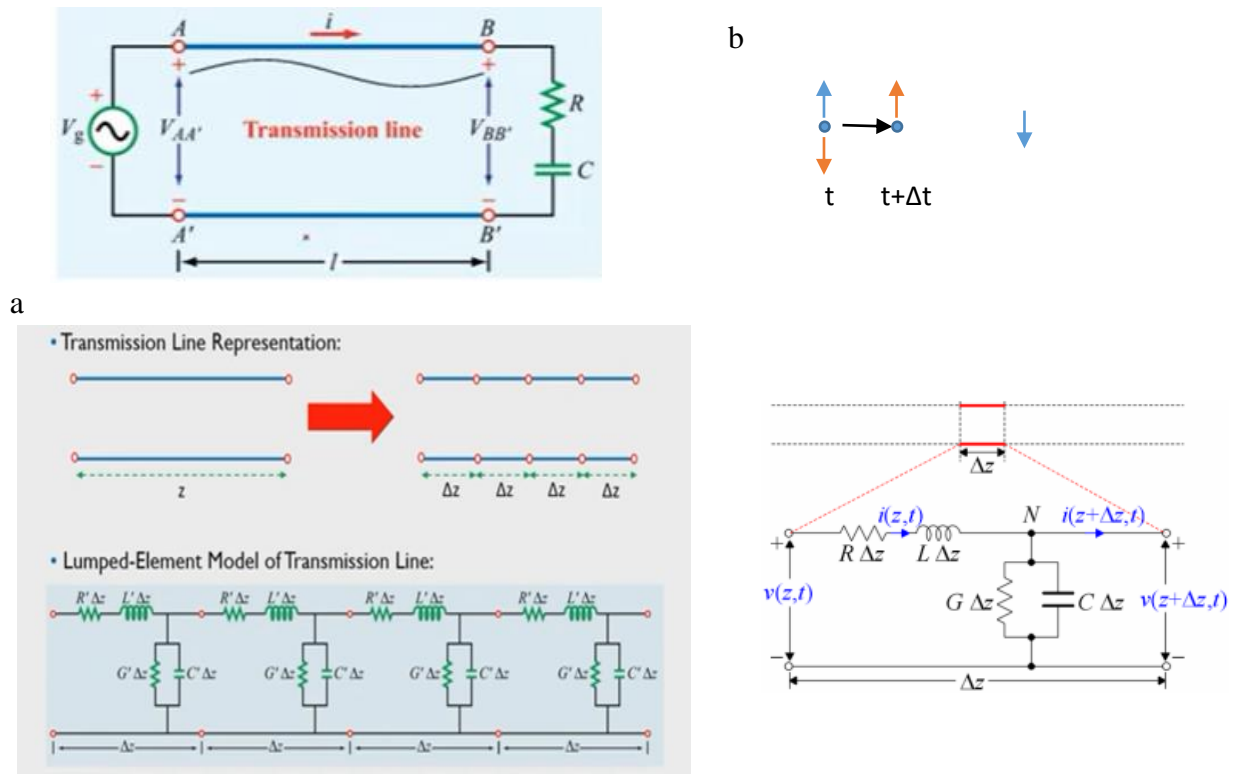


Figure II-2: a-Representation of transmission line and its lumped element model. b- the phase and magnitude of voltage and current changing over the length. c- electric field changing in time [Yang, 2018]

As represented in figure II-3-a, the voltage $V_{AA'}$ is different to $V_{BB'}$, this is due because of the electrical and magnetic fields are traveling over space and depending on how fast the magnitude of electric field is changing (figure II-3 b). At some times it can be pointed up (or down) and after Δt , the electrical field travels to another point (with another direction) which is true in TL too.

The voltage is frequency dependent and it takes time to travel from one point to another. That means if the frequency is low, the voltage travel without being changing at the other point ($V_{AA'}$ is approximately equal to $V_{BB'}$) which is the basis for circuit theory. However, for a very fast voltage, it already changes in polarity but the wave has not traveled yet a significant distance before the voltage has shifted. Consequently, it seems like the voltage (traveling voltage wave) is traveling from A to B along the transmission line. Therefore, to derive how fast the voltage travels and how it behaves, the figure II-3-c is considered, where the transmission line is breaking into small part (Δz). The changing in voltage over Δz is very small where the TL is represented by lumped element model of transmission line. It is a series RL and in a parallel (R/G)C circuit,

these elements are the characteristics of the TL (per unit length) and explained in Appendix A. Thus, it is distributed evenly over the whole TL.

Two types of transmission lines are common, the coaxial line and microstrip line as shown in figure II-4. They are illustrations of transverse electromagnetic (TEM) transmission lines. A TEM line uses a single electromagnetic wave (mode) having and magnetic field vectors in perpendicular directions to the axis of the line, as shown in Figures II-4-b.

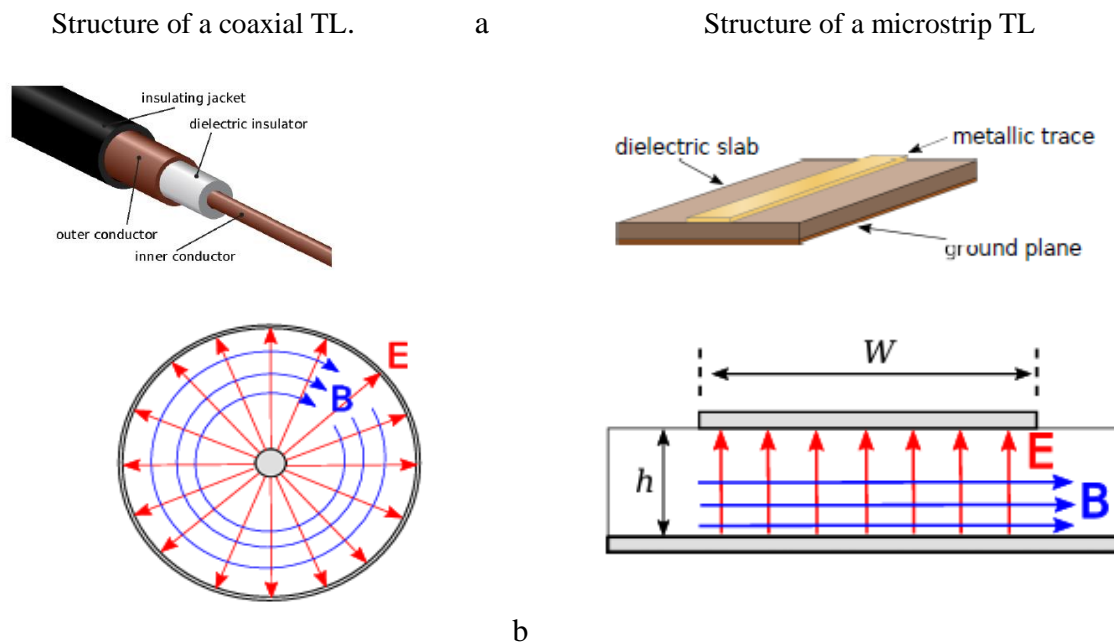


Figure II-4: types of transmission lines structure and the electric and magnetic fields within transmission lines [Ellingson, 2018]

TEM transmission lines generally appear in radio frequency applications. Knowing that not all transmission lines exhibit a TEM field structure. In non-TEM transmission lines, the magnetic and electric field vectors can be not perpendicular to the axis of the line, and the structure of the fields is more complex compared to the TEM lines field's structure. The waveguide is a case where a transmission line has a non-TEM field structure. Waveguides are the most dominant at radio frequencies and tend to appear in applications where it is important to achieve very low loss or when power levels are very high. Another example is the common "multimode" optical fiber. The optical fiber presents a complex field since the wavelength of light is quite short compared to the cross-section of the fiber, which makes excitation and propagation of non-TEM waves hard to escape. This problem is overcome by using single-mode fiber but it is considerably difficult and expensive to manufacture.

II-3 Transmission line characteristics

Taking into consideration figure II-4-c right, the study and the analysis of transmission line is fully studied in Appendix A. some interesting and useful characteristics of transmission line needed in filter analysis are summarized under the table II-2.

By using the equivalent circuit, analysis of electric and magnetic vector fields is substituted by that of scalar voltage between and current along the line, significantly simplify the process. Applying Kirchhoff's voltage and current laws at $\Delta z \rightarrow 0$, the two first-order PDE are obtained for the current and voltage which form the system of telegrapher's equation (Table II-2).

the telegrapher's equations in phasor Table II-2, has the main advantage over the time-domain versions where only derivatives with respect to distance remain which greatly eases the equations.

The characteristic impedance or surge impedance of a uniform transmission line, habitually written Z_0 , and it is the ratio of the amplitudes of a single pair of voltage and current waves propagating along the line in the single direction. Nevertheless, if two counter-propagating waves coexist, it can not be constant given in Table II-2. For microstrip line, the expressions Z_0 directly in terms of h/W and ϵ_r are used also given in Table II-2.

The propagation constant γ (m^{-1}) considers the effect of materials, geometry, and frequency in determining the variation in potential and current versus distance on a TEM transmission line (Table II-2). It is equal to $\gamma = \alpha + j\beta$, where β is the $\text{Im}(\gamma)$ (rad/m) and expresses the rate at which phase changes as a function of distance and. The real part α (1/m) is the attenuation constant, and it is the rate at which magnitude diminishes as a function of distance.

To define the lossless or low loss transmission lines. First recall that loss refers to magnitude reduction during the wave propagation. In the lumped-element equivalent circuit model, the parameters R' and G' of the represent physical mechanisms associated with loss.

Indeed R' represents the resistance of conductors, where G' represents the unwanted current induced between conductors through the spacing material. And by using the propagation constant equation given in Table II-2, the low loss is attributed to the conditions $R' \ll \omega L'$ and $G' \ll \omega C'$

and $\gamma = j\omega\sqrt{L' C'}$, thus $\alpha \approx 0$ and $\beta \approx \omega\sqrt{L' C'}$ and $Z_0 \approx \sqrt{\frac{L'}{C'}}$ and for the line strictly lossless line $R' = G' = 0$.

The phase velocity v_p represents the speed at which a point of constant phase travels along the transmission line.

The voltage reflection coefficient Γ , given in table II-2, determines the magnitude and phase of the reflected wave given the incident wave, the characteristic impedance of the transmission line, and the terminating impedance.

When there are waves moving in opposite directions, the concept of standing wave (SW) is made up. These waves add up to create a different variation in amplitude with distance that does not vary with time. Their period is $\lambda/2$ (one half of a wavelength). The standing wave ratio may also be calculated by taking the line's terminating impedance and the line's characteristic impedance, and dividing the higher of the two values by the smaller and in terms of potential it is $SWR = \text{maximum}\tilde{V} / \text{minimum}\tilde{V}$.

Telegrapher's equations	$\begin{cases} -\frac{\partial v(z,t)}{\partial z} = R' i(z,t) + L' \frac{\partial i(z,t)}{\partial t} \\ -\frac{\partial i(z,t)}{\partial z} = G' v(z,t) + C' \frac{\partial v(z,t)}{\partial t} \end{cases}$ $\Delta z \rightarrow 0$
Telegrapher's equations in phasor	$\begin{cases} -\frac{\partial \tilde{V}(z)}{\partial z} = [R' + j\omega L'] \tilde{I}(z) \\ -\frac{\partial \tilde{I}(z)}{\partial z} = [G' + j\omega C'] \tilde{V}(z) \end{cases}$
Propagation constant $\gamma (/m)$ $\gamma = \alpha + j\beta$	$(\sqrt{R' + j\omega L'}) (G' + j\omega C')$
Characteristic impedance (Ω) $Z_0 = \sqrt{R' + j\omega L'} / (G' + j\omega C')$	$Z_0 \approx \frac{60\Omega}{\sqrt{\epsilon_r}} \ln \frac{b}{a}$ low loss - Coaxial line
	$Z_0 \approx \frac{42.4\Omega}{\sqrt{\epsilon_r + 1}} \times \ln \left[1 + \frac{4h}{W'} \left(\Phi + \sqrt{\Phi^2 + \frac{1 + \frac{1}{\epsilon_r} \pi^2}} \right) \right]$ <p>where $\Phi = \frac{14 + 8/\epsilon_r}{11} \left(\frac{4h}{W'} \right)$ Microstrip Line</p>
The phase propagation constant $\beta = \omega \sqrt{\mu\epsilon}$.	$\omega \sqrt{\mu_0 \epsilon_{r,eff} \epsilon_0}$ Microstrip Line
	$\omega \sqrt{L'C'}$ Coaxial line
The phase velocity $vp = \frac{\Delta z}{\Delta t} = \frac{\omega}{\beta} = \lambda \cdot f$ With $\lambda = \frac{2\pi}{\beta}$	$\approx \frac{1}{\sqrt{L'C'}} = \frac{1}{\sqrt{\mu_0 \epsilon_0 \epsilon_r}}$ Coaxial line
	$\frac{c}{\sqrt{\epsilon_{r,eff}}}$ Microstrip line
voltage reflection coefficient	$\Gamma = \frac{Z_L - Z_0}{Z_L + Z_0}$
The input impedance (The transmission line -open or short-circuited)	$Z_{in}(l) = Z_0 \frac{1 + \Gamma \cdot e^{-j2\beta l}}{1 - \Gamma \cdot e^{-j2\beta l}}$

Table II-2: The main equations and characteristics of Transmission line (Coaxial line or Microstrip Line) see Appendix A.

II-4 On the way to 5G and Internet of Things (IoT)

The evolution of mobile communication has a deep impact on the daily life of millions of people all over the world. In just a few decades, we have witnessed a revolution in the way people communicate, share ideas and live. The table II-3 summarizes the differences and history over communication networks generations. This evolution is still happening and will continue in the future.

Generation	Differences
1G	The 1980s carried the first generation of networks with voice-only, analog service. The maximum data transmission speed on a 1G network reached about 2.4 kbp.s.
2G	Started in Finland in 1991, letting mobile phones to go digital. Encryption of calls and text messages, SMS, picture messages and MMS is possible. The maximum speed of the second generation was about 50 kbps.
3G	The emergence of a 3G network started in 1998. It offers the user the ability to simultaneously transfer data and voice over the same network in the form of instant messaging, emails and downloads. 3G is the heir of 2G, and it offers relatively better broadband capacity and supports a larger customer base for data and voice at a much lower incremental cost. 3G networks reach 2 Mbps on fixed or stationary devices and 384 kbps on devices in moving vehicles.
4G	The current standard for cellular networks, came out in the late 2000s, 500 times faster than 3G. It was able to support more than high definition mobile TV, video conferencing. When a device is in motion, such as walking when using the phone or in a car, the maximum speed can be 10s of Mbps, while when the device is stationary, it can be hundreds of Mbps. The 20 MHz bandwidth sector has a maximum capacity of 400 Mbps. However, since users share available sector capacity among others, users' observable speed experiences are usually 10-100 Mbps. As more people gain access to mobile devices and the IoT expands, up to 24 billion devices are expected to need cellular network support by 2024. is where 5G comes in.

Table II-3: The differences and history over communication networks generations

Nowadays, people are able to use mobile devices to connect to the internet due to 3G and 4G. This phenomenon is stated as people-to-thing communication. Aiming to connect people and objects everywhere at anytime, the Internet of Things (IoT) is upcoming-happening. So, the key catalyzer of the IoT is the 5G and the subsequent trend of the previous generations. Its full deployment was anticipated during 2020 [Onoe, 2020].

The requirements for this technology are exposed in Figure II-5-a, and comparing them to 4G. conjointly to conventional requirements for higher data rate and spectrum efficiency, connection density, area traffic capacity, and latency become key characteristics [Reynaert et al, 2017]. Besides, these specifications must be respected while obtaining 100 times better network efficiency [ITU-R, 2015].

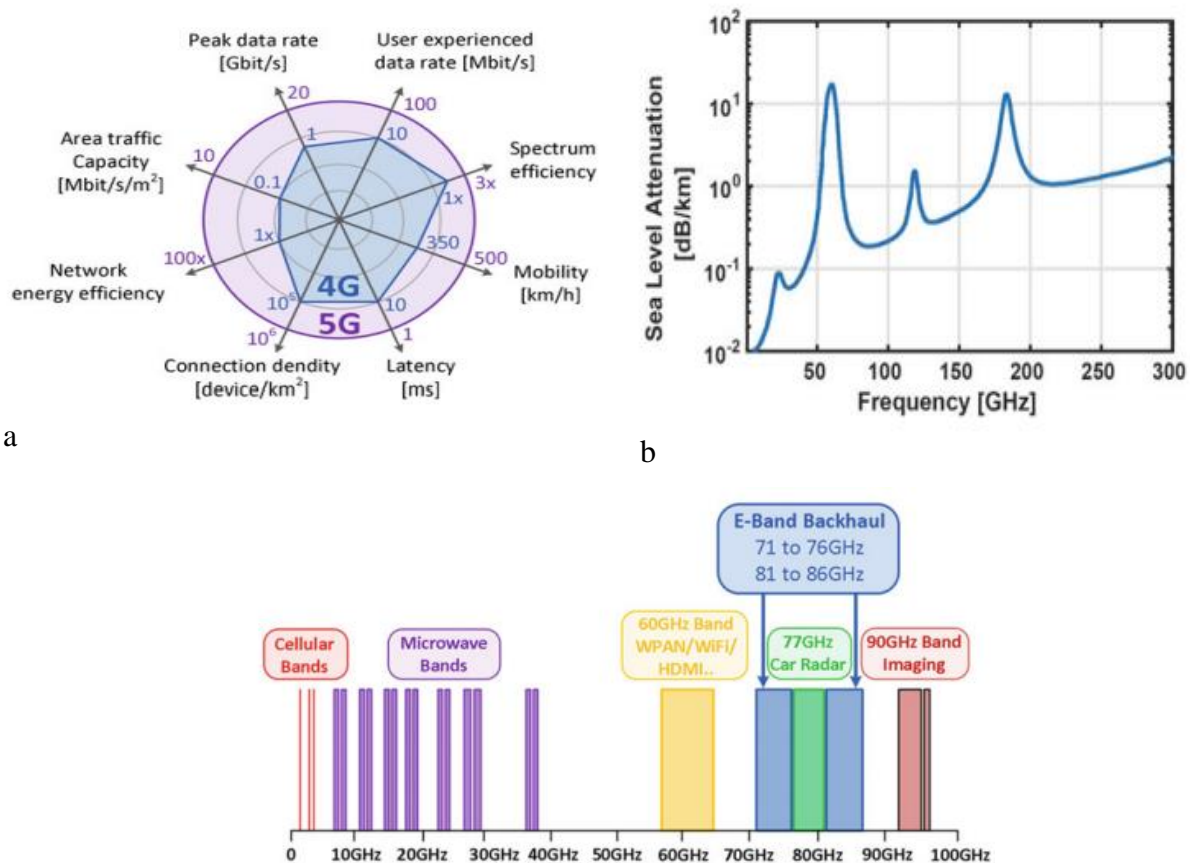


Figure II-5: a-5G requirements and comparison against 4G [ITR-R, 2015; Reynaert et al, 2017]. b: Sea level attenuation against frequency. c: Major spectrum allocation in the United States [Reynaert et al, 2017]

5G will allow better healthcare, smart objects and safer transport, additionally improving the quality of life. The IoT consequently, requires a low-cost, low-power technology, to enable every object around us to become smart while requiring a small battery or no battery. In fact, for mass-production digital circuitry, the CMOS technology is privileged for these same reasons. The scaling of CMOS technology has followed Moores law for over 50 years. Each new generation makes it possible to integrate more transistors (means more functions) in the same area (so at the same cost), while reducing consumption. therefore, CMOS acts a key role in the IoT [Holt, 2016].

Along with this win-win relationship between lower cost and lower power, at each technology node the MOS transistors get faster. So digital processors take full advantage of scaling technology, but what about analog design in advanced CMOS?

II-5 mm-Wave Spectrum, Challenges and Opportunities

In order to reach the performance summarized in Fig. II-5-a, the 5th generation needs should be a leap forward over 4G which is not conceivable to accomplish by a simple incremental advance on previous technologies. The fundamental limit of the channel capacity (C) as function to channel bandwidth (BW) was demonstrated [Shannon, 1948] as follows:

$$C = BW \log_2(1 + SNR) \quad \text{II-1}$$

where the signal-to-noise ratio SNR . This is why industries and research institutes are pushing towards solutions at higher frequencies, where more bandwidth is accessible. But, the need for higher frequency faces many challenges. The transmitted signal undergoes attenuation in free space (so-called free space path loss, FSPL) is expressed as

$$FSPL = (4\pi df/c)^2 \quad \text{II-2}$$

where d , f c are the distance, the frequency, and the speed of light respectively.

However, as the frequency goes higher, the loss follows it, also the signal will propagate through air which is not in free space. The resulting attenuation at sea level is shown in Figure II-5-b where the oxygen O_2 in the atmosphere causes a clear peak at 60 GHz, followed by an atmospheric window between 70 and 90 GHz. The different propagation characteristics of the medium are the reason for allocating specific services in certain parts of the spectrum.

So, the 5G is again be compatible to 3G and 4G, and benefits from similar technology and solutions. Also, to increase further the data rate, mm-Wave frequencies will be a major development from to the previous technologies [Onoe, 2020]. Figure II-5-c shows that the 57-66 GHz channel is kept to high-speed short range wireless communications. The high atmospheric absorption of ≈ 12 dB/km allows the coexistence of many different WPAN, WiFi and HDMI services in a small area. These wireless personal area networks will not be able to extend their signals through the domestic walls, making interference from a network operating at the same frequency in the next room minimal [Reynaert et al, 2017]. The two bands of 5 GHz each from 71 to 76 GHz and 81 to 86 GHz are reserved for backhauling systems. Taking advantage from low atmospheric attenuation (<0.5 dB/Km), these systems could deliver multi Gb/s links to extend or replace fiber along short to medium distances [Wells, 2010]. The extended frequency range from 77 to 81 GHz is designated for automotive radar applications. These radars will make Advanced Driver Assistance Systems (ADAS) reality, significantly improving the safety on the roads [Reger, 2016]. All of these applications will benefit from a fully integrated, low-power, low-cost CMOS solution.

However, strong scaling of the technology, the high-frequency analog front-end faces serious challenges. Figure II-6-a, shows the cut-off frequency as function of minimum channel length [Sansen, 2015]. In fact, each technology node has a clear advantage in terms of speed. Although in sub-micron deep technology, the velocity saturation effect also becomes dominant at moderate values of the Inversion Coefficient (IC), reducing the slope by 20 to 10 dB/dec. Figure II-6-b, illustrates two main challenges facing any analog designer at mm-Wave frequencies.

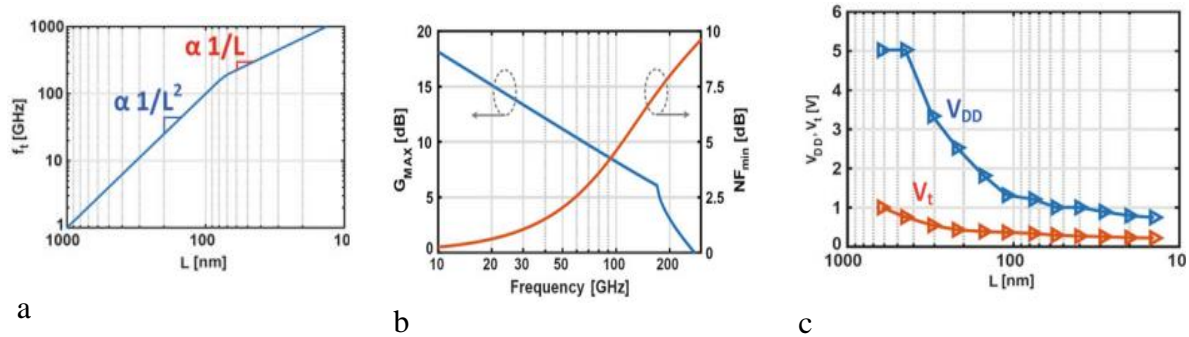


Figure II-6: a- Cut-off frequency versus channel length [Sansen, 2015; Reynaert et al, 2017]]. b- $G_{MAX}(f)$ and $NF_{min}(f)$ of a single transistor ($W/L=1.05 \times 24 \mu\text{m}/28 \text{ nm}$) common source amplifier .c- V_{DD} and V_t against minimum channel length [ITRS; Vigilante and Reynaert, 2017]

The circuit noise figure is defined as the signal-to-noise ratio at the input to the signal-to-noise ratio at the output [Razavi, 2011] and it is a measure of excess noise produced by the circuit.

$$NF = \frac{SNR_{IN}}{SNR_O} = \frac{N_O}{G \cdot N_{IN}} \quad \text{II-3}$$

N_{IN} and N_O are the noise power at the circuit input and output, and G is the gain of the circuit. At higher frequencies the transconductor exhibits lower gain and consequently the noise figure increases (Figure II-6-b). Thus, in one side transistors become faster, but on the other side at higher frequencies the performance degradation will impact seriously the circuit design. Besides, to guarantee reliability while the minimum channel length aggressively scales, the supply voltage must follow. This tendency is obviously shown in Figure II-6-c.

- (1) The phase noise in a voltage-controlled oscillator (VCO) is relative to the carrier power, which in turns is proportional to the supply voltage (for any oscillator topology).
- (2) The maximum output power that a power amplifier (PA) is able to deliver, is also proportional to V_{DD} (for any PA topology).
- (3) The number of devices that can be stacked to realize a cascode amplifier and/or a current source is limited by V_{DD} and V_t , and the latter can not scale as much (Figure II-6-c).

However, the more frequency increases, the smaller the antenna feature size of. The mm-Wave spectrum therefore not only enables the use of on-chip antennas, but also antenna arrays with a large elements count, making massive MIMO and beam forming key technologies for 5G [Onoe, 2020].

Antenna is as simple as metallic structure used as means for radiating or receiving radio waves; it is a connection of circuit to free space and consists of integrated part of any wireless communication system such as radio TV, satellite cellular Wi-Fi and more. From transmission line, a signal is sent to antenna, where the signal can be transformed into electromagnetic energy to be broadcasted through the space.

Sometimes, an electrical devices like antenna or aerial is used to change electrical power to electromagnetic signals and reciprocally. When an antenna is transmitting, it receives electrical signals from a transmission line and translates them into radio waves. The process in receiving antenna is rather opposite where it enables radio signals from the space and changes them into electrical signals, then delivers them to a transmission line.

Types of antennas (Table II-4) are selected based on size and shape. Based on the wavelength ($\lambda = \frac{c}{f}$), when the frequency increases, the size of antenna has to be reduced. Also, the radiation characteristics and application of antenna, its shape is chosen. So, these two options makes the foundation bases of antenna which are divided to, simple antenna (wire antennas, dipole, loop, ..etc), complex ones where the shaped radiation pattern (Yagi Uda antennas, aperture....etc) and the combination of identical antennas as example the phased arrays electrically shaped and steer antennas.

As frequency increase, the size of antenna has to increase too which is inconvenient for satellite as it leads to high cost, so to reduce that distinct the microstrip antenna are a kind of solution.

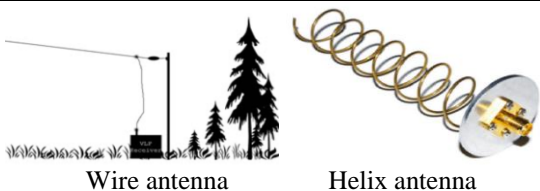
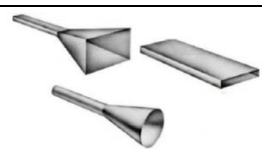
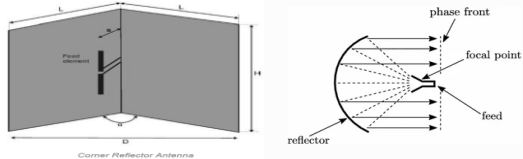
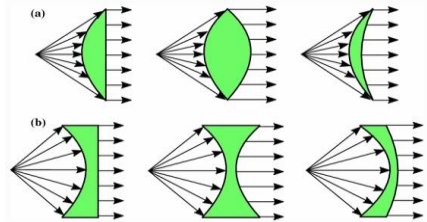
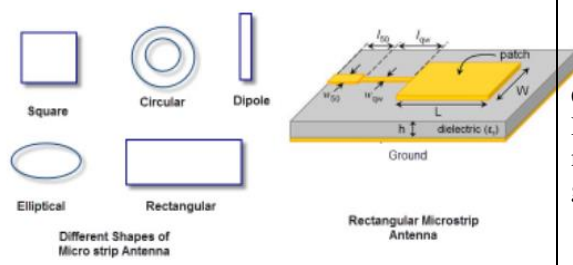
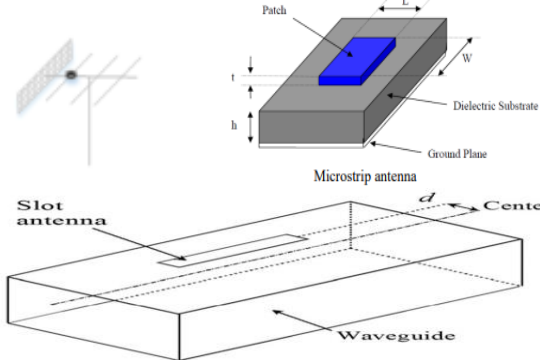
Antenna type	Shape	Examples-antenna	Applications
Wire	 <p>Wire antenna Helix antenna</p>	-Dipole -Monopole, Helix antenna, Loop	Personal applications, buildings, ships, automobiles, space crafts
Aperture		Waveguide (opening) Horn antenna	Flush-mounted applications, air-craft, space craft
Reflector	 <p>Corner reflectors - Parabolic reflectors</p>		Microwave communication, satellite tracking, radio astronomy
Lens	 <p>[Dupeez and Sinha,2016] Convex-plane, Concave-plane, Convex-convex, Concave concave lenses</p>		Used for very high frequency applications
Micro strip	 <p>Different Shapes of Micro strip Antenna</p> <p>Rectangular Microstrip Antenna</p>	Circular-shaped, Rectangular shaped metallic patch above the ground plane	Air-craft, space-craft, satellites, missiles, cars, mobile phones etc
Array	 <p>Slot antenna Microstrip antenna Waveguide</p>	Yagi-Uda Micro strip patch array Aperture array Slotted wave guide array	Used for very high gain applications, mostly when needs to control the radiation pattern

Table II-4: Different types of antennas.

II-6 Microstrip antenna

II-6-1 Microstrip structure and principle

It consists of a conducting patch and a parallel ground plane, separated by a dielectric substrate, usually fed by a microstrip line or a coaxial probe. The patch is usually made of conducting material such as copper or gold and can take any possible shape. Dielectric constant of the substrate (ϵ_r) is typically in the range 2.2 to 12 [Balanis, 2005].

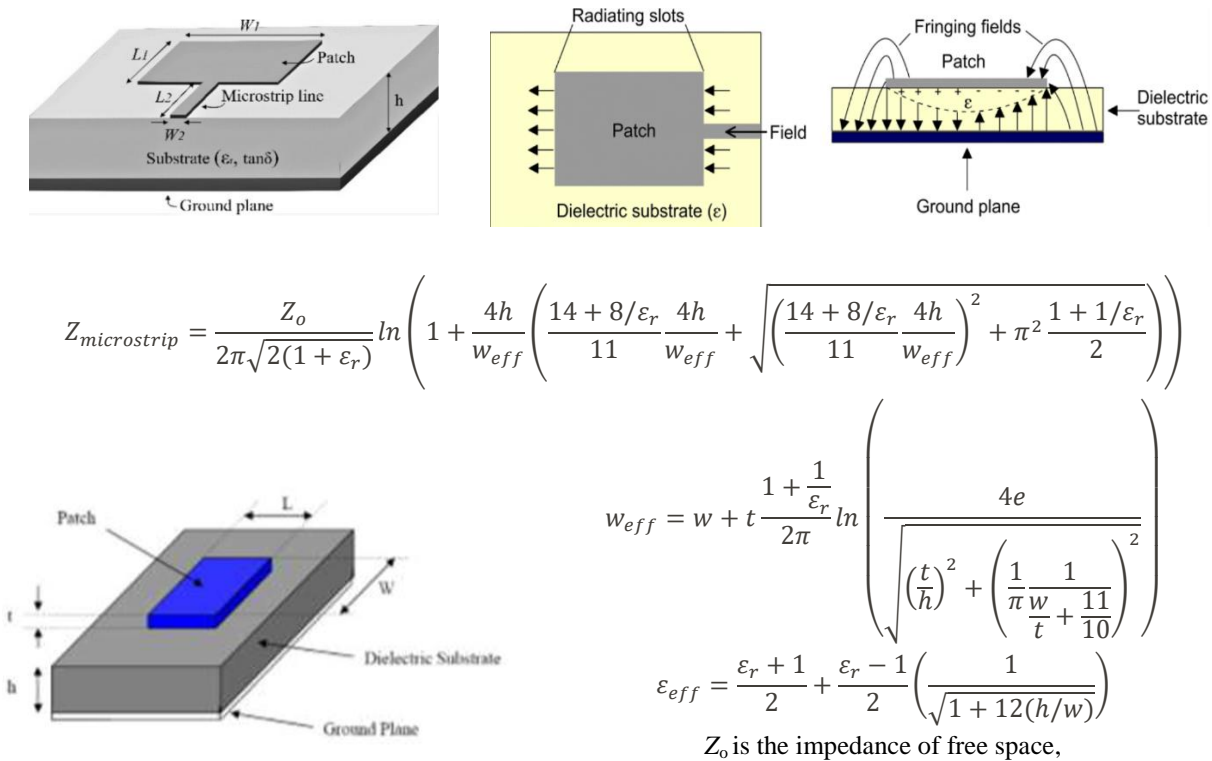


Figure II-7: Microstrip antenna, the top and side view and its radiation mechanism. The fringing field between the periphery of the patch and ground plane depend on the dimension of the patch and the high of the substrate [Chavali and Nikolova, 2019].

For advanced antenna performance, it is desirable to have a low dielectric constant with thick dielectric substrate, as it provides better radiation, better efficiency and larger bandwidth.

Transmission line model describes the microstrip antenna by two slots of width w and height h separated by transmission line of length L . Typically, the microstrip is an inhomogeneous of two dielectrics (the substrate plus the air). Most of the electric field lines locate partly in the air and rest in the substrate. As a result, the transmission line does not support transverse electric-

magnetic (TEM) mode of transmission, since the phase velocities will be different in substrate and in the air. Thus, the dominant propagation mode will be the *quasi-TEM mode*. An effective dielectric constant (ϵ_{reff}) must be obtained to account for wave propagation in the line and the fringes. The value of ϵ_{reff} must be smaller than ϵ_r , because the fringing fields across periphery of the patch were not completely included in the substrate, they also propagate in the air as shown in Figure II-7. To operate in the fundamental mode, the length of the patch must be slightly less than $\lambda/2$, where λ is the wavelength equal to $\lambda_0/\sqrt{\epsilon_{\text{reff}}}$. The TM_{10} implies that field varies by a cycle of $\lambda/2$ along the length, and width of the patch does not vary [Sandeep and Kashyap, 2012].

Thus, the microstrip patch antenna is represented by two slots, separated by a transmission line of length L and open circuited at both the ends as shown in Figure II-7 (top-right). The voltage is maximum across the width of the patch and due to the open ends the current is low. With respect to the ground plane, the boundary fields can be resolved into tangential and normal components. The electric field's normal components at the two edges along the width are in opposite directions and hence out of phase. Plus, because the patch has a length of $\lambda/2$ and so they cancel in the broad sense. Tangential components that are in phase mean that the resulting fields combine to provide a maximum radiated field normal to the surface of the structure. Therefore, the edges along the width can be represented as two radiating slots, $\lambda/2$ apart and excited in phase and radiating in the half-space above the ground plane.

So, the fringing fields along the width are modeled as radiating slots and electrically the microstrip antenna patch appears larger than its physical dimensions where the dimensions of the patch along its length have been extended at each termination by ΔL :

$$\Delta L = \frac{L_{\text{eff}} - L}{2} = \text{with } L_{\text{eff}} = \frac{c}{2L \cdot f_0 \cdot \sqrt{\epsilon_{\text{reff}}}} \quad \text{II-4}$$

So, to design an array of rectangular patch antennas of the center frequency f_c (GHz), sweeping between f_1 and f_2 . For a required gain, the three essential parameters are: 1- the operating frequency (f_0): The resonance antenna frequency should be chosen appropriately. 2- substrate dielectric constant (ϵ_r) [Pozar and Kaufman, 1987]. And 3- height of dielectric substrate (h): for the microstrip patch antenna, the height of the dielectric substrate is critical since the antenna shouldn't be bulky.

Frings factor is given as function of antenna patch dimensions:

$$\Delta L = 0.412 \cdot h \cdot \frac{(\epsilon_{reff} + 0.3) \left(\frac{w}{h} + 0.264 \right)}{(\epsilon_{reff} - 0.258) \left(\frac{w}{h} + 0.8 \right)} \quad \text{II-5}$$

And for rectangular microstrip, the resonance frequency for any TM_{10} mode is as follow:

$$f_0 = \frac{c}{2 \cdot \sqrt{\epsilon_{reff}}} \sqrt{(m/L)^2 + (n/w)^2} \quad \text{II-6}$$

Where c is the light speed, m and n are modes along L and w respectively.

The width and high are also given for efficient radiation:

$$\begin{cases} w = \frac{c}{2f_0 \cdot \sqrt{\frac{\epsilon_r + 1}{2}}} \\ h = \frac{0.3}{2\pi f \cdot \sqrt{\epsilon_r}} \end{cases} \quad \text{II-7}$$

II-6-2 Equivalent circuit of microstrip

The usual and simple equivalent circuit of the patch antenna is based on a transmission line model with capacitance and resistance on the radiating edges [Kumar, 2003] as shown on Figure II-8-a. And since the transmission line is characterized by its characteristic impedance Z_0 and electrical length $2\pi / \lambda_g L$. The transmission line model is not accurate, and doesn't describe neither the behavioral of the different structures that exist in the inset fed patch antenna nor the discontinuities between adjacent structures. So, instead of using a simple transmission line model, one can take into account the behavior of each structure used in its layout. As seen in Figure II-8-b, the antenna is the association of three parts: Part (a) is transmission line: TL_1 with characteristic impedance Z_{01} , and propagation constant β_1 , part (b) is conductor backed coplanar wave guide CBCPW [Simons, 2001] with characteristic impedance Z_{02} and propagation constant β_2 , and part (c) is a transmission line TL_2 with characteristic impedance Z_{03} , and propagation constant β_3 . When associating these three parts in series as in the layout of the patch antenna we obtain a new equivalent circuit of the patch antenna as shown on Figure II-8 d. By modeling the discontinuities between the Transmission line TL_1 and the conductor backed coplanar wave guide CBCPW in first step and between the CBCPW and transmission line 2 TL_2 in second step.

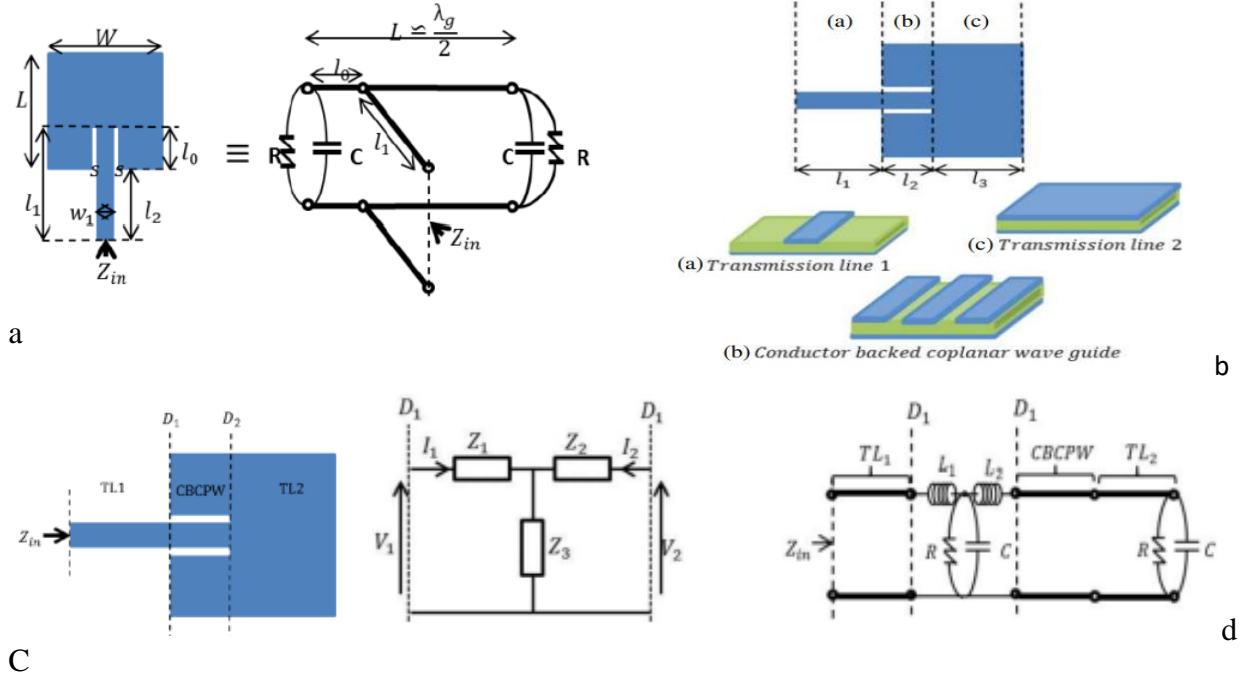


Figure II-8: Patch antenna equivalent circuit based on transmission line model with and without accounting discontinuity [Chouchene et al, 2017]

These two discontinuities: D1 and D2 are shown on Figure II-8 -c. The relation between each impedance Z1, Z2 and Z3, in the discontinuity [D1] in Figure 7 and the elements of the matrix

$$[D1] = \begin{bmatrix} A & B \\ C & D \end{bmatrix}$$

$$A = \frac{Z_1+Z_3}{Z_3}, B = \frac{Z_2(Z_2+Z_3)}{Z_1}, C = \frac{1}{Z_1+Z_3} \text{ and } D = -\frac{Z_2+Z_3}{Z_3} \tag{II-8}$$

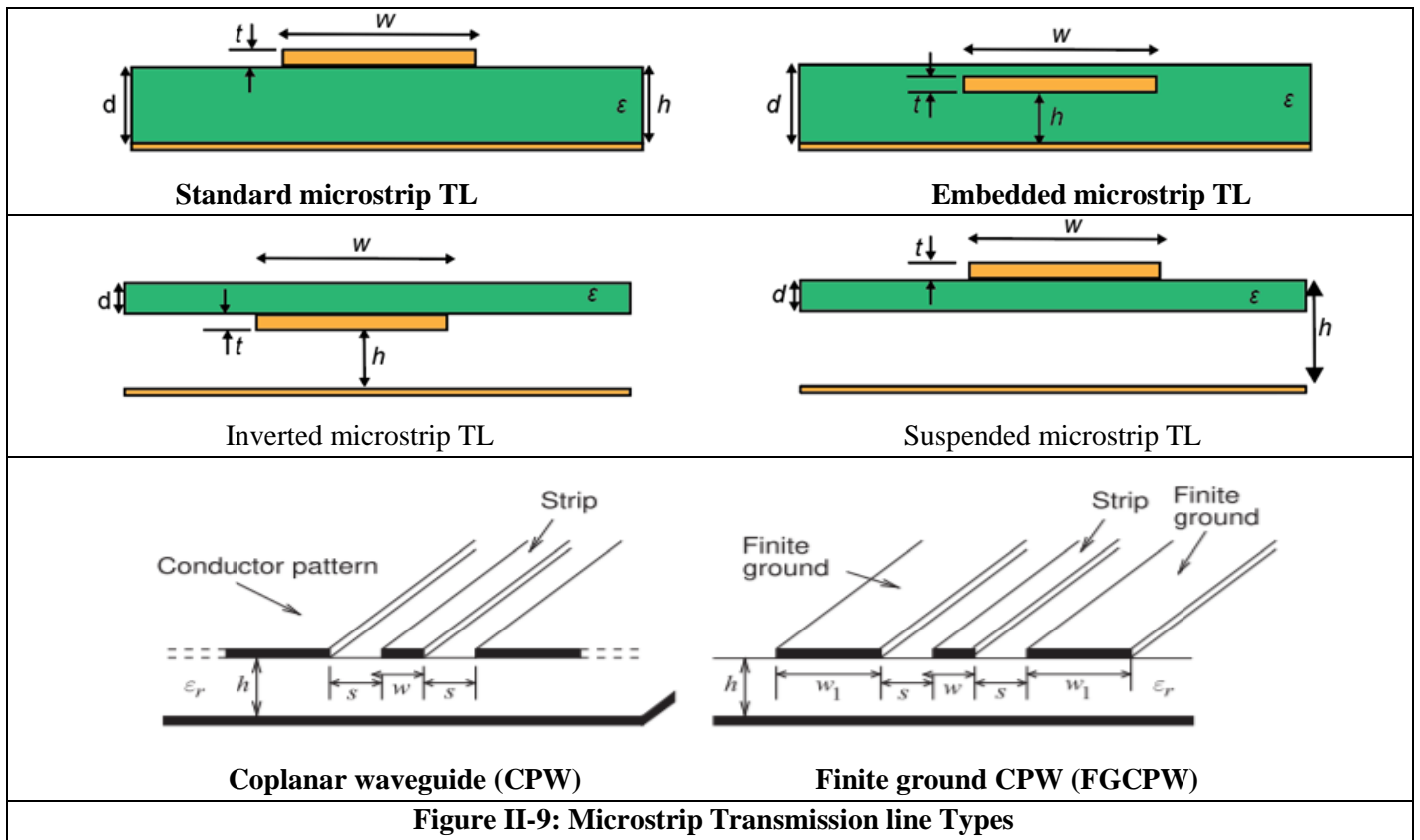
So, one can deduce the nature and the value of the elements circuit as [Chouchene et al,2017]:

$$\begin{cases} Z_1 = j\omega L_1 \\ Z_2 = j\omega L_2 \\ Z_3 = \frac{1}{R} + j\omega C \end{cases} \tag{II-9}$$

II-6-3 Types of microstrip

Diverse types of discontinuities exist in the design of the RF/microwave layout. These include bends, T-junctions, cross-junctions, width steps, couplings, and open ends. The parasitic effect introduced by these discontinuities is reduced by the use of cones with constant impedance for example; curved turns are used instead of sharp turns. Sharp edges are replaced with curved

edges in the RF layout. In some cases, radial stubs of various types (series and shunt) are used. As many as they can be, Figure II-9 shows some of them.



In embedded (or buried) microstrip line, the microstrip conductor is embedded in a dielectric. where, the dielectric is composed of two dielectric layers. Typically, signals passing through an integrated circuit ML runs nearly 20% slower than standard microstrip line. The impedance of an embedded microstrip line is rather more controllable, since the dielectric constant is the same above and below the transmission line. The additional layer of dielectric material has more effect on the effective dielectric constant of a narrow strips line.

Inverted microstrip lines use an air gap under the substrate, leading to reduce significantly the dispersion of the line parameters and lessens losses since the majority of electromagnetic field is concentrated in the air gap area. This type of microstrip line provides the benefit of low ohmic losses due to the RF current is concentrated in the highly-conductive copper conductors of printed circuit technology (PCB).

Suspended and inverted lines offer a higher Q -factor ($Q=500-1500$) than the general microstrip line ($Q=250$). The dispersion rises when increasing substrate permittivity (ϵ_r) and reducing the strip width (w). The air gap reduces the effective dielectric constant of the medium, which in turn increases physical dimensions of components. Another effect of lower effective dielectric constant is an increased width of the strip conductor. This means that the dimensional tolerances can be relaxed, which is very important at higher frequencies, including millimeter-wave frequencies. Inverted and suspended microstrip lines permit a broader range of achievable impedances. These lines are among the principal transmission media used in the upper microwave and lower millimeter-wave bands [Maloratsky, 2011].

Among the solution forms to microstrip problems, a coplanar waveguide (CPW) (Figure II-9) is a central strip flanked by two metal half-planes which carry the return current. The outer conductors can be considered as ground, but they are not necessarily connected to ground. At condition that the substrate is thick enough but in practice, this means that the substrate thickness is twice or three times larger than both strip width w and the metal separation s , the electrical characteristics of CPW are entirely determined by the lateral dimensions, because all of the metallization is on one layer. Indeed, the infinite half-grounds of CPW cannot be created so a practical implementation of CPW is finite ground CPW (FGCPW), where the signal return conductors are of finite width.

II-7 CMOS-Technology

In fact, as various applications are arisen in the millimeter wave frequency range (for instance: future broadband telecommunications and video streaming will operate around 60 GHz, automotive radars will operate around 77 GHz, and RF imaging will process 94 GHz, 140 GHz and above). Consequently, the high frequency transmission line development for the design of passive circuits (such as power dividers, baluns, matching networks, phase shifters and filters) is of an immense importance. Also, since the filters require huge performances and enable testing of advanced technologies and in particular insertion loss and on-chip area requirements. Nowadays mm wave filters on CMOS technology are reported and are based on a thin-film microstrip structure (TFMS) with a signal strip placed on the top metal layer, with the ground plane being located on the bottom ones M1 and/or M2 in a CMOS process. This easy-to-use topology allows

preventing the mm-wave signal from penetrating the lossy silicon substrate, thus minimizing the dielectric loss. Various microstrip filter topologies were realized with the TFMS [Sun et al, 2007; Hsiao and Tseng, 2010]. In 2003, a new type of slow-wave CPW T Lines was presented in [Cheung et al, 2003]. Then, many of authors experimental results were published and carried out on various CMOS technologies but before diving farther into the CMOS technology, it is beneficial to briefly recall some technology parameter. Those parameters describe the physics of the transistor and can be found in [Sun et al, 2007].

Complementary Metal Oxide Semiconductor (CMOS) is one of the most common technologies in the computer chip design industry. It is largely used in order to create integrated circuits in numerous and varied applications (computer memories, CPUs, cell phones, microprocessors microcontroller chips, memories like RAM, ROM due to its advantages by using both P and N channels semiconductor as represented in figure II-10-a, which depicts a cross-section of fabricated NMOS and PMOS field-effect transistors in an integrated circuit CMOS process.

The two MOS have four terminals: gate (G), source (S), drain (D), and body (B). Their schematic drawing symbols are shown in Figure II-10-b. When the voltage between source and drain terminals is large enough that the MOSFET is not in the triode region, the operation of MOSFET can be divided into two modes depending on the voltages between gate and source (G and S): strong inversion and weak inversion (or subthreshold) operations as presented in Figure II-10-c.

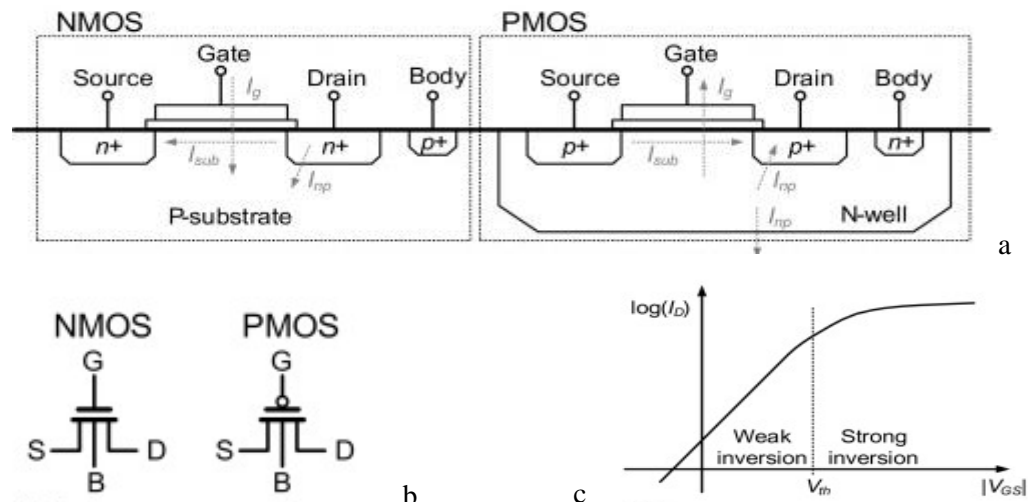


Figure II-10: Cross-section of NMOS and PMOS FETs fabricated in a CMOS process, (B) their schematic drawing symbols, and (C) logarithm of the drain current I_D as a function of the gate-source voltage with the body tied to the source, and the drain-source voltage biased

in the saturation region [Ha et al, 2019]

Contrary to standard practices in analog CMOS circuit design, the low inversion (subthreshold) region of CMOS operation has been shown to be a benefit regime for low-power biomedical circuit design [Ha et al, 2019]. In the conventional design and especially for high-speed applications, weak inversion operation has been considered as non-ideal in the cut-off region and its current has been termed as leakage current. Recently, weak inversion has become increasingly important as its low power and low bandwidth characteristics are well suited for biomedical and other low power sensor applications, due to its superior transconductance efficiency. Additionally, transistors in deep submicron technologies operating at weak inversion do not suffer from many of the process-dependent problems that affect the strong inversion region above threshold, such as the gain-limiting effects of velocity saturation. in the mobility of electrons and holes [Ha et al, 2019].

The transistor model equations in weak inversion are simpler and scale over a wider range than in strong inversion. Independent of the process technology, the electron energy of a transistor in weak inversion is entirely based on the Boltzmann distribution. The drain current through the channel of the transistor does not flow by drift, but by diffusion, and follows an exponential function versus the gate bias. Accordingly, the mode of operation is mainly appropriate to the implementation of translinear circuits and log-domain filters.

The drain current I_D , the transconductance g_m and the unity gain frequency f_t are expressed in weak inversion mode as follows [Ha et al, 2019]:

$$\begin{cases} i_D = i_{D0} \cdot \left(\frac{w}{L}\right) e^{\frac{v_{GS}}{nV_t}} \left(1 - e^{\frac{-v_{DS}}{V_t}}\right) \\ g_m = \frac{i_D}{nV_t} \propto I_D \\ f_t = \frac{I_D}{2\pi nV_t(C_{gs} + C_{gd} + C_{gb})} \propto I_D \end{cases} \quad \text{II-10}$$

Since, the transconductance g_m is linearly proportional to the drain current I_D , so is the unity-gain frequency. So, the trade-off between the current and bandwidth is very simple: the bandwidth is linearly proportional to the current in weak inversion.

II-8 CMOS - Inversion

CMOS circuits are built such that all PMOS transistors essentially have either an input from the voltage source or from another PMOS transistor. As well as, all NMOS transistors must either have an input from ground or from another NMOS transistor. The PMOS composition produces a small resistance between its source and drain contacts when the applied gate voltage is low and a high resistance if the applied gate voltage is high. On the other hand, the composition of an NMOS transistor creates a high resistance between the source and the drain when a low gate voltage is applied and a low resistance when a high gate voltage is applied.

CMOS accomplishes current reduction by completing every NMOS with a PMOS and connecting both gates and both drains together. A high voltage on the gates will cause the NMOS to conduct and the PMOS to block, while a low voltage on the gates causes the contrary.

This arrangement greatly reduces power consumption and heat generation. However, during the switching time, both MOSFETs conduct briefly as the gate voltage goes from one state to another. This induces a brief spike in power consumption and becomes a serious issue at high frequencies.

Figure II-11 shows what happens when an input is connected to both a PMOS and an NMOS. V_{dd} is positive voltage connected to a power supply and V_{ss} is ground (A is the input and Q is the output). When, the voltage at A is low (almost V_{ss}), the NMOS channel is in a high resistance state, disconnecting V_{ss} from Q. The PMOS transistor's channel is in a low resistance state, connecting V_{dd} to Q. therefore, the Q-voltage is equal to V_{dd} .

On the other hand, when the A-voltage is high (almost V_{dd}), the PMOS is in a high resistance state, disconnecting V_{dd} from Q. The NMOS is in a low resistance state, connecting V_{ss} to Q. So, now, the Q-voltage is equal to V_{ss} .

To summarize, the outputs of the PMOS and NMOS transistors are complementary in a way that when one is low, the other is high, no matter what the input is, the output is always the opposite. Because of this behavior of input and output, the CMOS circuit's output is the inverse of the input. The transistors' resistances are never exactly equal to zero or infinity, so Q will never exactly equal V_{ss} or V_{dd} , but Q will always be nearer to V_{ss} than A was to V_{dd} (or vice versa).

CMOS offers relatively high speed, low power dissipation, high noise margins in both states, and will operate over a wide range of source and input voltages (provided the source voltage is fixed).

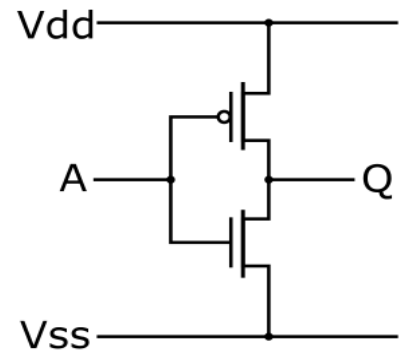


Figure II-11: CMOS inverter.

References of Chapter II

[Balanis,2005] C. A. Balanis, Antenna Theory: Analysis and Design, John Wiley & Sons, 2005.

[Bowrothu and Zhang, 2018] Bowrothu R, Yoon YK, Zhang J. ‘Through Glass Via (TGV) Based Band Pass Filter for 5G Communications’. IEEE68th Electronic Components and Technology Conference (ECTC)(pp. 1097-1102). IEEE; 2018

[Chavali and Nikolova, 2019] Murthy S. Chavali, Maria P. Nikolova Metal oxide nanoparticles and their applications in nanotechnology, SN Applied sciences, 2019

[Chen et al, 2009] Chen M, Lin YC, Ho MH. ‘Quasi-lumped design of bandpass filter using combined cpw and microstrip’. Prog Electromagn Res Lett.9:59-66, 2009

[Cheung et al, 2003] T. S. D. Cheung, J. R. Long, K. Vaed, R. Volant, A. Chinthakindi, C. M. Schnabel, J. Florkey, and K. Stein, “On-chip interconnect for mm-wave applications using an all-copper technology and wavelength reduction,” in Proc. IEEE Int. Solid-State Circuits Conf., San Francisco, CA, Feb. 13, 2003, pp. 396–501

[Chouchene et al, 2017] Wissem Chouchene, Chiraz Larbi, and Taoufik Aguil, ‘New Electrical Equivalent Circuit Model of the Inset Fed Rectangular Patch Antenna’, Progress in Electromagnetics Research Symposium- Spring (PIERS), St Petersburg, Russia, 2017

[Choudhury et al, 2018] Choudhury SR, Sengupta A, Das S. ‘Bandpass filters using multi-layered microstrip structures’. In 2018 Emerging Trends in Electronic Devices and Computational Techniques (EDCT) pp. 1–3. IEEE; 2018.

[Dupez and Sinha, 2016] Millimeter-Wave Antennas: Configurations and Applications, Book, Signals and Communication Technology Series, 2016

[Ellingson, 2018] Ellingson, Steven W., ‘Electromagnetics (Volume 1)’, Book, Blacksburg, Virginia, 2018

[Ha et al, 2019] Sohmyung Ha, Chul Kim, Patrick Mercier, and Gert Cauwenberghs ‘High-Density Integrated Electro cortical Neural Interfaces, Book, *Academic Press (Elsevier)*, 2019

[Holt, 2016] W.M. Holt, '1.1 Moore's law: a path going forward', IEEE International Solid-State Circuits Conference (ISSCC), San Francisco, CA, pp. 8–13, 2016

[Hsiao and Tseng, 2010] Y. C. Hsiao and C. H. Tseng, "Design of 60 GHz CMOS bandpass filters using complementary-conducting strip transmission lines," in Proc. IEEE MTT-S Int. Microw. Symp. Dig., Anaheim, CA, pp. 1712–1715, 2010.

[Hu et al, 2017] S. Hu, F. Wang, H. Wang, A 28GHz, 37GHz, 39GHz multiband linear Doherty power amplifier for 5G massive MIMO applications, in 2017 IEEE International Solid-State Circuits Conference - (ISSCC) Digest of Technical Papers (San Francisco, CA, 2017), pp. 1–3

[Ieu et al, 2018] Ieu W, Zhang D, Lv D, Wu Y. Dual-band microstrip bandpass filter with independently-tunable passbands using patch resonator. Electron Lett.;54(10):665-667,2018.

[ITRS] ITRS, International technology roadmap for semiconductors, <http://www.itrs.net/reports.html>

[ITU-R, 2015] ITU-R (International Telecommunication Union)-Recommendation M.2083-0, IMT vision, 'framework and overall objectives of the future development of IMT for 2020 and beyond', p. 21, 2015

[Kumar and Karthikeyan, 2018] Phani Kumar KV, Karthikeyan SS. Microstrip lowpass filter with flexible roll-off rates. Int J Electron Commun. 86:63-68,2018

[Kumar and Ray,2003] Kumar, G. and K. P. Ray, Regularly Shaped Broadband MSAs in Broadband Microstrip Antennas, 30–114, Artech House, 2003.

[Maloratsky, 2011] Leo G. Maloratsky, 'Using Modified Microstrip Lines to Improve Circuit Performance' High Frequency Electronics, Aerospace Electronics Company, Technical Media, LLC, 2011

[Onoe, 2020] S. Onoe, '1.3 evolution of 5G mobile technology toward 1 2020 and beyond', IEEE International Solid-State Circuits Conference (ISSCC), San Francisco, CA, pp. 23–28, 2016

[Pozar and Kaufman, 1987] D.M.Pozar and B.Kaufman, "Increasing the Bandwidth of a Microstrip Antenna by Proximity Coupling", Electronic Letters, Vol- 23, pp [12-14] April-1987.

[Razavi, 2011] B. Razavi, 'RF Microelectronics', 2nd ed. Prentice Hall, New Jersey, 2011

- [Reger, 2016] L.Reger, '1.4 the road ahead for securely-connected cars', IEEE International Solid-State Circuits Conference (ISSCC), San Francisco, CA, pp. 29–33, 2016
- [Reynaert et al, 2017] P. Reynaert, W. Steyaert, M. Vigilante, RF CMOS. Nanoelectronics: Materials, Devices, Applications, 2 Volumes, 2017
- [Sandeep and Kashyap, 2012] B.Sai Sandeep S.Sreenath Kashyap, ' Design and simulation of microstrip patch array antenna for wireless communications at 2.4 Ghz', International journal of scientific & engineering research, volume 3, issue 11, 2012.
- [Sansen, 2015] W. Sansen, '1.3 analog CMOS from 5 micrometer to 5 nanometers', IEEE International Solid-State Circuits Conference-(ISSCC) Digest of Technical Papers, San Francisco, CA,pp. 1–6,2015
- [Shaman et al, 2014] Shaman H, Almorqi S, Haraz O, Alshebeili S, Sebak AR. 'Milli-meter-wave microstrip diplexer using elliptical open-loop ring resonators for next generation 5G wireless applications.' Mediterranean Microwave Symposium (MMS2014) (pp. 1–4). IEEE; 2014.
- [Shannon, 1948] C.E. Shannon, 'A mathematical theory of communication'. Bell Syst. Tech. J. 27(3), 379–423, 1948
- [Simons, 2001] Simons, R. N., "Conductor-backed Coplanar Waveguide" in Coplanar Waveguide Circuits, Components, and Systems, 87–90, John Wiley & Sons, 2001.
- [Sun et al, 2007] S. Sun, J. Shi, L. Zhu, S. C. Rustagi, and K. Mouthaan, "Millimetre-wave bandpass filters by standard 0.18- μm CMOS technology," IEEE Electron Device Lett., vol. 28, no. 3, pp. 220–222,2007
- [Strytsin et al, 2018] Strytsin I, Shen M, Pedersen GF. Antenna integrated with a microstrip filter for 5G mm-wave applications, International Conference on Electromagnetics in Advanced Applications (ICEAA) (pp. 438-441). IEEE; 2018.
- [Vigilante and Reynaert, 2017] Marco Vigilante and Patrick Reynaert,' 5G and E-Band Communication Circuits in Deep-Scaled CMOS, Analog Circuits and Signal Processing (eBook),2017

[Wang et al, 2014] Wang CX, Haider F, Gao X.' Cellular architecture and key technologies for 5G wireless communication networks'. IEEE Commun Mag. 2014;52(2):122-130.

[Wells, 2010] J. Wells, 'Multigigabit Microwave and Millimeter-Wave Wireless Communications', Artech House, Boston, 2010

[Yang et al, 2018] Yang K, Hoang MH, Bao X, McEvoy P, Ammann MJ. 'Dual-stub Ka-band Vivaldi antenna with integrated bandpass filter'. IET Microw Antennas Propag. 12(5):668-671,2018

[Yang, 2018] Shan-Da Yang, 'electromagnetics courses, National Tsing Hua University, Taiwan,2018

III-1 Introduction

5G is recently a condensed research and development field as it can make high data rate available and meets the requirements of Gbps (Giga bits per second) communications for multiple users (speed, quality, massive network capacity, reliability...). Higher performance as well as improved efficiency allow new user experiences and connects new industries [Choudhury, 2015; Gao and Rebeiz, 2021].

Indeed, 5G as it widely used and expanded over the world (Figure III-1-a), it expresses also the 5th generation in mobile network which It is the global wireless standard after the prior networks (Figure III-1-b) [Yang, et al, 2018; Park et al, 2019; Gao and Rebeiz, 2021]

The communications systems involve RF/microwave devices, such the filter which is with imperative role. Since it offers the possibility to eliminates, select, or separates signals in predefined frequency bands [Shen et al, 2001; Richard et al, 2018]. It is extensively used as key components in transmitter and receiver systems. These microwave filters realization is associated directly to the technological properties which is used as substrate-integrated waveguide (SIW) [Benotmane, 2014] or as planar [Rampnoux, 2003; Benhaddi, 2017], The technological choice relays on the type and the performance of application envisaged.

In this chapter, a compact microstrip band pass filter based on a rectangular shaped resonator for 5G and others wireless communications systems like WIMAX (Worldwide interoperability for Microwave Access) and WLAN (Wireless Local Area Network) has been introduced. The simulation of the proposed band pass filter has realized by Advanced Design System “ADS” using FR4 substrate having relative permittivity of 4.4 a thickness of 1.6 mm and a tangent loss of 0.01. then a CMOS filter is also proposed by using its direct electrical equivalent form and by the lumped elements. The purpose of this work is to understand and cover the simulation of the performance of the microstrip and CMOS band pass filter in term of adaptation, bandwidth and resonant frequency. Compared to other work, the proposed filter is characterized by a miniaturized chip size, low insertion loss and high return loss. The suggested first compact structure (microstrip) of the band pass filter is developed in two major steps; the first is interested about the theories of the T-shaped resonator band pass filter, while the second is concerned about the simulation of the band pass Shaped resonator filter. For the second CMOS structure, it was investigated under its electrical for and by means of lumped elements after their evaluation.

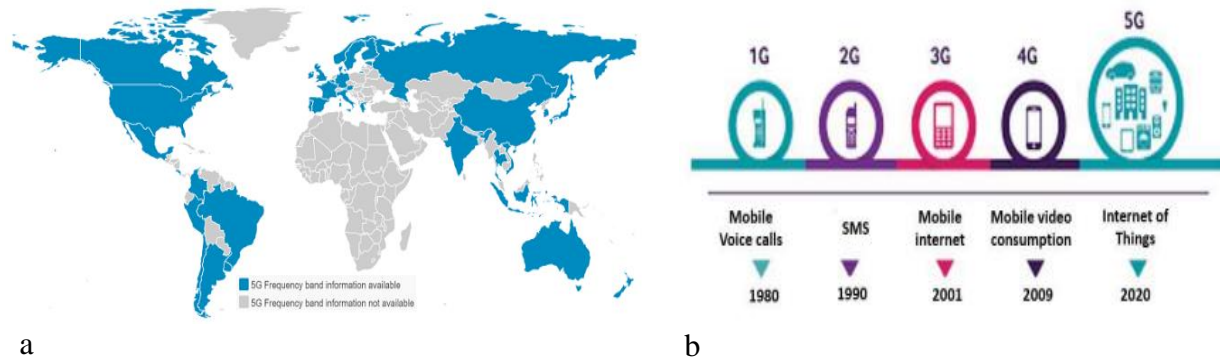


Figure III-1: a-5G frequency bands across the world [EverythingRF, 2021], b-f mobile communications evolution from 1G to 5G [BenHaddi et al, 2020]

Produced by a division of Keysight Technologies, PathWave Design, the Advanced Design System (ADS) is an electronic design computer software that makes available an integrated design environment of RF electronic products. Every step of the design process such as schematic capture, layout, design rule checking, frequency and time domain circuit simulation, and electromagnetic field simulation is supported by ADS, tolerating the characterization and fully optimization of a RF design in the same environment tool.

Since ADS focuses on the RF and microwave design, so the devices library is mostly on microwave devices. It provides also to design the device by mean of circuit simulation where it is possible to make some analysis such as: DC analysis, transient analysis where it runs the time domain analysis on the circuits and considers the nonlinearity of the elements, the AC analysis which consists of the small signal analysis and use the linear model of elements on their bias point. So, the nonlinear elements as transistors are replaced by a linear model (small signal circuit) that consist of resistors, capacitors, inductors and voltage and current sources. Additionally, the Scattering parameters of the components (S-parameters) and their variation over different range of frequencies. It is also used for calculating noise figure and group delay.

Momentum is based on a numerical discretization technique called the Method of Moments. This technique is used to solve Maxwell's electromagnetic equations for planar structures embedded in a multilayered dielectric substrate. The simulation modes available in Momentum (microwave and RF) are both based on this technique, but use different technologies to achieve their results. It combines full-wave and quasi-static EM solvers to provide insight into EM behavior of MMIC, RFIC, RF Board, Signal Integrity, and antenna designs. The Momentum simulation engine is integrated into Keysight ADS and Keysight Genesys. Moreover, the layout is which integrated

with ADS software and represents an integrated circuit in its geometric planar shape terms that correspond to the patterns of metal, oxide, or semiconductor layers which make up the components of the integrated circuit.

Starting ADS: All design work must be done in a project directory. Working in project directories enables you to organize related files within a predetermined file structure. This predetermined file structure consists of a set of subdirectories. These subdirectories are used in the following manner: - networks contains schematic and layout information, as well as information needed for simulating

-data is the default directory location for input and output data files used or generated by the simulator

-mom_dsn contains designs created with the Agilent EEsof planar electromagnetic simulator, Momentum

- synthesis contains designs created with DSP filter and synthesis tools verification contains files generated by the Design Rule Checker (DRC), used with Layout.

III-2 Design of Microstrip band pass filter

III-2-1 Specification of the proposed filter:

In this modest thesis, it is interested to form an antenna based on band pass filter (BPF) microstrip structure, and based on the constraints imposed by a set of specifications based on mobile communications system; specially 5G as well, the specifications of the proposed structure (microstrip) of band pass filter are summarized in the following table (Table III-1 and III-2). The main parts for the design of each band pass filter based on linear resonator are:

1-First, the theoretical synthesis of the filter permits to identify the structure of the filtering circuit, and to define the values (impedance, electrical length).

2- The design and simulation of the band pass microstrip (T-shaped) as second step.

The frequency band (GHz)	Central frequency (GHz)	Insertion loss (dB)	Return loss (dB)
1.8-3	2.4	<-2	<-12

Table III-1: Microstrip filter specifications.

III-2-1-1 Patch characterization

Operating frequency, the dielectric substrate has a relative permittivity of 4.4 with high of 1.6 mm and the velocity of free space is $v=3e8$ m/s. So, the wavelength $\lambda=$ velocity/frequency ($\lambda=(3e8/2.4e9)=125$ mm). For an antenna operating frequency F_r of 2400 MHz and an efficient radiator, an effective radiation efficiency is given by a practical width W of:

$$W = \frac{v}{2F_r} \sqrt{\frac{2}{\epsilon_r + 1}} \quad \text{III-1}$$

So, by substituting the velocity of light v with its value $3e8$ m/s and the other parameters values, the width results as 38.04 mm. Figure III-2 illustrates the shape of microstrip antenna under study.

For the rest of need patch microstrip parameters, the Appendix A shows clearly how to calculate them while in this section, we just recall those equations and use them.

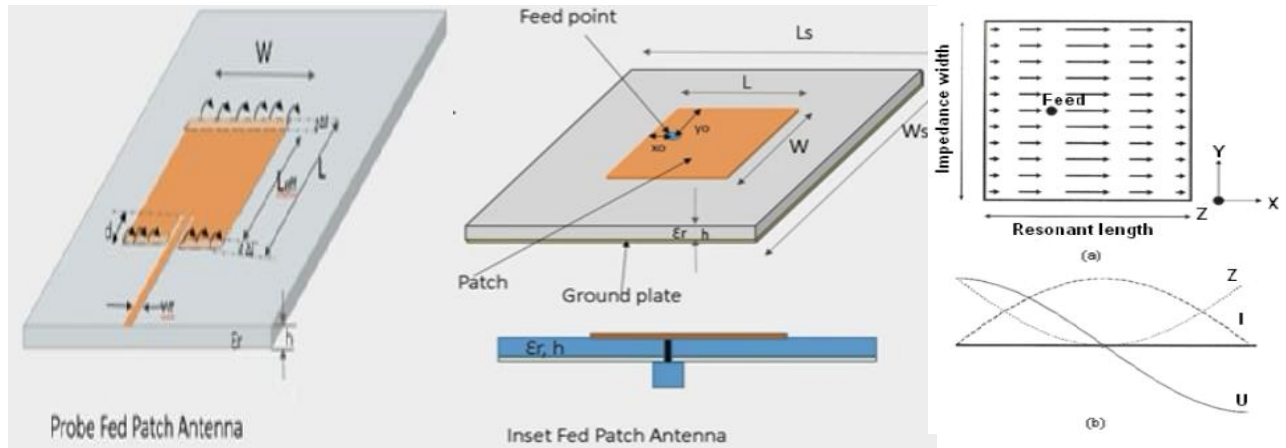


Figure III-2: left/a geometric form of antenna Microstrip structure. Right/(a) Current distribution on the patch surface. (b) Voltage U , current I and impedance Z distribution along the patch's resonant length [Alayesh, 2007].

The microstrip antenna-effective dielectric constant, the extension of the length ΔL and the actual length are given as:

$$\left\{ \begin{array}{l} \epsilon_{eff} = \frac{\epsilon_r + 1}{2} + \frac{\epsilon_r - 1}{2} \left(1 + \frac{12d}{W} \right)^{-0.5} \\ \frac{\Delta L}{h} = \frac{0.412(\epsilon_{eff} + 0.3) \left(\frac{W}{h} + 0.264 \right)}{(\epsilon_{eff} - 0.256) \left(\frac{W}{h} + 0.8 \right)} \\ L = \frac{v}{2F_r \sqrt{\epsilon_{eff}}} - 2\Delta L \end{array} \right. \quad \text{III-2}$$

with $1 < \epsilon_{eff} < \epsilon_r$ and if ϵ_{eff} is a function of frequency, so when frequency of operation increases, most of the electric field lines concentrate in the substrate. The parameters values are summarized in Table III-2 where the substrate height is h and the width of microstrip line is W .

Parameters	ϵ_r	$h(\text{mm})$	$W(\text{mm})$	ϵ_{eff}	$\Delta L(\text{mm})$	$L(\text{mm})$
Value	4.4	1.6	38.04	4.086	0.7384	29.42

Table III-2: Microstrip antenna parameters and dimensions.

III-2-2 Theoretical Synthesis of the Filter

From the magnitude of the current and voltage view, the impedance is minimum (\sim zero Ω) in the middle of the antenna patch and maximum (\sim 200 Ω) near the edges. Additionally, the electric field is zero at the center of the patch, maximumly positive at one side and minimally negative at the opposite side. The maximum and minimum continuously change side according to the instantaneous phase of the applied signal resulting in zero current at the middle and multi-mode voltage. Thus, the feeding point is the point where the impedance is 50 Ω . somewhere along the resonant length used to couple electromagnetic in and /or out of the patch.

Also, as every standard antenna impedance so we need to add the impedance allowing the antenna to match the standard device which lead to calculate the impedance at the edges. The input impedance and the transition impedance are given by equations III-3, since the Z_c does not match with 50Ω s standard microstrip antenna, therefore, a quarter wavelength transformer is needed to connect them

$$\begin{cases} Z_c = \frac{90 \cdot \epsilon_r^2}{\epsilon_r - 1} \left(\frac{L}{W}\right)^2 \\ Z_T = \sqrt{50 * Z_c} \end{cases} \quad \text{III-3}$$

Thus, the transition line characteristics impedance of the line can be evaluated by equation III-4 as:

$$\begin{cases} Z_0 = \frac{60}{\sqrt{\epsilon_r}} * \ln\left(\frac{8 \cdot h}{W_T} + \frac{W_T}{4 \cdot h}\right) \\ \frac{Z_0}{\frac{60}{\sqrt{\epsilon_r}}} = \ln\left(\frac{8 \cdot h}{W_T} + \frac{W_T}{4 \cdot h}\right) \end{cases} \quad \text{III-4}$$

By putting $Z_0 = Z_T$, one can calculate the transition line width W_T and to calculate the transition line length, the relative permittivity calculation is important, which follows the next equation

$$\epsilon_{re} = \frac{\epsilon_r + 1}{2} + \frac{\epsilon_r - 1}{2} \left(1 + \frac{12d}{W_T}\right)^{-0.5} \quad \text{III-5}$$

Hence, the length of transition line (quarter wavelength) line should be:

$$L_T = \frac{\lambda}{4} = \frac{\lambda_0}{4 \sqrt{\epsilon_{re}}} \quad \text{III-6}$$

The W_f and the length L_f of 50Ω microstrip feed line are calculated via using the characteristic impedance as follow:

$$\begin{cases} W = \frac{8 \cdot h \cdot e^A}{e^{2A} - 2} \text{ for } w \leq 2h \\ W = \frac{2h}{\pi} \left[B - 1 - \ln(B - 1) + \frac{\epsilon_r - 1}{2\epsilon_r} \cdot \ln(B - 1) + 0.39 - \frac{0.61}{\epsilon_r} \right] \text{ for } w > 2h \end{cases} \quad \text{III-7}$$

Where:

$$\begin{cases} A = \frac{Z_c}{60} \sqrt{\frac{\epsilon_r + 1}{2}} + \frac{\epsilon_r - 1}{2} (0.23 + 0.11/\epsilon_r) \\ B = 377 \cdot \pi / (2 \sqrt{\epsilon_r} Z_c) \end{cases} \quad \text{III-8}$$

So, the feedline length is

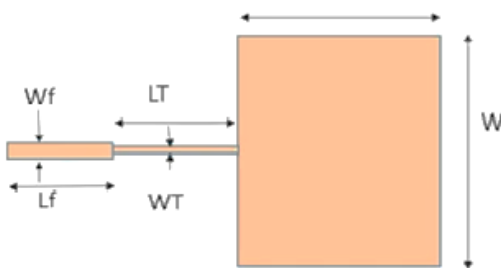
$$L_f = \frac{\lambda}{4} = \frac{\lambda_0}{4 \sqrt{\epsilon_{reff}}} \quad \text{III-9}$$

Table III-3 summarized the value of parameters included in the simulation and evaluated from the previous equations.

Z_c (Ω)	Z_T (Ω)	W_T (mm)	ϵ_{re}	L_T (mm)	A	W_f (mm)	L_f (mm)
306.36	123.82	0.169	2.859	18.48	1.53	3.058	15.46

Table III-3 The geometrical parameters value of microstrip patch antenna.

If the microstrip line width is too small as shown in figure III-3, where W_T is too tightly for fabrication it is convenient to use an alternative design where the inset feed is employed and the recessed distance (the length cutting into the patch) is given as:



$$R_{in}(x = x_0) = R_{in}(x = 0) \cdot \cos\left(\frac{\pi}{L * x_0}\right)$$

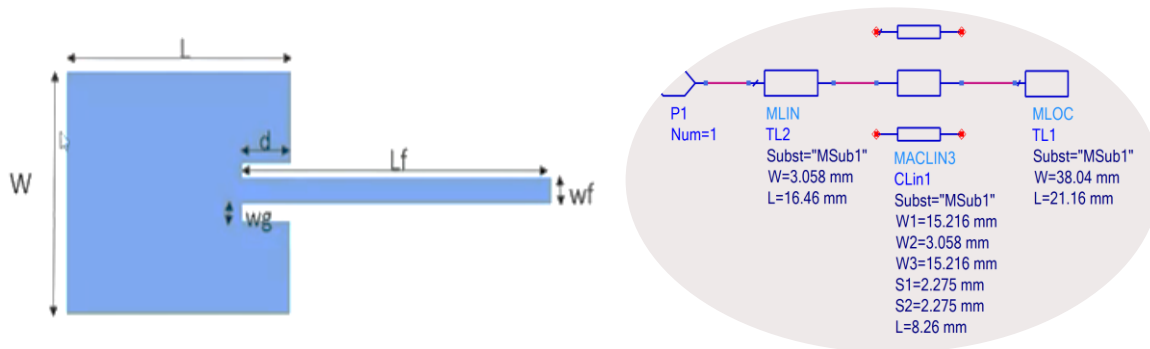
$$R_{in}(x = x_0) = 50 \text{ ohms}$$

$$R_{in}(x = 0) = Z_c = 123.82 \text{ ohms}$$

$$\text{Which gives } x_0 = 8.26 \text{ mm}$$

FigureIII-3: The patch antenna with all its parameters and the inset feed recess distance calculation

Consequently, the antenna microstrip patch changes to figure III-4, the new configuration of the



patch antenna.

Figure III-4: left/ the new patch antenna, right/ the equivalent schematic circuit under ADS Agilent.

$x_0 = d$ is the inset distance. In the purpose to design our microstrip, we first generate open the ADS Agilent and choose either use the schematic or layout to generate proceed since from each domain (schematic or layout), one can generate the second form of the patch (the equivalent circuit or the geometrical structure). Then, from there, it is possible to define the EM parameters such as the substrate definition material and dimensions. The figure III-5 summarizes all the steps needed to execute in order to design the device.

It is important to name the project and introduce any new materials included from the library or importing files.

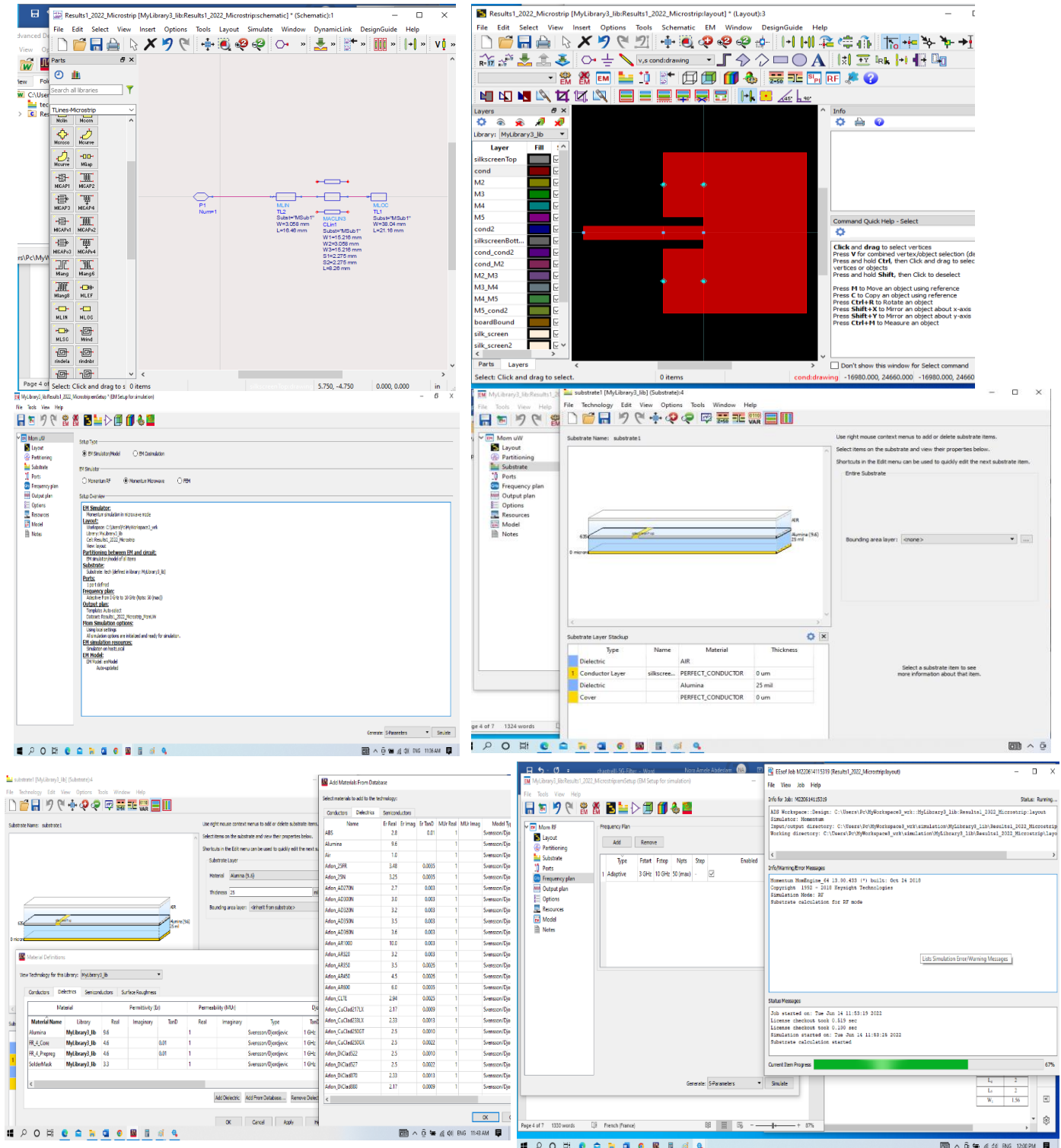


Figure III-5: Steps to follow for designing the microstrip antenna via the schematic circuit or via the layout (physical form of the patch).

The results of this simulation are given in figure III-6. Scattering parameters have fundamental role where they express the reflection coefficient and the gain as given by figure III-7.

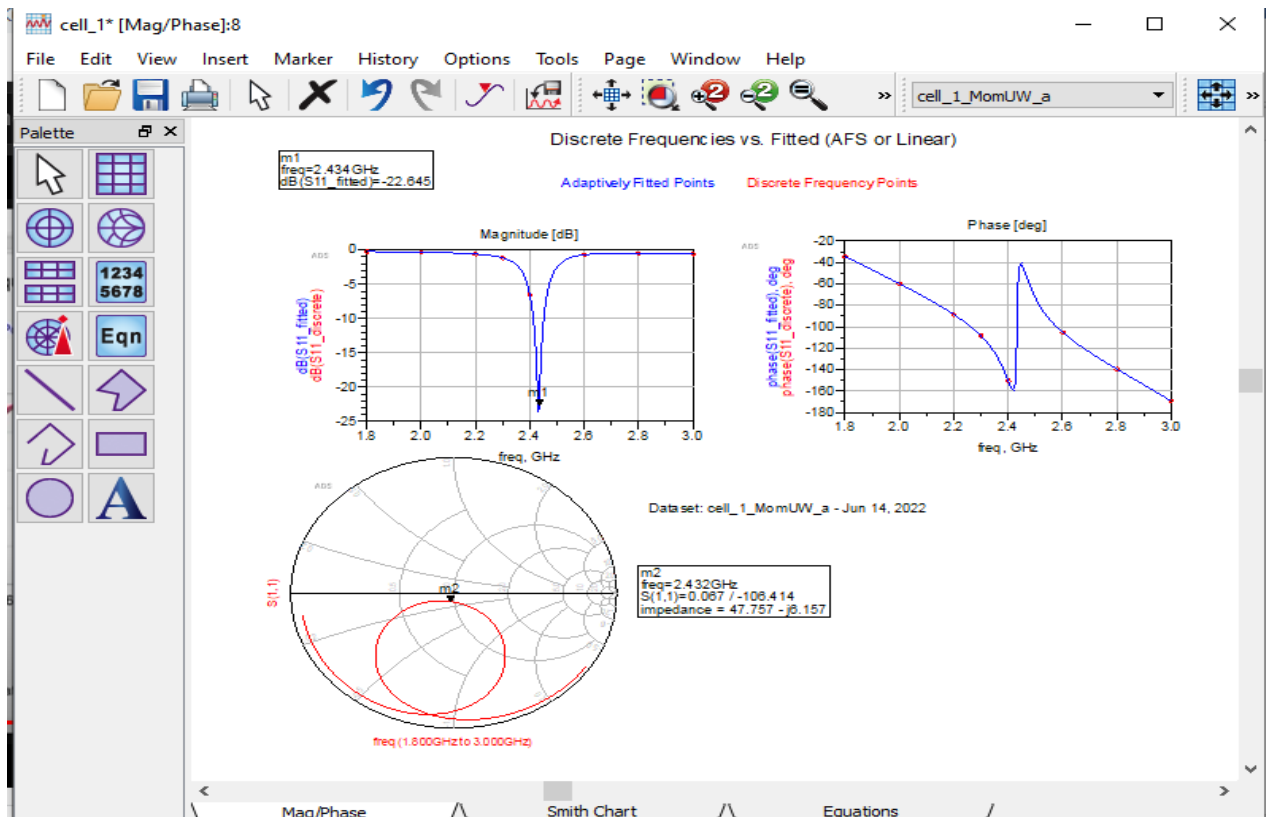


Figure III-6: The magnitude and phase of S11 -scattering parameter.

From the smith chart one can find the impedance 47.757 ohms which is almost nearly 50 ohms that is good as ideal impedance.

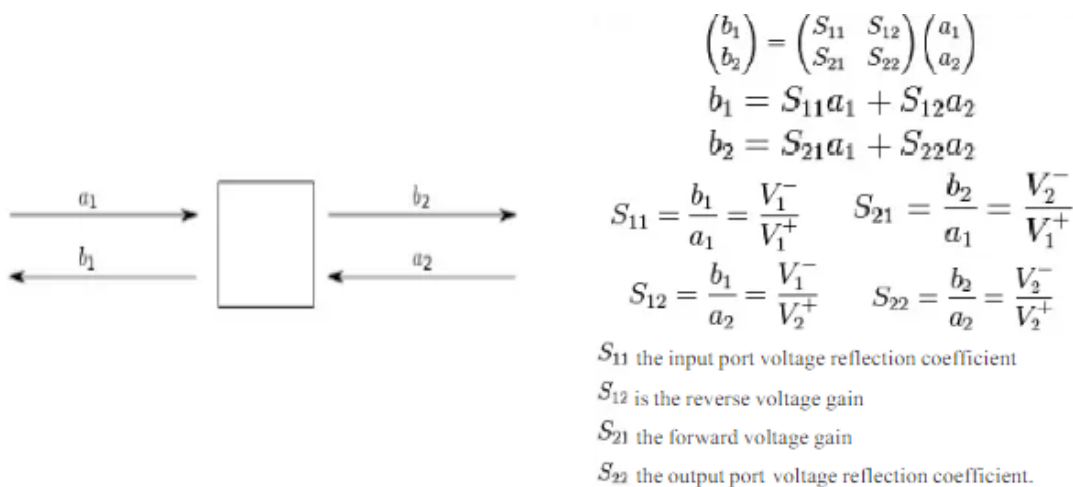


Figure III-7: Scattering parameters relationships [Qing and Chen, 2010]

The return loss S_{11} or $S(1,1)$ characterizes the power amount reflected from the antenna, it why it is known as the reflection coefficient (sometimes written as γ : or return loss). If $S_{11}=0$ dB, then all the power is reflected from the antenna and nothing is radiated.

So, to optimize the output of the design, one can go back to the schematic and add some blocs as shows the figure III-8.

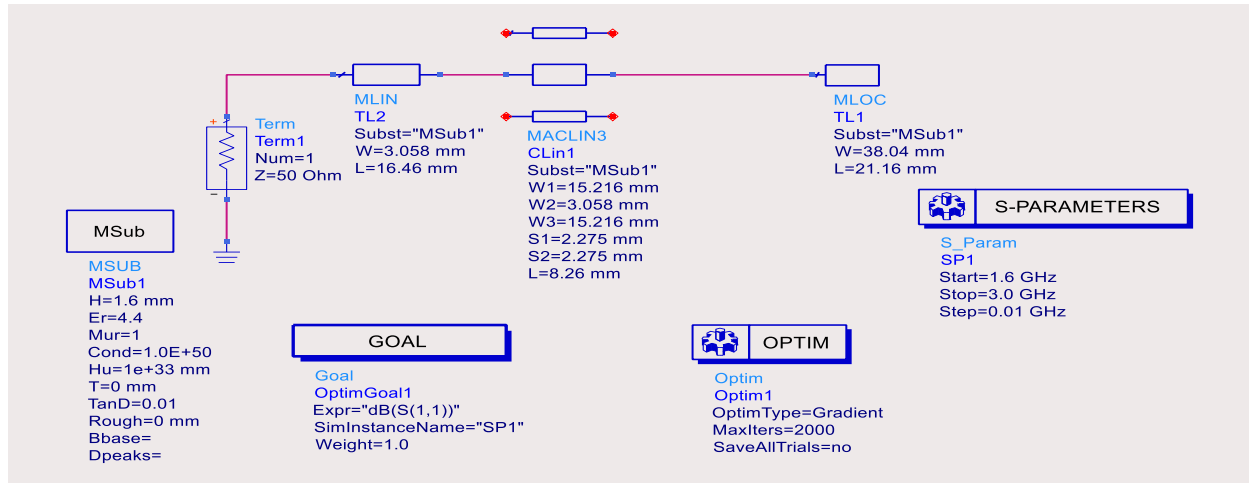


Figure III-8: The schematic circuit of microstrip antenna with optimization blocs.

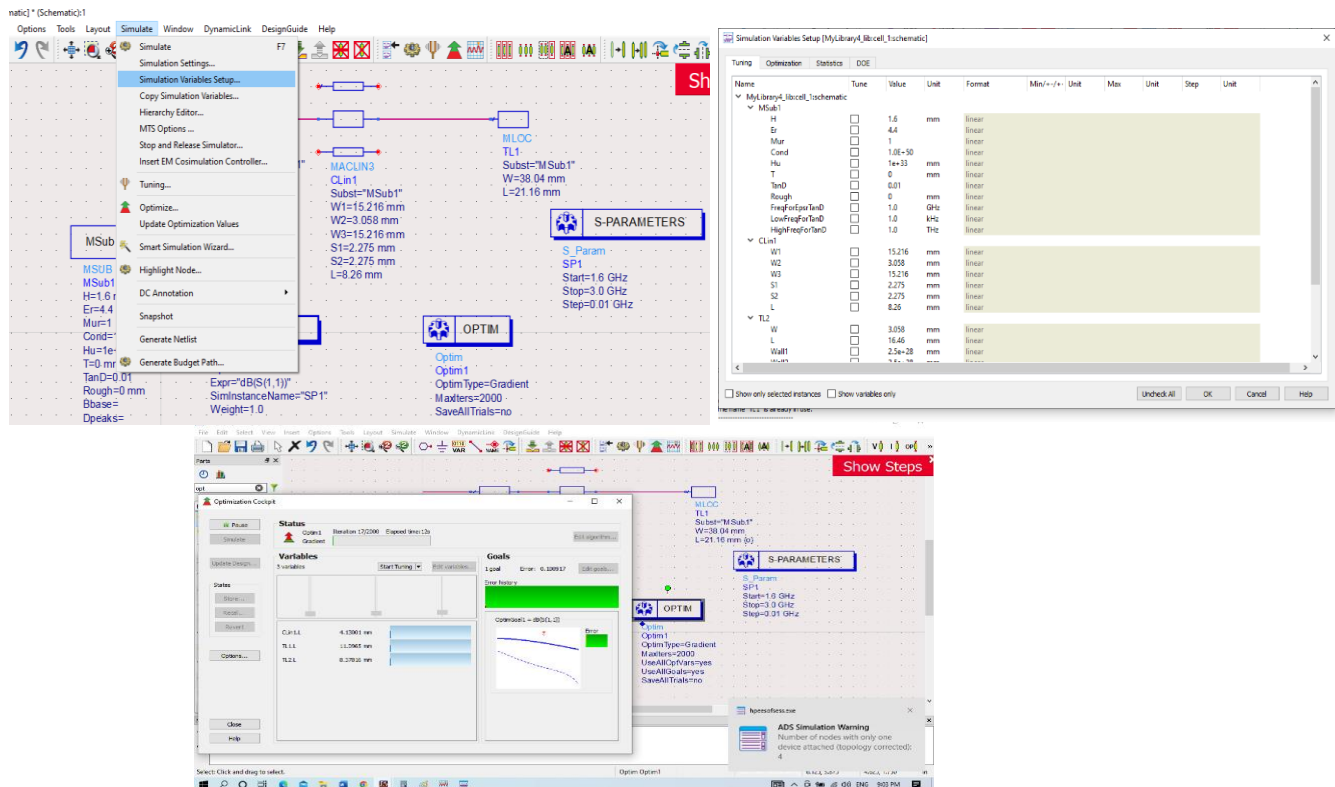


Figure III-9: Steps to proceed the optimization of parameters within the schematic circuit.

Then, in order to simulate the new design, one can push the simulation icon, and get some other steps are needed and can be done as presented on figure III-9.

It is also possible to take a view on the distribution of electric fields via the Momentum 3D Preview on MyLibrary (EM cell) as illustrated on figure III-10.

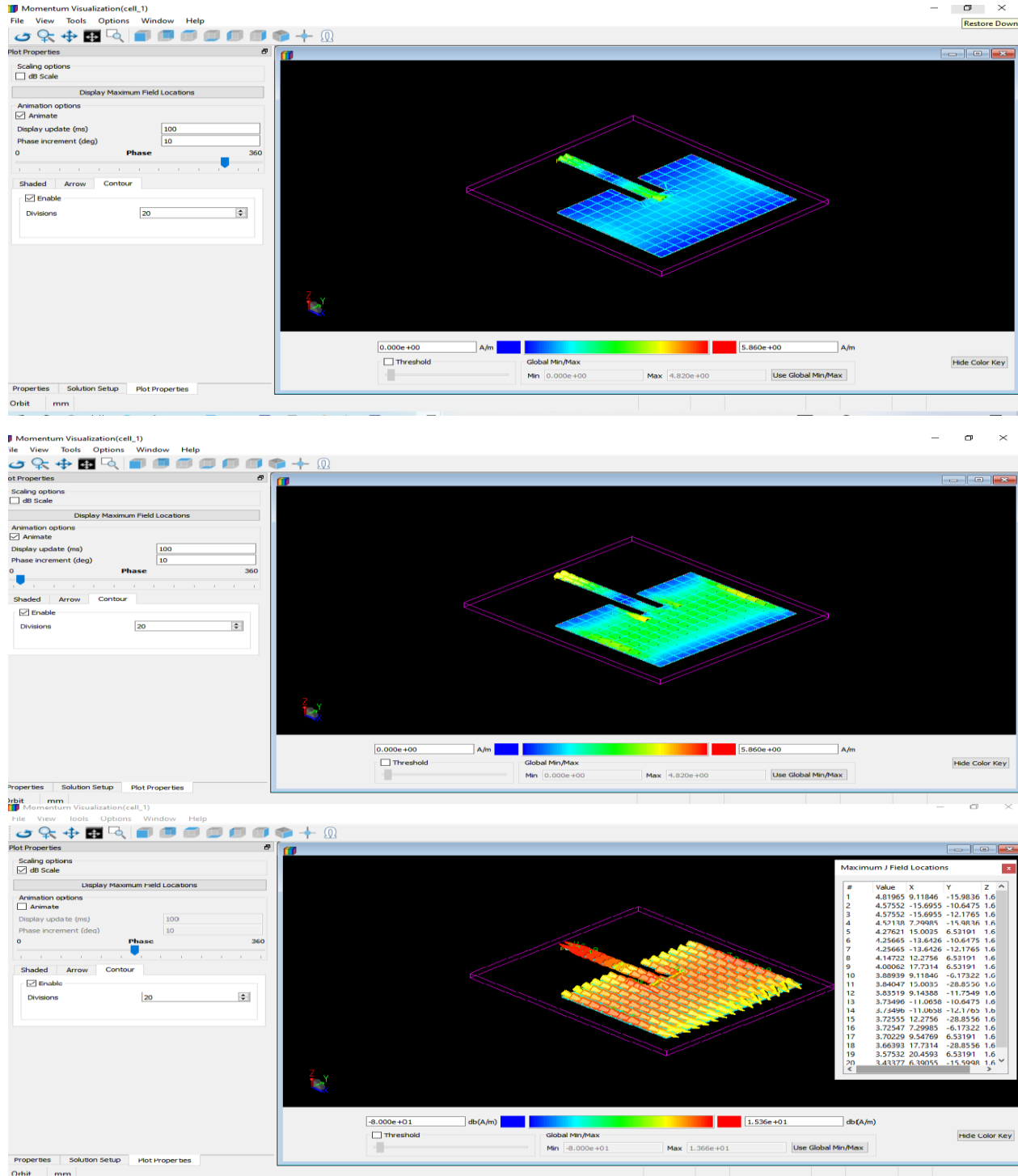


Figure III-10: 3 D view (animated) of the electric field microstrip antenna on ADS Agilent.

Or for more option one can use the far field in the same location as shown in figure III-11. And from there, one can display the device characteristics as well. The characteristics are shown in figure III-12.

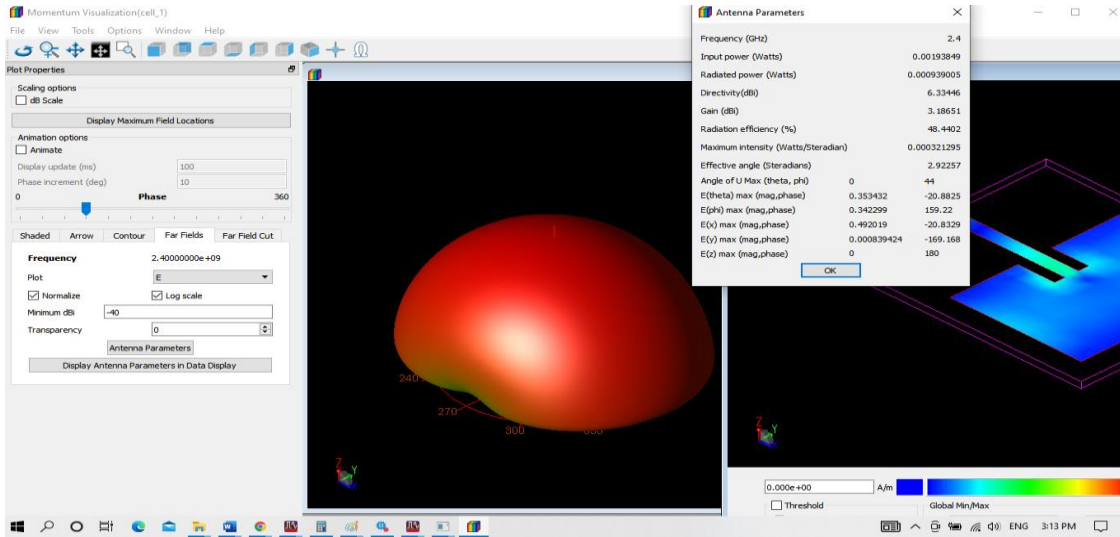


Figure III-11: Far field View of the microstrip electric field.

Antenna Parameters vs Frequency

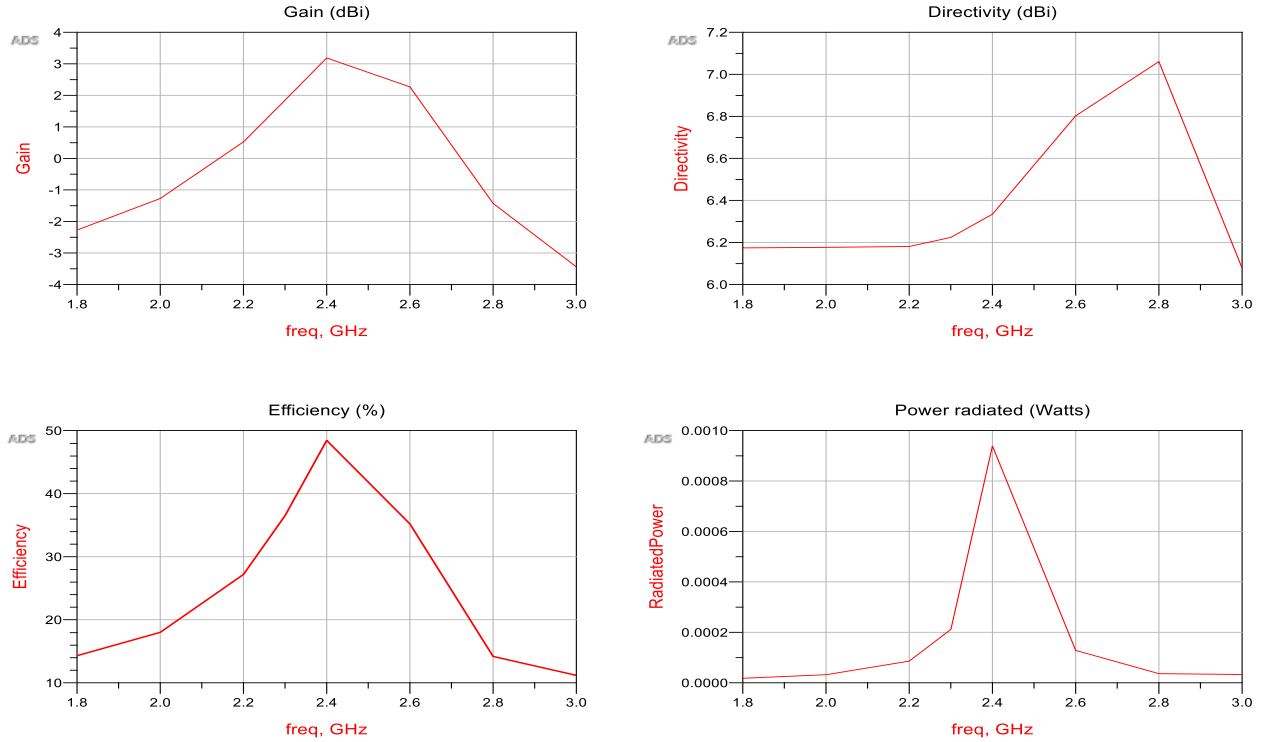
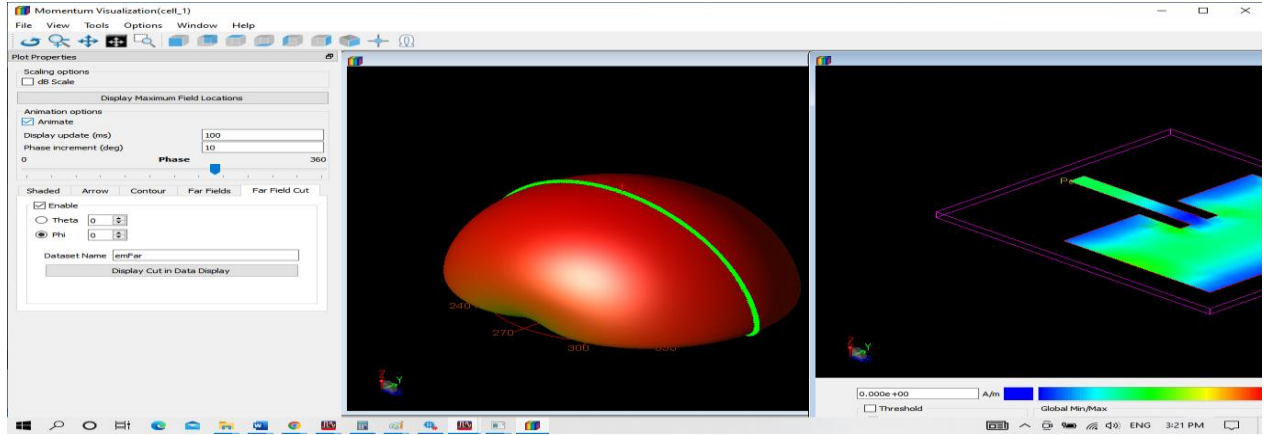


Figure III-12: The microstrip antenna characteristics as function of frequency (from 1.8 to 3.0 GHz)



Dataset: emFar - Jun 15, 2022

Frequency	E_max	Theta_max	Phi_max	Directivity_max	Gain_max	RadiatedPower	InputPower	Efficiency	CutType	CutAngle
2.400E9	0.492	0.000	44.000	6.334	3.187	9.390E-4	0.002	0.484	Phi	0.000

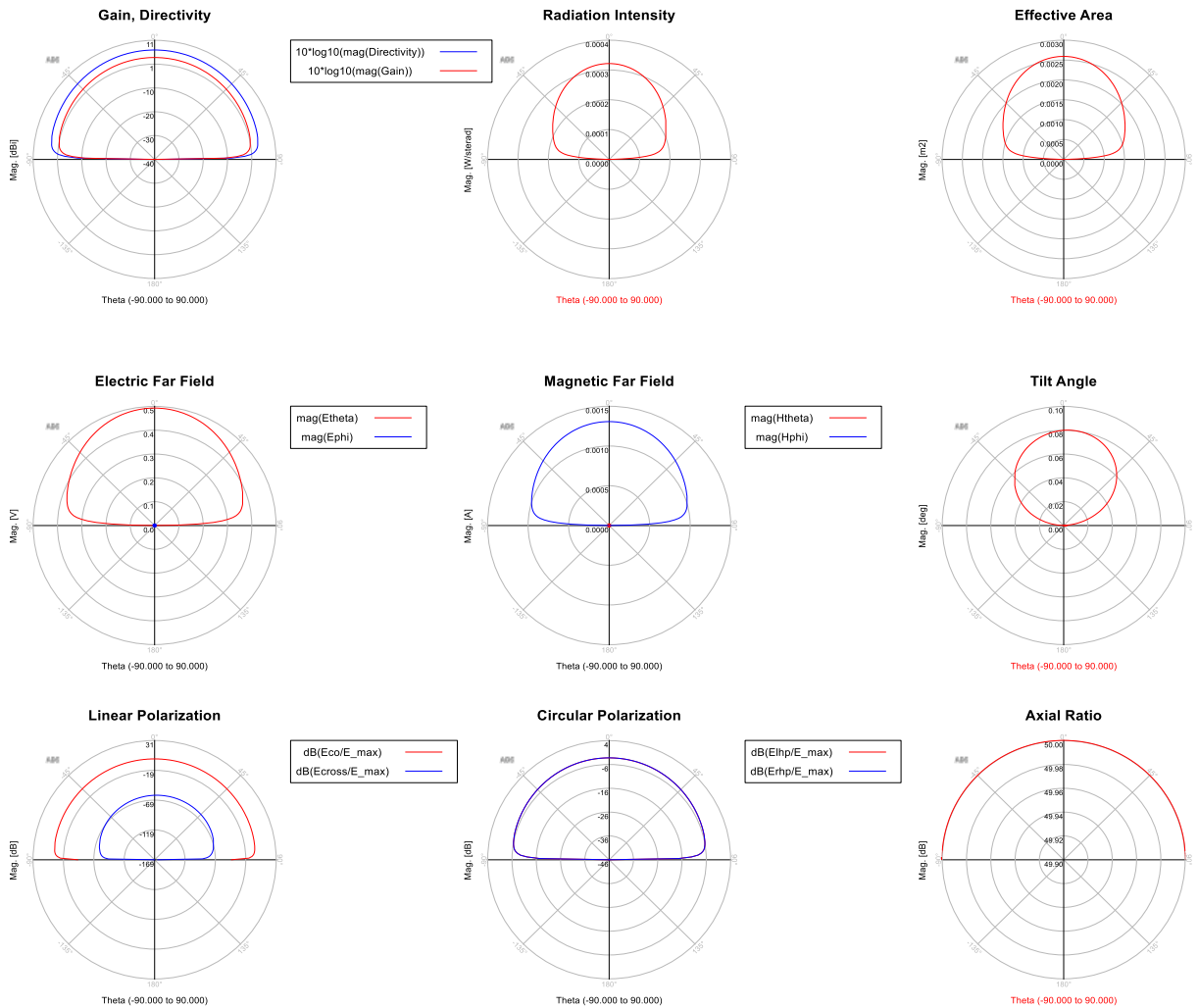


Figure III-13: the top figure shows the Far field windows and possible data display, The bottom presents all the possible characteristics of the antenna device.

Additionally, the Far field icon the displayed window allows to further extract data as shown in figure III-13 -top and bottom. For 5G application, this patch could be just doubled by 4*4 antenna is a basic perspective to a future work.

III-3 CMOS Filter

The ever-increasing congestion of the radio spectrum as a very rare resource, and the need to transmit and receive very large amount of data to support near future's wireless communication services such as big-data networks, 5G (-and beyond) and IoT leads to take advantage of very high frequency ranges where a large usable bandwidth yet has to be discovered. Nevertheless, notable technological challenges are standing relating to the development of advanced RF hardware to enable these modern radio systems.

Certainly, millimeter wave bandpass filters and notch filters are key representatives of this tendency, since they are required to obtain such ultra-wideband radio signals and lessen out-of-band from external RF sources. Many classes of millimeter-wave wide band (Band pass and band stop) Filters in bulk technology CMOS are existing. The stated solutions were mainly aimed at further reducing the physical footprint of the on-chip filter through different design strategies for use in cost-effective and highly integrated RF systems.

III-3-1 CMOS design

Starting by the schematic window, one can design the CMOS circuit

By using spice model files provided a BSIM4 CMOS technology are available under 32nm, 45nm,65nm,90nm and 130nm dimensions but since they all are from 2006 which means old technology, they are used in this section just for training purpose, because they are not compatible with 5G requirements.

As shown in figure III-14 for equivalent circuit, the CMOS is defined by the two different MOS (n-type and p-type), where the NMOS must be directly polarized by negative voltage while the PMOS is inversely biased from the source so, it continuously states ON, and also polarized with fixed potential on gate. The input voltage is sinusoidal (depends on frequency) since it is an amplifier device. To define the NMOS and PMOS, one can use the NETLIST INCLUDE, by which the file data of 130nm CMOS [BSIM4, 2012] is introduced. After simulation, figure III-14

V_{out} and V_{in} versus time are resulting with their sinusoidal forms. From these two graphs, the gain can be concluded via simple equation $(m1-m2)/V_{in}$.

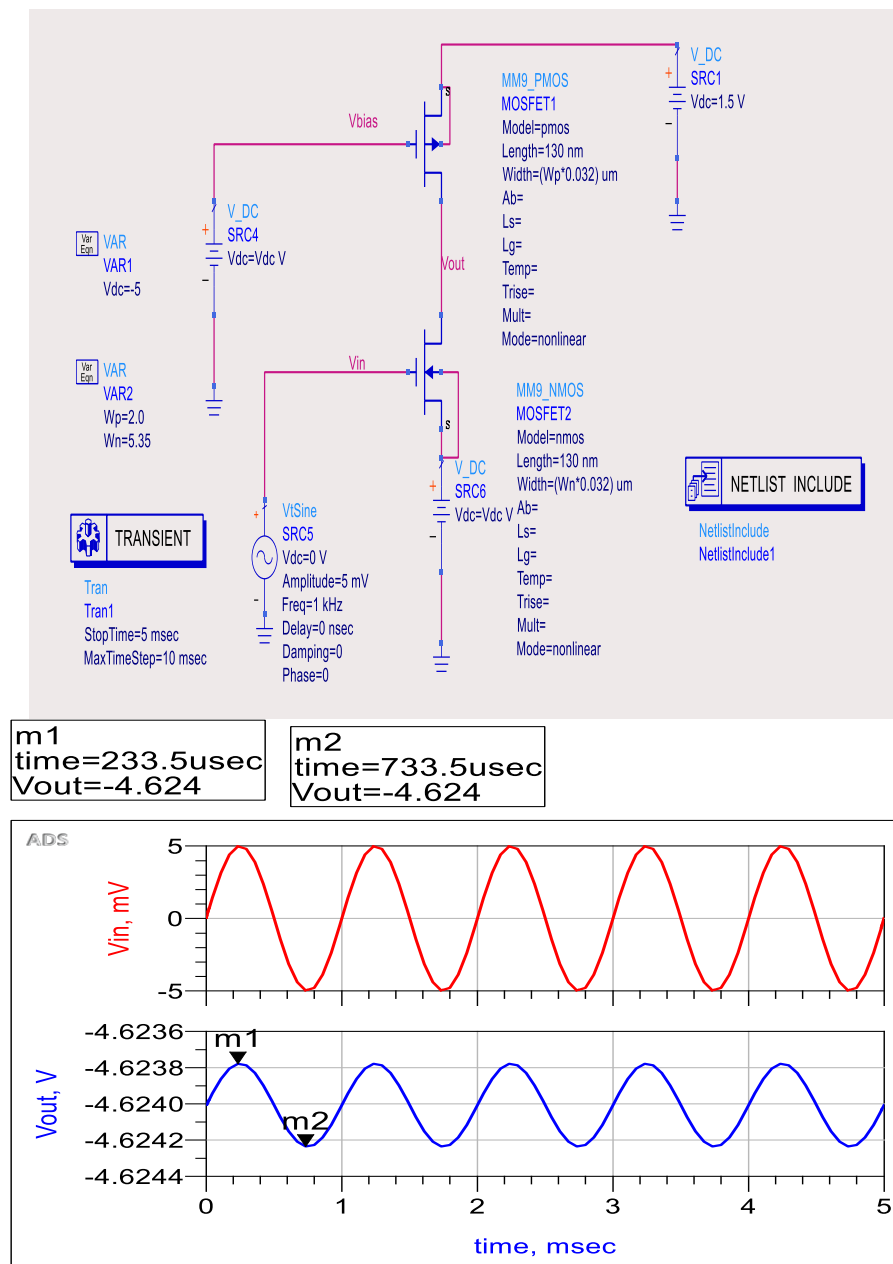


Figure III-14: The equivalent circuit and the response V_{out} (time) of the CMOS.

It is also possible to design the CMOS as physical structure by the mean of layout with introducing the different layers and electrical properties, plus the effect between each layer and the adjacent one. Nevertheless, this technique is very complicated and need much time to cover it. This is a pushing reason toward the lumped elements-based design and it is not that easy but conceivable.

III-3-2 CMOS filter under lumped element form

In order to design a pass band filter, it is typical to start from the low pass filter then just shift the band along the frequency, meaning adding lumped element as example, the following test is executed:

To design a bandpass filter (maximum flat response with 3rd order(N), the center frequency is 2 GHz, and 15% of bandwidth), the input impedance 50 ohms. For this aim, the element values are given by equation III-10 and the elements are obtained by replacing k by 1,2,3 consecutively $g_1 = 1$, $g_2 = 2$ and $g_3 = 1$. Figure III-15 shows how to convert a low pass to the bandpass Filter.

$$g_k = 2\sin\left(\frac{(2k-1)}{2N}\pi\right)$$

III- 10

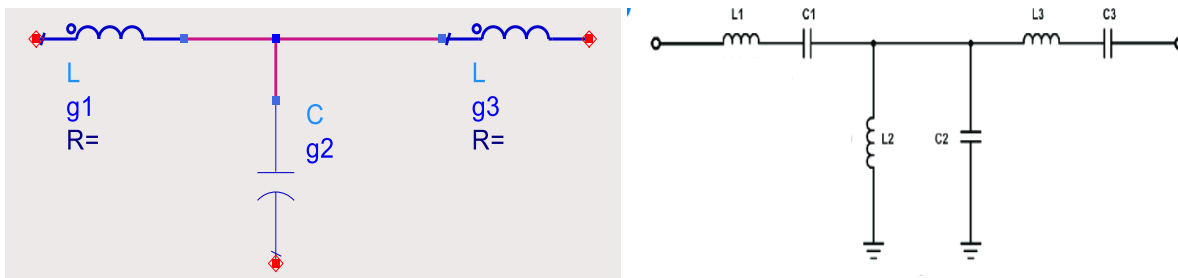


Figure III-15: on the left-low pass, on the right- band pass (3rd order filter).

One can calculate the value of all the element as follow:

From g_1 , L_1 and C_1 formula are

$$\begin{cases} L_1 = \frac{g_1 \times 50}{2\pi \times 2e8 \times 0.15} = 26.5 \text{ nH} \\ C_1 = \frac{0.15}{g_1 \times 2\pi \times 2e8 \times 50} = 0.238 \text{ pF} \end{cases}$$

From g_3 , L_3 and C_3 are

$$\begin{cases} L_3 = \frac{g_3 \times 50}{2\pi \times 2e8 \times 0.15} = 26.5 \text{ nH} \\ C_3 = \frac{0.15}{g_3 \times 2\pi \times 2e8 \times 50} = 0.238 \text{ pF} \end{cases}$$

And from g_2 , L_2 and C_2 are

$$\begin{cases} L_2 = \frac{0.15 \times 50}{2\pi \times 2e8 \times g_2} = 0.298 \text{ nH} \\ C_2 = \frac{g_2}{0.15 \times 2\pi \times 2e8 \times 50} = 21.2 \text{ pF} \end{cases}$$

Thus, by simulation, the results of return loss S_{11} and S_{21} is presented on figure III-17.

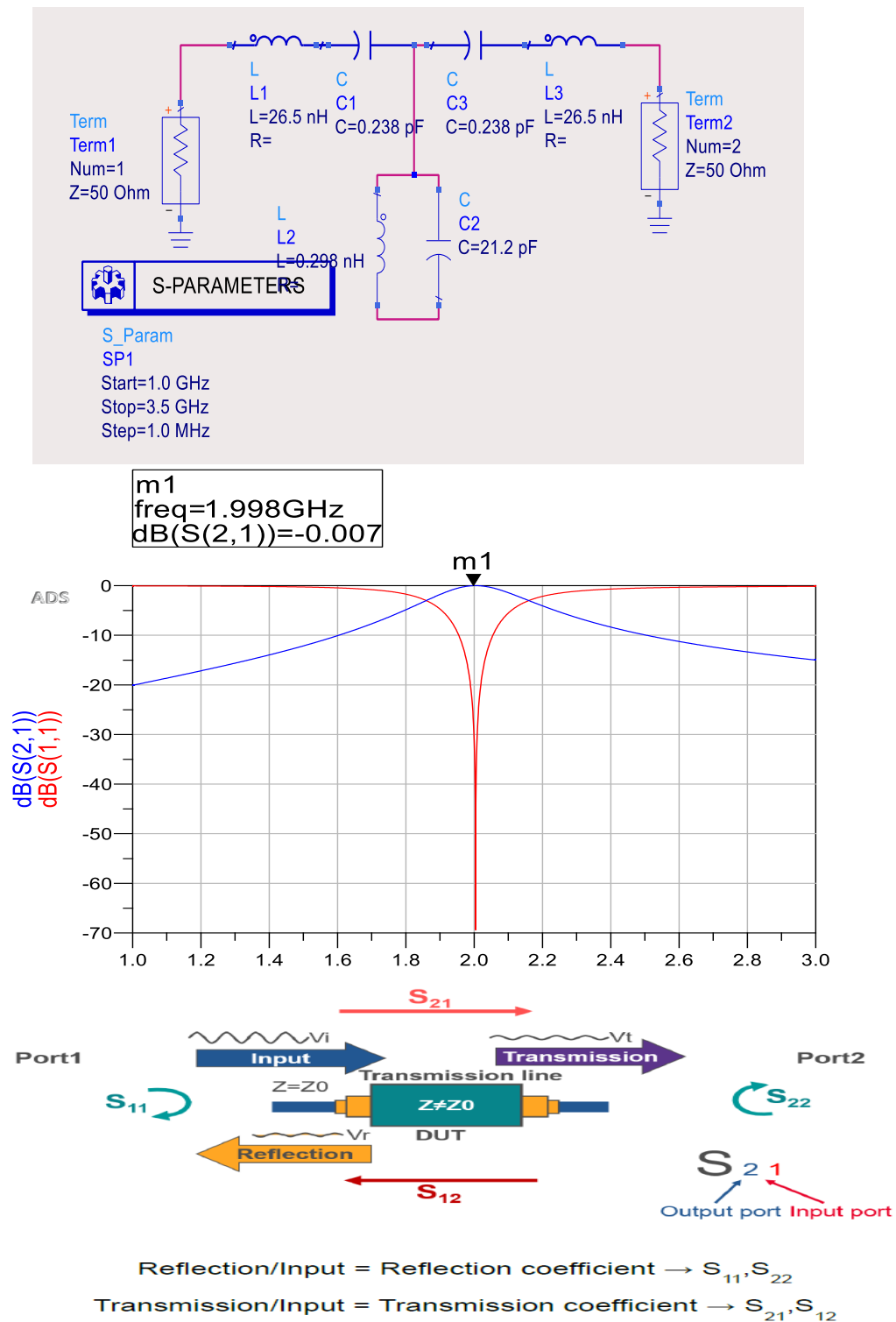


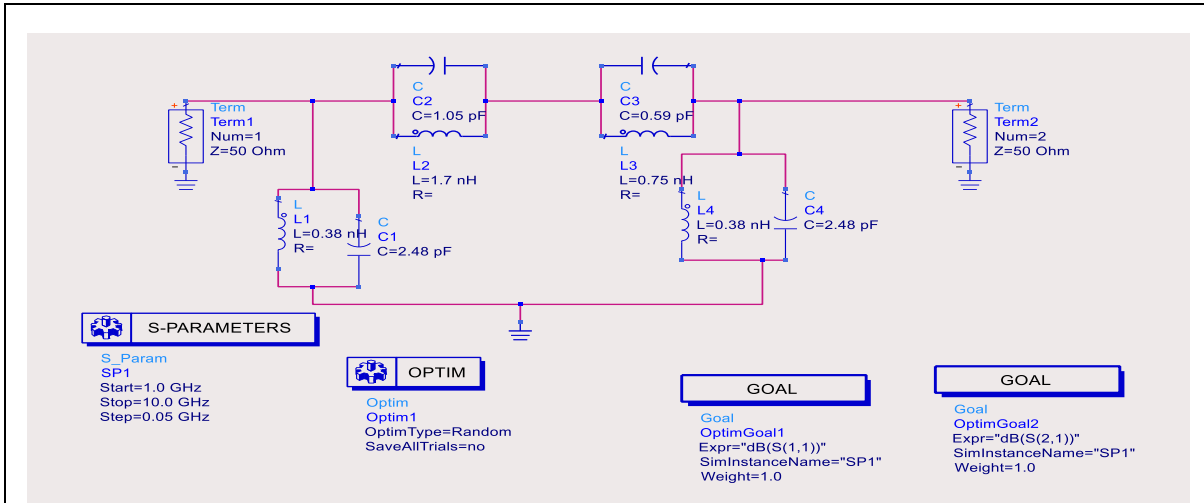
Figure III-17: the schematic circuit of bandpass filter based on lumped elements, the Scattering results and a schematic view of the meaning of scattering parameters for the transmission line (Image of Keysight technologies, [Schweber, 2019]).

As built-in low insertion loss (IL) RF filters are continuously needed for wireless communication system, since high IL reduces spurious free dynamic range. Which requires that filters should be upgraded to adequate everyday applications. For this aim, CMOS-MEMS inductors are used to improve the on-chip bandpass filter performance for a 5 GHz application [Chen, 2018].

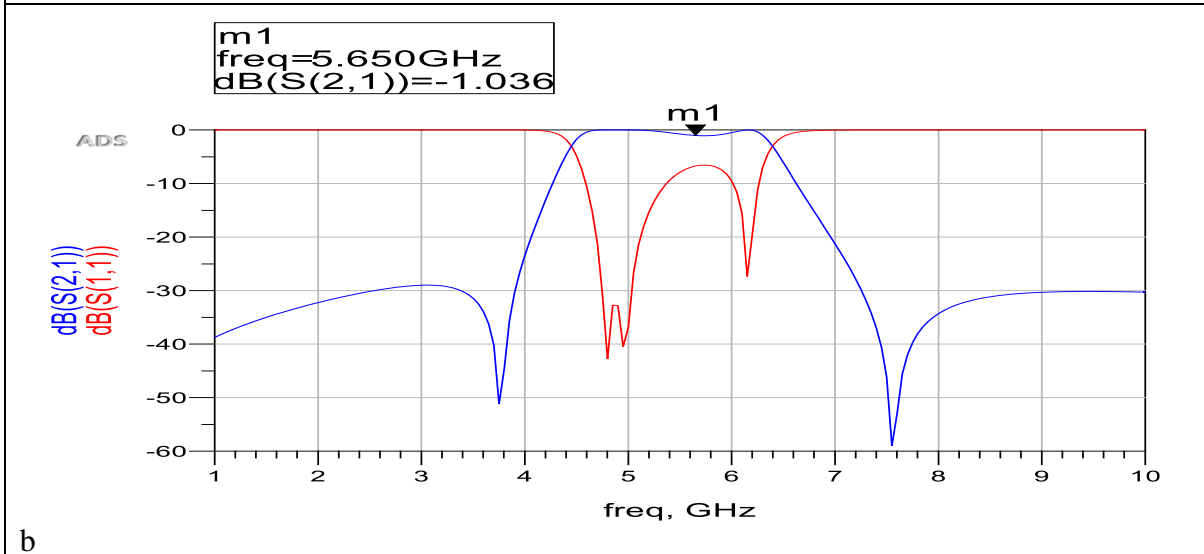
The planned filter was implemented using the TSMC 0.18 μm mono-poly-six metal (1P6M) CMOS process. The on-chip capacitor construction in the CMOS process is metal-insulator-metal (MIM), where the fifth metal layer is the bottom plate and an additional thin metal layer is the top plate between the fifth and sixth metal layers. The dielectric thickness is 38 nm .

CMOS inductors are spiral wound and constructed using the fifth and sixth metal layers and via. The fifth and sixth metal layers are composed of Al and Cu with physical thicknesses of 0.53 and 2.34 μm , respectively. The thick insulating layer between the fifth and sixth metal layers is 1 μm and made of silicon oxide. Passive component dissipation effects must be considered in filter design because non-ideal effects deteriorate filter performance, resulting in an increase of IL, frequency shifts in the passband, and reduction of rejection in the stop band.

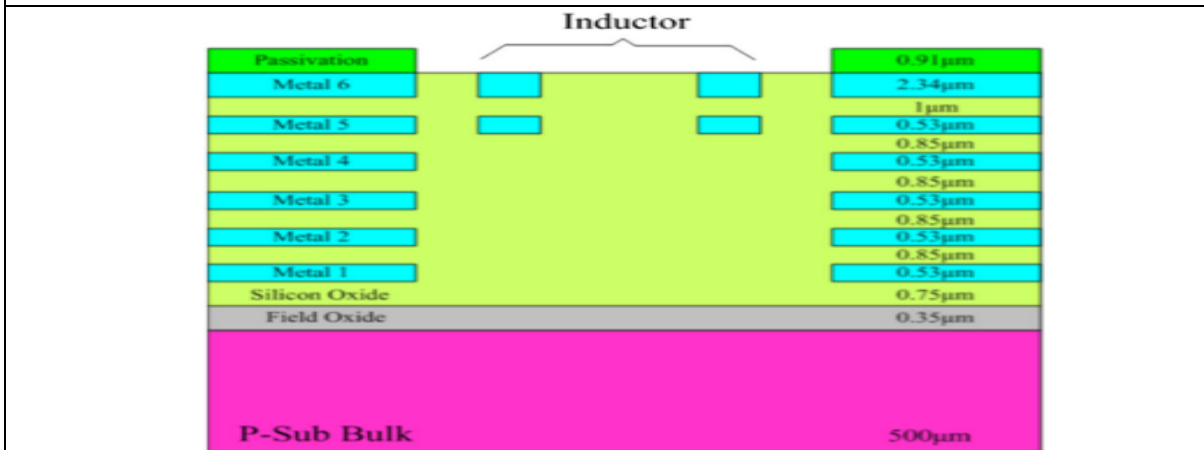
As first step is always specification of the filter, where the frequency range is near 5GHz (4.5 GHz to 5.6 GHz), the insertion loss (<4 dB) and attenuation (<21.5 for frequency under 3.8 GHz). Hence, the value of lumped components can be calculated as previously mentioned and then simulated the equivalent circuit with the obtained element values as represented on Figure III-18-a. The characteristics of this filter is on figure III-18-b. the CMOS under its physical layered form is on Figure III-18-c.



a



b



c [Chen, 2018]

Figure III-18: a- The filter equivalent circuit in ADS. b- The filter characteristics. c- the CMOS technology

References of Chapter III

- [Alayesh, 2007] Mahmoud AyeshAlayesh, 'Analysis and Design of Reconfigurable Multi-Band Stacked Microstrip Patch Antennas (MSAs) for Wireless Applications', Electrical engineering, Matser thesis, The University of New Mexico, 2007
- [BSIM4, 2012] <http://ptm.asu.edu/latest.html>
- [BenHaddi et al, 2020] S.BenHaddi, A.Zugari, A.Zakriti and S.Achraou, 'A Compact Microstrip T-Shaped Resonator Band Pass Filter for 5G Applications', IEEE, 2020
- [Chen, 2018] Ja-Hao Chen, 'Enhancement of 5 GHz on-chip bandpass filter performance by using CMOS-MEMS inductors', *Microsystem Technologies* 24:2371–2377,2018
- [Choudhury, 2015] D. Choudhury, "5G wireless and millimeter wave technology evolution: An overview," 2015 IEEE MTT-S International Microwave Symposium, Phoenix, AZ, pp. 1-4, 2015
- [EverythingRF, 2021] EverythingRF, <https://www.everythingrf.com/community/5g-frequency-bands>, 2021
- [Gao and Rebeiz, 2021] Li Gao and Gabriel M. Rebeiz, 'Wideband Bandpass Filter for 5G Millimeter Wave Application in 45-nm CMOS', *IEEE Electron Device Letters*, vol. 42, No. 8, 2021
- [Qing and Chen, 2010] Xianming Qing and Zhi Ning Chen, 'Comments on 'Measuring the Impedance of Balanced Antennas by an S-Parameter Method'', *IEEE Antennas and Propagation Magazine*, Vol. 52, No.1, February 2010
- [Shen et al, 2001] J. Shen, G. Hong and M.J. Lancaster, "Microstrip filters for RF/microwave applications", John Wiley & Sons Inc., U.S.A. 2001
- [Richard et al, 2018] Richard J. Cameron, Chandra M. Kudsia, Raafat R. Mansour, "Microwave Filters for Communication Systems", John Wiley & Sons, Inc, 2018
- [Rampnoux, 2003] E. Rampnoux, Analyse, "conception et réalisation de filtres planaires millimétriques appliqués à la radiométrie spatiale", thèse de doctorat en Electronique des Hautes Fréquences et Optoélectronique, universite de limoges, 2003

[Schweber, 2019] Bill Schweber, <https://www.analogictips.com/what-are-the-functions-and-principles-of-s-parameters-part-1/>, An EE word online resource, Analog IC, october,2019

[Park et al, 2019] J. Park, S. Lee, D. Lee, and S. Hong, “A 28 GHz 20.3%-transmitterefficiency 1.5-phase-error beamforming front-end IC with embedded switches and dual-vector variable-gain phase shifters,” IEEE Int. SolidState Circuits Conf. (ISSCC) Dig. Tech. Papers, pp. 176–178, Feb. 2019, doi: 10.1109/ISSCC.2019.8662512.

[Pozzar, 2012] D.M. Pozzar, Microwave engineering, 3rd edition, John Wiley sons, U.S.A. 2012

[Yang, et al, 2018] B. Yang, Z. Yu, J. Lan, R. Zhang, J. Zhou, and W. Hong, “Digital beamforming-based massive MIMO transceiver for 5G millimeter-wave communications,” IEEE Trans. Microw. Theory Techn., vol. 66, no. 7, pp. 3403–3418, doi: 10.1109/TMTT. 2018. 2829702, Jul. 2018

[Y.Benotmane, 2014] Y.Benotmane El amine CHIKH , “Conception des Filtres Opérants en Bande S et C en Technologie Guides d’Ondes Intégrés aux Substrats “, thèse de doctorat en réseaux et systèmes de télécommunications, universite aboubekr belkaid – TLEMEN, 2014

Conclusion

Regarding the important and critical role of the filter in the transceiver block, the present work is dedicated to the study of two types of filters for the benefit of 5G.

The microstrip antenna was created in order to permit a practical integration of antenna and other control circuits of a communication system onto a shared printed circuit board or semiconductor chip [Carver and Mink, 1981; Pozar, 1992]. further with other consequential benefits, integrated circuit technology allowed high dimensional accuracy, which if not was tough to realize with conventional industrial methods.

The substrate in microstrip is with a high importance since it provides adequate spacing and mechanical support between the radiating patch and the ground plane. Often, substrate with high dielectric-constant materials are used to load the patch and reduce its size at the expense of the bandwidth and radiation efficiency [Mohamed, 2017; Lakshmu et al, 2017].

The dielectric substrate is of a certain thickness d , having complete metallization on one side and a metallic patch on the other. Usually, the thin of substrate d has to be very small to the wavelength λ . The metal patch on the front surface can have different shapes, a rectangular shape is the one chosen in this work. The antenna can be excited via various methods [Pozar, 1992; Pozar and Schawbert, 1995]. the general approach is to feed from a microstrip line, connecting the microstrip antenna to the center of one of its edges. The microstrip line can be connected to a power circuit or directly alimented via connecting a signal source between the microstrip line and the ground plane.

The microstrip antenna produces maximum radiation in the broadside direction perpendicular to the substrate and ideally no radiation along the substrate surface. This leads to define the effective substrate dielectric. The size of the antenna is usually designed such that the antenna resonates at the operating frequency, producing a real input impedance. For a rectangular microstrip antenna, the length L is needed to be equal to $\lambda/2$ in the dielectric medium. While the width of the antenna W determines the level of the input impedance Z_{in} . The microstrip antenna can be of as a rectangular cavity with open sidewalls. The fringing fields through the open sidewalls are responsible for the radiation.

As well, numerous millimeter-wave broadband BPFs and BSFs categories in low-cost mass CMOS technology are existing primarily aiming at further reducing the physical footprint of the on-chip filter through different design strategies for use in highly integrated and cost-effective RF systems.

For these objectives filters based microstrip and CMOS technology was explored. Analytical method was followed to obtain the microstrip parameters based on the central frequency designed in this work, a 2.4 GHz was selected. Then a design was made via circuit window leading to the microstrip layout which consists on the real physical band pass filter (microstrip). As second section, a CMOS transistor was designed under two forms, the electrical schematic with using data file data of 130nm CMOS [BSIM4, 2012]. This type of file contains almost all the fabrication parameters and electrical properties and also the layers constituent definitions. The second way was by mean of analytical study to obtain the lumped elements of low pass filter, then convert it to band pass filter. Then simulation was done with circuit schematic. The reached results were enough satisfying for master project.

References of Conclusion

[BSIM4, 2012]. <http://ptm.asu.edu/latest.html>

[Carver and J. W. Mink, 1981] K. R. Carver and J. W. Mink, "Microstrip Antenna Technology," IEEE Transactions on Antennas and Propagation', Vol. 29, No. 1, pp. 2-24. doi:10.1109/TAP.1981.1142523, 1981,

[Mohamed, 2017] Mohamed BE, Design and Analysis of Rectangular Microstrip Patch Array Antenna for Fifth Generation of Mobile Technology, SciFed Journal of Telecommunic 1:1, pg.1-9, 2017

[Lakshmu et al, 2017] M. Lakshmu Naidu, B. Rama Rao, C. Dharma Raj, Compact Rectangular Microstrip Patch Antenna with Defected Ground Structure (DGS) of Swastik Shape for LTE Applications, International Journal of Applied Engineering Research ISSN 0973-4562 Volume 12, Number 20, pp. 10063-10067, 2017

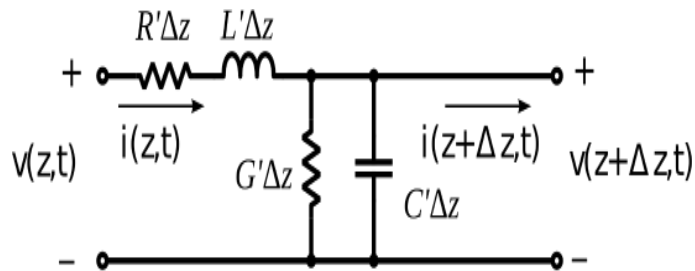
[Pozar, 1992] Pozar, D.M, 'Microstrip Antennas'. Proceedings of the IEEE, 80, 79-91. <https://doi.org/10.1109/5.119568> , 1992

[Pozar and Schaubert, 1995] Pozar, D.M. and Schaubert, D.H, 'Microstrip Antennas', John Wiley & Sons Ltd., Hoboken. <https://doi.org/10.1109/9780470545270>, 1995

Appendix A

A-1 Equivalent circuit

Because the voltage and current of a transmission line change along the length z (and over the time t), one needs to characterize it by using a distributed circuit model and considering an infinitesimal line of length Δz . The currents produce a magnetic field between the conductors by Ampere's law, causing magnetic flux. When currents are time-varying, so is the magnetic flux, and a voltage variation along the conductor based on electromotive force is induced by Faraday's law trying to drive the currents oppositely by Lenz's law. This behavior can be modeled by a series inductor $v = L \frac{di}{dt}$. Meanwhile, the two separated conductors form a capacitor. Since the upper and lower conductors of adjacent infinitesimal lines are connected respectively, the capacitive behavior of an infinitesimal line can be modeled by a shunt capacitor. Also, due to the presence of imperfect conducting and imperfect insulating materials, voltage drop along the conducting line and leakage current between them, and this can be translated by a series resistor and a shunt conductor, respectively. The resulting equivalent circuit of transmission line is shown in figure A-1, where R , L , G , C represent resistance, inductance, conductance, and capacitance



per unit length. Transmission line is lossless in the absence of R and G .

FigureA-1: Lumped-element equivalent circuit transmission line model [Ellingson, 2018].

A-1-1 Role of different components:

1-Inductance L'

The inductance makes the current appear to have inertia, which means that with a large inductance it is difficult to increase or decrease the flow of current at any given point. A large inductance L causes the wave to travel slower, just as waves travel slowly down a heavy cord

than a light string. Also, the large inductance increases the surge impedance of the line (extra voltage is needed to drive the same AC-current through the line).

2-Capacitance C

The capacitance controls how much the gathered-up electrons within each conductor repel, attract, or divert the electrons in the other conductor. By deflecting some of these bundled electrons, the wave's speed and its strength (voltage) are both reduced. With a larger capacitance C , there is less repulsion, since the other line is always opposite charged, partially cancels out these repulsive forces inside each conductor. Larger capacitance equals weaker restoring forces, which slightly slows down the movement of the wave and furthermore gives the TL a lower surge impedance (less voltage needed to drive the same AC-current through the line).

3-Resistance R

It corresponds to the internal resistance of the two lines combined. It dissipates a small part of the voltage along the line as heat left in the conductor, causing the current unchanged. Usually, at radio frequencies, the line resistance is very small, compared to the inductive reactance ωL . For simplicity, it is taken as zero, and any voltage dissipation or wire heating being taken into account after the fact, with slight corrections to the lossless line. calculation deducted later, or simply ignored.

4-Conductance G

The ability of current to leak from one line to the other represents the conductance between the lines. So, higher G dissipates more current as heat, deposited in all what can serve as insulation between the two conductors, generally, wire insulation (as well as air) is quite good. The conductance is almost zero compared to the capacitive susceptance ωC it is why it is treated as if it were zero in purpose to simplifying; the caveat is that materials that are good insulation at low frequencies are often leaky at very high frequencies.

These L , C , R and G parameters depend on the material used to build the cable or feedline. They all change with frequency and while R , and G tend to increase for higher frequencies, L and C tend to drop.

A-2 The telegrapher equations

The equations that govern the potential $v(z,t)$ and current $i(z,t)$ along a transmission line are derived, that is oriented along the z axis. For this, the lumped-element model is employed as

follow: -To start, the voltages and currents are defined as shown in figure A-1. assigning the variables $v(z,t)$ and $i(z,t)$ to represent the potential and current on the left side of the segment, with reference polarity and direction. Similarly the variables $v(z+\Delta z,t)$ and $i(z+\Delta z,t)$ are assigned to represent the potential and current on the right side of the segment, also with reference polarity and direction.

By applying Kirchoff's voltage law from the left port, through $R'\Delta z$ and $L'\Delta z$, and returning via the right port, one obtains:

$$v(z, t) - (R'\Delta z)i(z, t) - (L'\Delta z) \frac{\partial i(z,t)}{\partial t} - v(z + \Delta z, t) = 0 \quad \text{A-1}$$

Moving terms referring to current to the right side of the equation and then dividing through by Δz , one obtains

$$-\frac{v(z+\Delta z,t)-v(z,t)}{\Delta z} = R'i(z, t) + L' \frac{\partial i(z,t)}{\partial t} \quad \text{A-2}$$

Then taking the limit as $\Delta z \rightarrow 0$:

$$-\frac{\partial v(z,t)}{\partial z} = R'i(z, t) + L' \frac{\partial i(z,t)}{\partial t} \quad \text{A-3}$$

Applying Kirchoff's current law at the right port, one can get obtain:

$$i(z, t) - (G'\Delta z)v(z + \Delta z, t) - (C'\Delta z) \frac{\partial v(z+\Delta z,t)}{\partial t} - i(z + \Delta z, t) = 0 \quad \text{A-4}$$

Moving terms referring to potential to the right side of the equation and then dividing through by Δz , the last equation becomes:

$$-\frac{i(z+\Delta z,t)-i(z,t)}{\Delta z} = G' v(z + \Delta z, t) + C' \frac{\partial v}{\partial t}(z + \Delta z, t) \quad \text{A-5}$$

Taking the limit as $\Delta z \rightarrow 0$:

$$-\frac{\partial i(z,t)}{\partial z} = G' v(z, t) + C' \frac{\partial v(z,t)}{\partial t} \quad \text{A-6}$$

Equations A-3 and A-6 are the telegrapher's equations. These coupled differential equations are simultaneously solved. The time-domain telegrapher's equations are usually more than enough.

So, if only interested in the response to a sinusoidal stimulus, then considerable simplification is possible using phasor representation.

First $\tilde{V}(z)$ and $\tilde{I}(z)$ phasors are defined through the typical relationship:

$$v(z, t) = \text{Re}\{\tilde{V}(z)e^{j\omega t}\} \quad \text{A-7}$$

$$i(z, t) = \text{Re}\{\tilde{I}(z)e^{j\omega t}\} \quad \text{A-8}$$

As one can see

$$\frac{\partial v(z, t)}{\partial z} = \frac{\partial}{\partial z} \text{Re}\{\tilde{V}(z)e^{j\omega t}\} = \text{Re}\left\{\left[\frac{\partial \tilde{V}(z)}{\partial z}\right] e^{j\omega t}\right\} \quad \text{A-9}$$

In other words, $\frac{\partial v(z, t)}{\partial z}$ expressed in phasor representation is simply $\frac{\partial \tilde{V}(z)}{\partial z}$; and

$$\begin{cases} \frac{\partial i(z, t)}{\partial t} = \frac{\partial}{\partial t} \text{Re}\{\tilde{I}(z)e^{j\omega t}\} = \text{Re}\left\{\left[\frac{\partial \tilde{I}(z)}{\partial t}\right] e^{j\omega t}\right\} \\ \frac{\partial i(z, t)}{\partial t} = \text{Re}\{[j\omega \tilde{I}(z)]e^{j\omega t}\} \end{cases} \quad \text{A-10}$$

Accordingly, $\frac{\partial i(z, t)}{\partial t}$ expressed in phasor representation is $j\omega \tilde{I}(z)$. Therefore, equation A-3 and equation A-6 are re-written in phasor representation as:

$$\begin{cases} -\frac{\partial \tilde{V}(z)}{\partial z} = [R' + j\omega L']\tilde{I}(z) \\ -\frac{\partial \tilde{I}(z)}{\partial z} = [G' + j\omega C']\tilde{V}(z) \end{cases} \quad \text{A-11}$$

So, the last equations system represents the telegrapher's equations in phasor representation.

The principal advantage of these equations over the time-domain versions is that it is no longer need to struggle with derivatives with respect to time – only derivatives with respect to distance remain. This considerably simplifies the equations.

A-3 TEM Transmission Line -wave Equation

By knowing that TEM transmission line aligned along the z axis, the Telegrapher's Equations under its phasor form relate the potential phasor $\tilde{V}(z)$ to the current phasor $\tilde{I}(z)$ and to the lumped-element model equivalent circuit parameters (R' , G' , C' , L') as equation A-11. But an obstacle stands up when using these equations, which is the need to solve both equations for either the potential or the current. So, reducing these equations to a single equation is solution it

is called a wave equation, that is more convenient to use and provides some additional physical insight.

One can start by differentiating both sides of Equation A-11 for voltage with respect to z , and eliminating $\tilde{I}(z)$ for the Equation A-11 for the current, and the equation system obtained is:

$$\begin{cases} -\frac{\partial^2}{\partial z^2} \tilde{V}(z) = [R' + j\omega L'] \frac{\partial}{\partial z} \tilde{I}(z) \\ -\frac{\partial^2}{\partial z^2} \tilde{V}(z) = [R' + j\omega L'] [G' + j\omega C'] \tilde{V}(z) \end{cases} \quad \text{A-12}$$

The second equation in A-12 system is re-written as follows:

$$\frac{\partial^2}{\partial z^2} \tilde{V} - \gamma^2 \tilde{V}(z) = 0 \quad \text{A-13}$$

$$\begin{cases} \frac{\partial^2}{\partial z^2} \tilde{V} - \gamma^2 \tilde{V}(z) = 0 \\ \frac{\partial^2}{\partial z^2} \tilde{I}(z) - \gamma^2 \tilde{I}(z) = 0 \end{cases} \quad \text{A-14}$$

With $\gamma^2 = (R' + j\omega C')(G' + j\omega C')$, and γ (/m) is the propagation constant which captures the effect of materials, geometry, and frequency to determine how the potential and current vary with distance on a TEM transmission line. Both $\tilde{V}(z)$ and $\tilde{I}(z)$ satisfy the same linear homogeneous differential equation. They can differ by no more than a multiplicative constant which must be an impedance known as the characteristic impedance. The general solutions to equations A-14 (the wave equations) are:

$$\begin{cases} \tilde{V}(z) = V_0^+ e^{-\gamma z} + V_0^- e^{+\gamma z} \\ \tilde{I}(z) = I_0^+ e^{-\gamma z} + I_0^- e^{+\gamma z} \end{cases} \quad \text{A-15}$$

Where $V_0^+, V_0^-, I_0^-,$ and I_0^+ are complex-valued constants. These equations represent sinusoidal waves propagating in $+z$ and $-z$ directions along the line length. The constants may represent sources, loads, or simply discontinuities in the materials and/or geometry of the line. The values of the constants are determined by boundary conditions (constraints on $\tilde{V}(z)$ and $\tilde{I}(z)$ at some position(s) along the line).

A-4 Characteristic Impedance

The ratio of voltage to current for a wave that is propagating in single direction on a transmission line characterizes the characteristic impedance already mentioned. It is a crucial parameter for

analysis and design the circuits and systems using transmission lines. To define this parameter and derive an expression for this parameter in terms of the equivalent circuit model, let's consider a transmission line aligned along the z axis. Using the results from last section (A-3), the phasor form of the wave equations A-14 and since $\tilde{V}(z)$ is potential and $\tilde{I}(z)$ is current, that constant is expressed in units of impedance. More precisely, it is the characteristic impedance, so-named because it only counts on the materials and cross-sectional geometry of the transmission line that is on the elements that determine γ and not length, excitation, termination, or position along the line. To obtain the characteristic impedance, first recall that the general solutions to equations A-14 are equations A-15. Also, the use of the telegrapher's equations A-11, one can begin by differentiating A-15 with respect to z , which yields:

$$\frac{\partial}{\partial z} \tilde{V}(z) = \gamma [V_0^+ e^{-\gamma z} - V_0^- e^{+\gamma z}] \quad \text{A-16}$$

Eliminating $\frac{\partial}{\partial z} \tilde{V}(z)$ from the equation by using equation A-11 for voltage, one can obtain

$$\gamma [V_0^+ e^{-\gamma z} - V_0^- e^{+\gamma z}] = [R' + j\omega L'] \tilde{I}(z) \quad \text{A-17}$$

So, the current is:

$$\tilde{I}(z) = \frac{\gamma}{R' + j\omega L'} [V_0^+ e^{-\gamma z} - V_0^- e^{+\gamma z}] \quad \text{A-18}$$

And by comparing the equation A-15 for the current, one can note:

$$\begin{cases} I_0^+ = \frac{\gamma}{R' + j\omega L'} V_0^+ \\ I_0^- = \frac{-\gamma}{R' + j\omega L'} V_0^- \end{cases} \quad \text{A-19}$$

Thus,

$$\begin{cases} Z_0 = \frac{R' + j\omega L'}{\gamma} \\ \frac{V_0^+}{I_0^+} = \frac{-V_0^-}{V_0^-} = Z_0 \end{cases} \quad \text{A-20}$$

As expected, it is found that coefficients in the potentials and currents equations are linked by an impedance, namely, z_0 . It can be written entirely in terms of the equivalent circuit parameters by substituting γ yielding:

$$Z_0 = \sqrt{\frac{R' + j\omega L'}{G' + j\omega C'}}$$

A-21

It is important to know that Z_0 is not the ratio of $\tilde{V}(z)$ to $\tilde{I}(z)$ in general; rather, Z_0 relates only the potential and current waves traveling in the same direction.

To conclude, the transmission lines are (as a rule) designed to have an all-real characteristic impedance, i.e., with no imaginary part. This is because the imaginary component of an impedance represents energy storage (capacitors and inductors), while the objective of a transmission line is energy transfer.

A-5 Wave propagation on a TEM TL.

by demonstrating that the phasor equations A-15 when it assumed that the transmission line is aligned along the z axis represent sinusoidal waves, it points out some important features. First, one can define real-valued quantities α and β as the real and imaginary components of γ as $\gamma = \alpha + j\beta$ and then

$$\begin{cases} e^{\pm\gamma z} = e^{\pm(\alpha+j\beta)z} = e^{\pm\alpha z} e^{\pm j\beta z} \\ \text{Re}\{e^{\pm\gamma z} e^{j\omega t}\} = e^{\pm\alpha z} \cos(\omega t \pm \beta z) \end{cases} \quad \text{A-22}$$

it is easier to interpret γ expression by reverting to the time domain, consequently, $e^{-\gamma z}$ represents a damped sinusoidal wave traveling in the $+z$ direction, and $e^{+\gamma z}$ represents a damped sinusoidal wave traveling in the $-z$ direction. By using $\tilde{V}^+(z)$ and $\tilde{I}^+(z)$ associated with a wave propagating in the $+z$ direction. Then

$$\tilde{V}^+(z) = V_0^+ e^{-\gamma z} \quad \text{A-23}$$

or equivalently in the time domain:

$$v^+(z, t) = \text{Re}\{\tilde{V}^+(z) e^{j\omega t}\} = \text{Re}\{V_0^+ e^{-\gamma z} e^{j\omega t}\} = |V_0^+| e^{-\alpha z} \cos(\omega t - \beta z + \psi) \quad \text{A-24}$$

where ψ is the phase of V_0^+ .

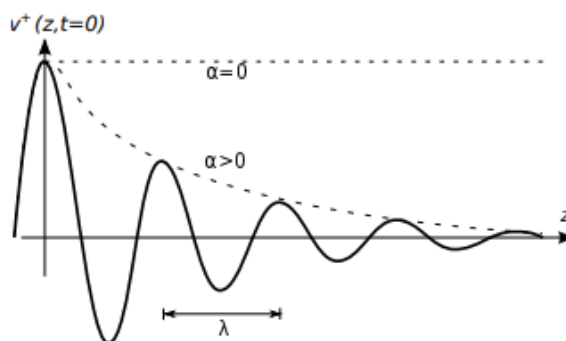


Figure A-2: The potential $v^+(z, t)$ of the wave traveling in the +z direction at $t=0$ for $\psi=0$

Figure A-2 shows $v^+(z, t)$ and from fundamental wave theory one can recognize β (rad/m) which is equal to imaginary part of γ , and it is the rate of phase changing versus to distance. Subsequently the wavelength in the line is:

$$\lambda = \frac{2\pi}{\beta} \quad \text{A-25}$$

Also, α which is the real part of γ given by 1/m or Np/m (nepers per meter) and it represents the attenuation constant. α is the rate at which magnitude diminishes as a function of distance. Noting that $\alpha=0$ for a wave that does not diminish in magnitude with increasing distance, in which case the transmission line is lossless. If α is positive, then the line is lossy (or low loss), and in this case the rate at which the magnitude decreases with distance increases with α .

To consider the speed of the wave (phase velocity at which a point of constant phase seems to move through space or what is the distance Δz does a point of constant phase traverse in time Δt , one can start with the phase of $v^+(z, t)$. $v^+(z, t)$ can be written generally as equation A-26 (1st) and at some time Δt later and some point Δz further along (2nd) with ϕ is a constant:

$$\begin{cases} \omega t - \beta z + \phi \\ \omega(t + \Delta t) - \beta(z + \Delta z) + \phi \end{cases} \quad \text{A-26}$$

The phase velocity $v_p = \Delta z / \Delta t$ when these two phases are equal; yield to $v_p = \frac{\omega}{\beta}$. Thus, $v_p = \lambda f$

A-6 Lossless and Low-Loss Transmission Lines

Generally, the loss in a transmission line is small enough that can be neglected leading to simplifying several aspects of transmission line theory.

Initially, the loss means a reduction of magnitude as a wave propagates through space. And knowing that in the lumped-element equivalent circuit model, the parameters R' and G' of the represent physical mechanisms associated with loss (R' represents the resistance of conductors, and G' represents the undesirable current induced between conductors through the spacing material).

Furthermore, since the propagation constant $\gamma = \sqrt{(R' + j\omega L')(G' + j\omega C')}$, low loss is defined as meeting the conditions $R' \ll \omega L'$ and $G' \ll \omega C'$. In this case, the propagation constant simplifies as $\beta \approx \sqrt{(j\omega L')(j\omega C')} \approx j\omega\sqrt{L'C'}$

and subsequently for low loss approximations one can obtain:

$$\left\{ \begin{array}{l} \alpha \triangleq \text{Re}\{\gamma\} \approx 0 \\ \beta \triangleq \text{Im}\{\gamma\} \approx \omega\sqrt{L'C'} \\ v_p = \frac{\omega}{\beta} \approx \frac{1}{\sqrt{L'C'}} \\ Z_0 = \sqrt{\frac{R' + j\omega L'}{G' + j\omega C'}} = \sqrt{\frac{L'}{C'}} \end{array} \right. \quad \text{A-27}$$

Of course, if the transmission line is strictly lossless ($R'=G'=0$) so these are the exact expressions. In practice, these approximations are so commonly used, because typically, practical transmission lines satisfy the conditions for low loss and the resulting expressions are much simpler. It is further observed that Z_0 and v_p are approximately independent of frequency when these conditions met.

But even if low loss does not mean that there is no loss, it is common to apply these expressions even for R' and/or G' is significantly large to yield important loss. As instance, a used coaxial cable to connect an antenna on a tower to a radio near the ground usually has important loss that consider in the analysis and design process, but still satisfies the low-loss expressions for β , but α cannot be approximated as zero.

A-7 Coaxial Line

Coaxial transmission lines consist of metallic inner and outer conductors separated by a spacer material as shown in following Figure A- 3a). The spacer material is typically a low-loss dielectric material having permeability approximately equal to that of free space ($\mu \approx \mu_0$) and permittivity ϵ_s which can range from ϵ_0 (air-filled line) to $2 - to 3 \times \epsilon_0$. The outer conductor is alternatively called a shield, because it provides a high degree of isolation from nearby objects and electromagnetic fields. Coaxial line is single-ended [Ellingson, 2018] which means that the conductor geometry is asymmetric and the shield is normally connected to ground at both ends. These characteristics make coaxial line attractive for connecting unbalanced circuits in largely

discrete locations and for connecting antennas to receivers and transmitters. Coaxial lines exhibit TEM field structure as shown in Figure A- 3 b).

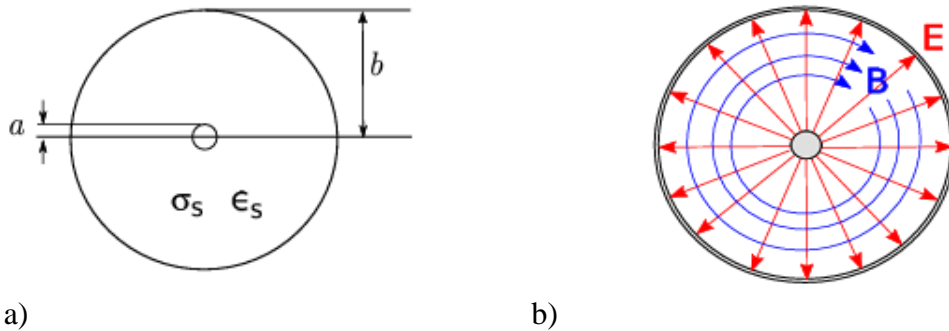


Figure A-3: a) Cross-section of a coaxial transmission line, indicating design parameters. b). the electric and magnetic fields within coaxial line [Ellingson, 2018]

Expressions for the equivalent circuit parameters C' and L' for coaxial lines can be obtained from basic electromagnetic theory and are given in the following Table A-1

The capacitance per unit length	$C' = \frac{2\pi\epsilon_s}{\ln\left(\frac{b}{a}\right)}$
Inductance per unit length	$L' = \frac{\mu_0}{2\pi} \ln\left(\frac{b}{a}\right)$
Loss conductance G'	$G' = \frac{2\pi\sigma_s}{\ln\left(\frac{b}{a}\right)}$
a and b are the radii of the inner and outer conductors, σ_s is the conductance	

Table A-1: the equivalent circuit parameters expressions for coaxial lines.

The resistance per unit length, R' , is relatively difficult to quantify. One obstacle is that the inner and outer conductors are usually made of different materials or compositions of materials. The inner conductor is not necessarily a single homogeneous material; as an alternative, the inner conductor can be made of a variety of materials selected by balancing between conductivity, strength, weight and cost. In the same way, the outer conductor can be not homogeneous; for various reasons, it may be a metal mesh, a braid, or a composite of materials. Furthermore, the resistance varies significantly with frequency which produce another complicating factor is that, while C' , L' , and G' exhibit small variation from their electro- and magnetostatic values. These factors make it difficult to devise a single expression for R' that is both as simple as those shown above for the other parameters and generally applicable. Fortunately, it turns out that the low-loss

conditions ($R' \ll \omega L'$ and $G' \ll \omega C'$) are often applicable, so that R' and G' are important only if it is necessary to compute loss.

Because the low-loss conditions are frequently met, a convenient expression for the impedance is obtained from expressions of L' and C' respectively (Table A-1):

$$Z_0 \approx \frac{1}{\sqrt{L'C'}} = \frac{1}{2\pi} \sqrt{\frac{\mu_0}{\epsilon_s}} \ln \frac{b}{a} \quad (\text{low-loss}) \quad \text{A-28}$$

The spacer permittivity $\epsilon_s = \epsilon_r \epsilon_0$ and ϵ_r is the relative permittivity of the spacer material. Since $\sqrt{\frac{\mu_0}{\epsilon_s}}$ is a constant, the above expression is commonly re-written as

$$Z_0 \approx \frac{60\Omega}{\sqrt{\epsilon_r}} \ln \frac{b}{a} \quad (\text{low-loss}) \quad \text{A-29}$$

Consequently, it is possible to express Z_0 directly in terms of parameters describing the geometry (a and b) and material (ϵ_r). In the same way, the low-loss approximation allows the phase velocity v_p to be expressed directly as function of the spacer permittivity:

$$v_p \approx \frac{1}{\sqrt{L'C'}} = \frac{1}{\sqrt{\mu_0 \epsilon_0 \epsilon_r}} \quad (\text{low-loss}) \quad \text{A-30}$$

So, for the low-loss coaxial line, the phase velocity is approximately equal to the speed of electromagnetic propagation in free space, divided by the square root of the relative permittivity of the spacer material. Therefore, the phase velocity in an air-filled coaxial line is approximately equal to speed of propagation in free space, but is reduced in a coaxial line using a dielectric spacer [Ellingson, 2016].

A-8 Microstrip Line

A microstrip transmission line consists of a narrow metallic trace separated from a metallic ground plane by a slab of dielectric material, as shown in Figure A- 4-a). It is a natural way to implement a transmission line on a printed circuit board, and thus represents a large and wide range of applications. the microstrip is different from stripline.

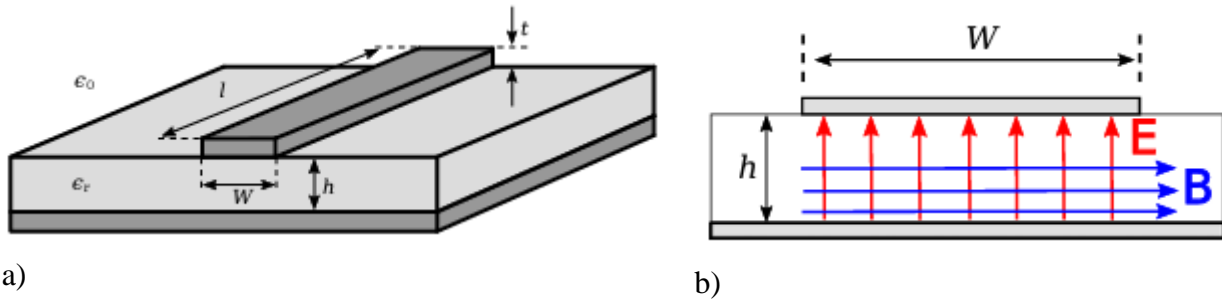


Figure A-4: a)-Microstrip transmission line structure and design parameters. b)- Structure of the electric and magnetic fields within microstrip line.

A microstrip line is single-ended since the conductor geometry is asymmetric and the one conductor—namely, the ground plane also typically serves as ground for the source and load. The spacer material is a low-loss dielectric material with permeability $\mu \approx \mu_0$ and ϵ_r in the range 2 to about 10. A microstrip line nominally exhibits TEM field structure.

This structure is shown in Figure A-4 -b). knowing that the electric and magnetic fields exist both in the dielectric and in the space above the dielectric, which is generally air (not always). This complex field structure makes it difficult to describe microstrip line concisely in terms of the equivalent circuit parameters of the lumped-element model. Instead, the expressions for Z_0 are used directly in terms of h/W and ϵ_r . A variety of these expressions are in common use, representing different approximations and simplifications. An-accepted and -applicable expression is:

$$\left\{ \begin{array}{l} Z_0 \approx \frac{42.4\Omega}{\sqrt{\epsilon_r+1}} \times \ln \left[1 + \frac{4h}{W'} \left(\Phi + \sqrt{\Phi^2 + \frac{1+\frac{1}{\epsilon_r}}{2} \pi^2} \right) \right] \\ \text{where} \quad \Phi = \frac{14+8/\epsilon_r}{11} \left(\frac{4h}{W'} \right) \end{array} \right. \quad \text{A-31}$$

and W' is W adjusted to account for the thickness t of the microstrip line. Typically, $t \ll W$ and $t \ll h$, for which $W' \approx W$. Simpler approximations for Z_0 are also used in microstrip lines design and analysis. These expressions are limited in the range of h/W for which they are valid and can generally be considered special cases or approximations of equation A-31. However, they are sometimes useful for quick “back of the envelope” calculations. Exact expressions for wavelength λ , phase propagation constant β , and phase velocity v_p are also difficult to obtain for microstrip line waves.

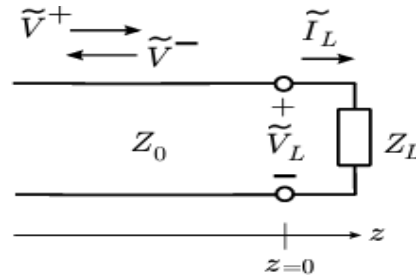
The result from the theory of uniform plane waves in unbounded media is used as an approximate technique where $\beta = \omega \sqrt{\mu \epsilon}$. It is proved that the electromagnetic field structure in the space between the conductors is well-approximated as that of a uniform plane wave in unbounded media having the same permeability μ_0 but a different relative permittivity, to which it is assigned the symbol $\epsilon_{r,eff}$. Then $\beta = \omega \sqrt{\mu_0 \epsilon_{r,eff} \epsilon_0}$ for low-loss microstrip so $\beta = \beta_0 \sqrt{\epsilon_{r,eff}}$. This means that, the phase propagation constant in a microstrip line can be approximated as the free-space phase propagation $\beta_0 = \sqrt{\mu_0 \epsilon_0}$ times a correction factor $\sqrt{\epsilon_{r,eff}}$, $\epsilon_{r,eff}$ is crudely approximated to $\epsilon_{r,eff} \approx \frac{\epsilon_r + 1}{2}$ which means that $\epsilon_{r,eff}$ is around the average of the relative permittivity of the dielectric slab and the relative permittivity of the free space. This assumption is true because part of the power in the guided wave is in the dielectric, and the rest is above the dielectric. Despite many availability calculations to improve this approximation, in practice, variations in the value of ϵ_r of the dielectric due to the manufacturing processes generally make a more precise estimate irrelevant. Using this concept, one can obtain [Wheeler, 1977]:

$$\left\{ \begin{array}{l} \lambda = \frac{2\pi}{\beta} = \frac{2\pi}{\beta_0 \sqrt{\epsilon_{r,eff}}} = \frac{\lambda_0}{\sqrt{\epsilon_{r,eff}}} \\ vp = \frac{\omega}{\beta} = \frac{c}{\sqrt{\epsilon_{r,eff}}} \end{array} \right. \quad \text{A-32}$$

Where λ_0 (c/f) is the free-space wave length and the phase velocity in microstrip is slower than c by a factor of $\sqrt{\epsilon_{r,eff}}$.

A-9 Voltage reflection coefficient

Taking into account Figure A-5. A wave coming from the left along a lossless TL having characteristic impedance Z_0 arrives at a termination located at $z=0$. The impedance looking into



the termination is Z_L , which can have a real value, imaginary or complex. The interesting questions are under what conditions is the reflection, means which wave is moving to the left, expected, and what exactly is that wave?

Figure A- 5: Arriving wave from the left incident on a termination located at $z=0$.

The incident wave potential and current are associated by the constant value of Z_0 . and, the potential and the current of the reflected wave are also related by Z_0 . So, it simply to study either the potential or the current. The potential, of the incident wave is expressed as:

$$\tilde{V}^+(z) = V_0^+(z)e^{j\beta z} \quad \text{A-33}$$

V_0^+ is determined by the source of the wave and actually be a given. Any reflected wave must have the form

$$\tilde{V}^-(z) = V_0^-(z)e^{j\beta z} \quad \text{A-34}$$

Thus, the problem is answered by determining the value of V_0^- given V_0^+ , Z_0 , and Z_L .

By definition $Z_L = \frac{\tilde{V}_L}{\tilde{I}_L}$, where \tilde{V}_L and \tilde{I}_L are the potential across and current through the termination, respectively. Also, the potential and current on either side of the $z=0$ interface must be equal. Thus,

$$\tilde{V}^+(0) + \tilde{V}^-(0) = \tilde{V}_L \quad \text{A-35}$$

$$\tilde{I}^+(0) + \tilde{I}^-(0) = \tilde{I}_L \quad \text{A-36}$$

Where $\tilde{I}^+(z)$ and $\tilde{I}^-(z)$ are the currents associated with $\tilde{V}^+(z)$ and $\tilde{V}^-(z)$, respectively. And because the voltage and current are related by Z_0 , the equation of Z_L is rewritten as follows:

$$\frac{\tilde{V}^+(0)}{Z_0} - \frac{\tilde{V}^-(0)}{Z_0} = \tilde{I}_L \quad \text{A-37}$$

Assessing equations A-35 and A- 37 left side at $z=0$, one can obtain equation A-38,

$$\begin{cases} V_0^+ + V_0^- = \tilde{V}_L \\ \frac{V_0^+}{Z_0} - \frac{V_0^-}{Z_0} = \tilde{I}_L \end{cases} \quad \text{A-38}$$

Substituting these expressions into the previous Z_L expression, one can obtain

$$Z_L = \frac{V_0^+ + V_0^-}{V_0^+/Z_0 - V_0^-/Z_0} \quad \text{A-39}$$

Then by solving for V_0^- , one can get:

$$V_0^- = \frac{Z_L - Z_0}{Z_L + Z_0} V_0^+ \quad \text{A-40}$$

Thus, the response of the question sat earlier is:

$$V_0^- = \Gamma \cdot V_0^+ \quad \text{A-41}$$

where $\Gamma = \frac{Z_L - Z_0}{Z_L + Z_0}$.

This quantity Γ is known as the voltage reflection coefficient and if the terminating impedance is equal to the characteristic impedance of the transmission line, then there is no reflection ($Z_L = Z_0$, $\Gamma = 0$, means $V_0^- = 0$).

But if, $Z_L \neq Z_0$, then $|\Gamma| > 0$, $V_0^- = \Gamma \cdot V_0^+$, and a leftward-traveling reflected wave exists. Since Z_L can be real-, imaginary-, or complex-valued, Γ also can take a real-, imaginary-, or complex-valued. Therefore, V_0^- can be different from V_0^+ in magnitude, sign, or phase. Also, note that Γ is not the ratio of I_0^- to I_0^+ The ratio of the current coefficients is actually $-\Gamma$.

The values of Γ that arise for commonly-encountered terminations is discussing as follow.

Matched Load ($Z_L=Z_0$): In this case, the termination may be a device with impedance Z_0 , or another transmission line with the same characteristic impedance. When $Z_L = Z_0$, $\Gamma=0$ and there is *no reflection*.

Open Circuit: An open circuit means the absence of a termination. This condition implies $Z_L \rightarrow \infty$, and subsequently $\Gamma \rightarrow +1$. Since the current reflection coefficient is $-\Gamma$, the reflected current wave is 180° out of phase with the incident current wave, making *the total current at the open circuit equal to zero*.

Short Circuit: It means $Z_L=0$, and subsequently $\Gamma=-1$. This means, the phase of Γ is 180° , and therefore, the potential of the reflected wave cancels the potential of the incident wave at the open circuit, making the *total potential equal to zero*, as it must be. Since the current reflection coefficient is $-\Gamma=+1$ in this case, *the reflected current wave is in phase with the incident current wave*, and the *magnitude of the total current at the short circuit non-zero*.

Purely Reactive Load: A purely reactive load, including that presented by a capacitor or inductor, has $Z_L = jX$ where X is the reactance. In particular, *an inductor is represented by $X > 0$ and a capacitor by $X < 0$* . So, $\Gamma = \frac{-Z_0 + jX}{+Z_0 + jX}$ The numerator and denominator have the same magnitude, so $|\Gamma| = 1$. Let φ be the phase of the denominator ($+Z_0 + jX$). Then, the phase of the numerator is $\pi - \varphi$. Then, the phase of Γ is $(\pi - \varphi) - \varphi = \pi - 2\varphi$. *Thus, the phase of Γ is no longer limited to be 0° or 180° , but can be any value in between*. The phase of reflected wave is then shifted by this amount.

Other Terminations: Any other termination, including series and parallel combinations of any number of devices, can be defined as a value of Z_L which is, generally, complex-valued. The associated value of $|\Gamma|$ is limited to the range 0 to 1. Note that $\Gamma = \frac{Z_L - Z_0}{Z_L + Z_0} = \frac{Z_L/Z_0 - 1}{Z_L/Z_0 + 1}$ knowing that the smallest possible value of $|\Gamma|$ occurs when the numerator is zero; i.e., when $Z_L=Z_0$. Consequently, the smallest value of $|\Gamma|$ is zero. The largest possible value of $|\Gamma|$ occurs when $Z_L/Z_0 \rightarrow \infty$, means an open circuit or when $Z_L/Z_0=0$ a short circuit, the result in either case is $|\Gamma|=1$. Thus, $0 \leq |\Gamma| \leq 1$.

A-10 Input Impedance for Open and Short-Circuit Terminations

Considering the input impedance of a transmission line TL that is terminated in an open- or short-circuit. Such a TL is sometimes referred to as a stub. From a lumped element circuit theory perspective, this does not have any particular application, but the fact that this structure exhibits an input impedance that depends on length ($Z_{in}(l) = Z_0 \frac{1+\Gamma.e^{-j2\beta l}}{1-\Gamma.e^{-j2\beta l}}$), and shown on figure A-6-a) enables some useful applications.

First, Let's answer on What is the input impedance when the transmission line is open or short-circuited? For a short circuit, $Z_L=0$, $\Gamma=-1$, so one can find

$$Z_{in}(l) = Z_0 \frac{1+\Gamma.e^{-j2\beta l}}{1-\Gamma.e^{-j2\beta l}} = Z_0 \frac{1-e^{-j2\beta l}}{1+e^{-j2\beta l}} \tag{A-42}$$

By multiplying the numerator and denominator of the last equation by $e^{+j\beta l}$, one can find

$$Z_{in}(l) = Z_0 \frac{e^{+j\beta l}-e^{-j\beta l}}{e^{+j\beta l}+e^{-j\beta l}} \tag{A-43}$$

By involving the trigonometric identities and replacing them in the equation, one can obtain:

$$Z_{in}(l) = Z_0 \frac{2j \sin\beta l}{2 \cos\beta l} = +jZ_0 \tan\beta l \tag{A-44}$$

The following Figure A-6-c shows that for $Z_{in}=0$ when $l=0$, since it is equivalent to a short circuit without a transmission line. Moreover, Z_{in} varies periodically with increasing length, with the period $\lambda/2$. What is particularly interesting now is that as $l \rightarrow \lambda/4$, $Z_{in} \rightarrow \infty$. Remarkably, the transmission line essentially turned the termination from short to open!

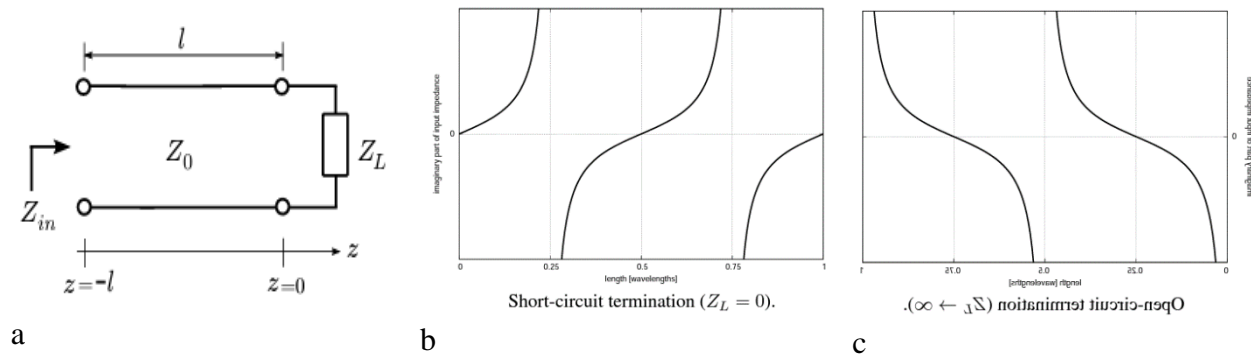


Figure A-6: a/A transmission line driven by a source on the left and terminated by an impedance Z_L at $z=0$ on the right. b and c/Input reactance ($\text{Im}(Z_{in})$) of a stub. $\text{Re}(Z_{in})$ is always zero [Ellingson, 2018].

For an open circuit termination, $Z_L \rightarrow \infty$, $\Gamma = +1$, and the input impedance is given as

$$Z_{in}(l) = Z_0 \frac{1 + \Gamma e^{-j2\beta l}}{1 - \Gamma e^{-j2\beta l}} \quad \text{A-45}$$

$$Z_{in}(l) = -jZ_0 \cos \beta l \quad \text{A-46}$$

Figure A-6-c shows the result for open-circuit termination. As expected, $Z_{in} \rightarrow \infty$ for $l=0$, and the same $\lambda/2$ periodicity is observed. What is of particular interest now is that at $l=\lambda/4$, $Z_{in}=0$. In this case, the transmission line has transformed the open circuit termination into a short circuit. Thus, the input impedance of a short- or open circuited lossless transmission line is completely imaginary-valued represented by equations A-44 and A-46, respectively. The input impedance alternates between open- ($Z_{in} \rightarrow \infty$) and short-circuit ($Z_{in}=0$) conditions with each $\lambda/4$ -increase in length.

The theory of open and shorted transmission lines - often called stubs. These structures have significant applications. In particular, they can be used to replace discrete inductors and capacitors in certain applications. To see this, consider the shorted line (Figure A-6 c). Note that each value of l less than $\lambda/4$ corresponds to a particular positive reactance; that is, the transmission line appears as an inductor. Also note that lengths between $\lambda/4$ and $\lambda/2$ result in negative reactance that is, the transmission line appears as a capacitor. Accordingly, it is possible to replace an inductor or a capacitor with a short-circuited transmission line of suitable length. So, at the design frequency, the input impedance of a similar transmission line is the same as that of the inductor or capacitor. The reactance variation versus frequency can be a problem depending on the application bandwidth and frequency response requirements. Open circuit lines can be used in the same way.

Taking advantage of this property of open- and short transmission lines, it is possible to implement impedance matching circuit, filters, and other devices entirely from transmission lines, with fewer or no discrete inductors or capacitors required. Transmission lines have not performance limitations of discrete devices at high frequencies and are less expensive. The disadvantage of these stubs in this application is the lines are much larger than the discrete devices they are meant to replace.

A-11 Quarter-Wavelength Transmission Line

Quarter-wavelength sections of transmission line play an important role in many systems at radio and optical frequencies. In order to perform more general analysis, one can consider not just open- and short-circuit terminations but any terminating impedance, and then some applications are addressed. The general expression for the input impedance of a lossless transmission line is represented by equation A-47

$$Z_{in}(l) = Z_0 \frac{1+\Gamma.e^{-j2\beta l}}{1-\Gamma.e^{-j2\beta l}} \quad \text{A-47}$$

and when $l = \lambda/4$, $2\beta l = 2 \cdot \frac{2\pi}{\lambda} \frac{\lambda}{4} = \pi$, subsequently the last equation becomes:

$$Z_{in}(l) = Z_0 \frac{1+\Gamma.e^{-j\pi}}{1-\Gamma.e^{-j\pi}} = Z_0 \frac{1-\Gamma}{1+\Gamma} \quad \text{A-48}$$

And by substituting the expression of $\Gamma = \frac{Z_L - Z_0}{Z_L + Z_0}$, then multiplying numerator and denominator by $(Z_L + Z_0)$, one obtains

$$Z_{in}\left(\frac{\lambda}{4}\right) = Z_0 \frac{(Z_L + Z_0) - (Z_L - Z_0)}{(Z_L + Z_0) + (Z_L - Z_0)} = Z_0 \frac{2Z_0}{2Z_L} \quad \text{A-49}$$

And thus,

$$Z_{in}\left(\frac{\lambda}{4}\right) = \frac{Z_0^2}{Z_L} \quad \text{A-50}$$

Thus, the input impedance is inversely proportional to the load impedance. This is why a transmission line of length $\lambda/4$ can be named a quarter-wave inverter or just an **impedance inverter**. Quarter-wave lines play an imperative role in radio engineering. In this case, they have the useful characteristic of transforming small impedances into large impedances, and reciprocally. To perceive how the quarter-wave lines are used for impedance matching, one can solve equation A-50 for Z_0

$$Z_0 = \sqrt{Z_{in}(\lambda/4) \cdot Z_L} \quad \text{A-51}$$

This equation shows that it is possible to match the local Z_L to a source impedance (represented by $Z_{in}(\lambda/4)$) simply by making the characteristic impedance equal to the value given by the above expression and setting the length to $\lambda/4$. Figure A-7 shown the scheme.

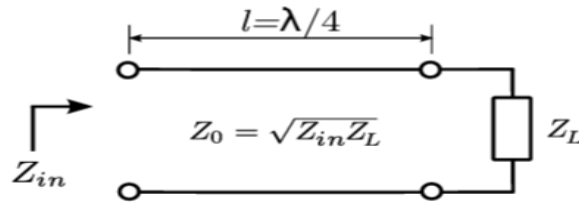


Figure A-7: Using a quarter wavelength transmission line for impedance-matching.

References -Appendix A

[Ellingson, 2016] S.W. Ellingson, ‘Differential Circuits’, Radio Systems Engineering, Cambridge Univ. Press, 2016.

[Wheeler, 1977] H.A. Wheeler, “Transmission Line Properties of a Strip on a Dielectric Sheet on a Plane,”IEEE Trans. Microwave Theory & Techniques, Vol.25, No.8, pp.631–47,1977.

[Ellingson, 2018] Ellingson, Steven W., ‘Electromagnetics (Volume 1)’, Book, Blacksburg, Virginia, VT Publishing. <https://doi.org/10.21061/electromagnetics-vol-1>.2018

Appendix B

In 5G technology, two classes of frequency bands are specified. First are Sub-six GHz bands in which the frequency transmitted from cell phone towers are smaller than 6 GHz (similar to 4G). On the other hand, the higher speeds that really set 5G apart from any of the 4G **LTE** links require high-frequency bands (mm-wave above 24 GHz). These high frequencies have very large bandwidths, so they are perfect for keeping the connection in busy environments like stadiums.

Consequently, 5G is classified into Frequency Range-1 (sub-six GHz) and Frequency Range-2 (mm-wave, above 24GHz).